INFORMATION TO USERS

This dissertation was produced from a microfilm copy of the original document. While the most advanced technological means to photograph and reproduce this document have been used, the quality is heavily dependent upon the quality of the original submitted.

The following explanation of techniques is provided to help you understand markings or patterns which may appear on this reproduction.

1. The sign or "target" for pages apparently lacking from the document photographed is "Missing Page(s)". If it was possible to obtain the missing page(s) or section, they are spliced into the film along with adjacent pages. This may have necessitated cutting thru an image and duplicating adjacent pages to insure you complete continuity.

2. When an image on the film is obliterated with a large round black mark, it is an indication that the photographer suspected that the copy may have moved during exposure and thus cause a blurred image. You will find a good image of the page in the adjacent frame.

3. When a map, drawing or chart, etc., was part of the material being photographed the photographer followed a definite method in "sectioning" the material. It is customary to begin photoing at the upper left hand corner of a large sheet and to continue photoing from left to right in equal sections with a small overlap. If necessary, sectioning is continued again — beginning below the first row and continuing on until complete.

4. The majority of users indicate that the textual content is of greatest value, however, a somewhat higher quality reproduction could be made from "photographs" if essential to the understanding of the dissertation. Silver prints of "photographs" may be ordered at additional charge by writing the Order Department, giving the catalog number, title, author and specific pages you wish reproduced.

University Microfilms

300 North Zeeb Road
Ann Arbor, Michigan 48106

A Xerox Education Company

Downloaded from SHAREOK. Persistent Handle URL: https://hdl.handle.net/11244/3327

72-24,383

BAHERI, Javad Motazed, 1934-
THE DIFFRACTION PATTERN PRODUCED BY A POINT SOURCE ILLUMINATING THE REGION BETWEEN TWO PLANE PARALLEL MIRRORS.

The University of Oklahoma, Ph.D., 1972
Physics, optics

University Microfilms, A XEROX Company, Ann Arbor, Michigan

© 1972

JAVAD MOTAZED BAHERI

ALL RIGHTS RESERVED

THIS DISSERTATION HAS BEEN MICROFILMED EXACTLY AS RECEIVED

THE UNIVERSITY OF OKLAHOMA

GRADUATE COLLEGE

THE DIFFRACTION PATTERN PRODUCED BY A POINT SOURCE ILLUMINATING THE REGION BETWEEN TWO PLANE PARALLEL MIRRORS

A DISSERTATION

SUBMITTED TO THE GRADUATE FACULTY

in partial fulfillment of the requirements for the

degree of

DOCTOR OF PHILOSOPHY

BY

JAVAD MOTAZED BAHERI

Norman, Oklahoma

1972

THE DIFFRACTION PATTERN PRODUCED BY A POINT SOURCE ILLUMINATING THE REGION BETWEEN TWO PLANE PARALLEL MIRRORS

APPROVED BY

J. N. Huffaker

Robert M. St. John

Ronald Rantowski

William N. Huff

Gerald Tuma

R. R. Bowrassa

PLEASE NOTE:

Some pages may have

indistinct print.

Filmed as received.

University Microfilms, A Xerox Education Company

Acknowledgement

This dissertation is a revision of an earlier draft [1], performed under the direction of Dr. Richard Day. Dr. J. Neal Huffaker directed the revision of the original work, and Dr. Robert St. John provided liason.

The completion of this work is due to the careful technical assistance of both my advisors and the encouragement of Dr. St. John. They deserve my sincere thanks. The National Aeronautical and Space Administration supported the original work through the grant NGR37-033-047 and The University of Oklahoma extended this support for the completion of this revision.

My wife continued to bear the burden of life with our children and gave me the opportunity to devote my time to my academic work. I thank all these sources of help.

A l s o I can not avoid mentioning the inspiration of both Dr. Huffaker throughout this work, and of Dr. William Huff in one of the most important chapters of the dissertation.

Suggestions made by Dr. Ronald Bourassa are greatly appreciated. Finally thanks to Dr. Ronald Kantowski and professor Gerald Tuma for serving on dissertation committee.

TABLE OF CONTENTS

Page

ACKNOWLEDGEMENT iii

LIST OF FIGURES v

LIST OF TABLES vi

ABSTRACT vii

Chapter

I. INTRODUCTION 1

II. SOLUTION BY IMAGE METHOD 5

1. The Image of an Electromagnetic Field 7

2. Unpolarized and Polarized Light 9

3. Derivation of Image Method Treatment of GIMBI 10

III. MODE THEORY TREATMENT OF GIMBI 15

1. Modes in Rectangular Coordinates 15

2. Coefficients of the Expansion in Modes for a Given Source 20

3. Propagation of Modes and Intensity of the Interference Pattern 23

IV. CALCULATIONS, RESULTS, AND CONCLUSIONS 25

1. Details of Mode-Method Calculations 26

2. Results 34

3. Conclusions 75

BIBLIOGRAPHY 76

APPENDIX 77

LIST OF FIGURES

FIGURE		PAGE
1.	Cross section of the GIMBI.	2
2.	Photograph of GIMBI	3
3.	Treatment of reflected rays by method of images. .	6
4.	Image of acharge,the forceon it,and the E field. .	8
5.	Image method for light polarized perpendicular to the plane of incidence.	11
6.	Image method for light polarized parallel to th plane of incidence.	13
7.	Schematics for the mode method treatment..	
8.	Graphical comparisons of the function..	32
9-27.	Plots Of Intensity.	.39-74

LIST OF TABLES

TABLES		PAGE
I.	Effect of using various numbers of cells on the Simpson's Rule.	29
II.	Values of $\left\|C_{TE_{(n)}}\right\|$ for several sets of parameters.	31
III.	Accuracy of Truncated Fourier series.	36
IV.	Parameters used in calculating figures 9-27. . .	38

ABSTRACT

Full vector-electromagnetic theory is used to calculate the diffraction pattern between two parallel perfectly conducting mirrors, illuminated by a point monochromatic source located equidistant from the mirrors. The method of solution of the problem involves four steps: (a) All possible modes of the electromagnetic field between two parallel mirrors are found. These modes form a complete set of orthogonal functions which are solutions to the vector Helmholtz equation, and satisfy Maxwell's equations subject to appropriate boundary conditions. (b) An appropriate expression for the radiation field of the source (in the absence of mirrors) is found. (c) The actual field between the mirrors due to the source is expressed as a linear combination of the modes found in (a). (d) Finally, the intensity of light on a screen just beyond the mirrors and perpendicular to them is calculated from the fields of part (c). The calculation is performed for several sets of values of the various parameters: mirror separation, distance of source from mirrors and screen, and wavelength of source.

A simpler theory for this problem, involving the method of images, is also described. A comparison between image method and mode calculations is given.

CHAPTER I

INTRODUCTION

In 1969, Day introduced [1] a new kind of interferometer, which he called the Grazing Incidence Multi-Beam Interferometer (GIMBI). It was hoped that this interferometer would be useful as a spectrometer in the ultraviolet region. The construction of the GIMBI is shown in Fig. 1.

Two plane mirrors are separated by a distance of 2a. A point light source which usually is outside the interferometer illuminates these mirrors and the pattern of interference between various reflected beams is observed on a screen located at a distance $z_I + z_o$ from the source. In Fig. 2 we show a photograph of one of the interferometers which were built in our laboratory.

Since the interferometer makes use solely of reflecting surfaces to obtain coherent beams (i.e., no transmitting elements are involved) it has unrestricted applications throughout the electromagnetic spectrum. In particular there is no impediment for its use in the ultraviolet range of the spectrum, unlike interferometers which involve transmission through glass plates.

Before such a device would become useful as a spectrometer,

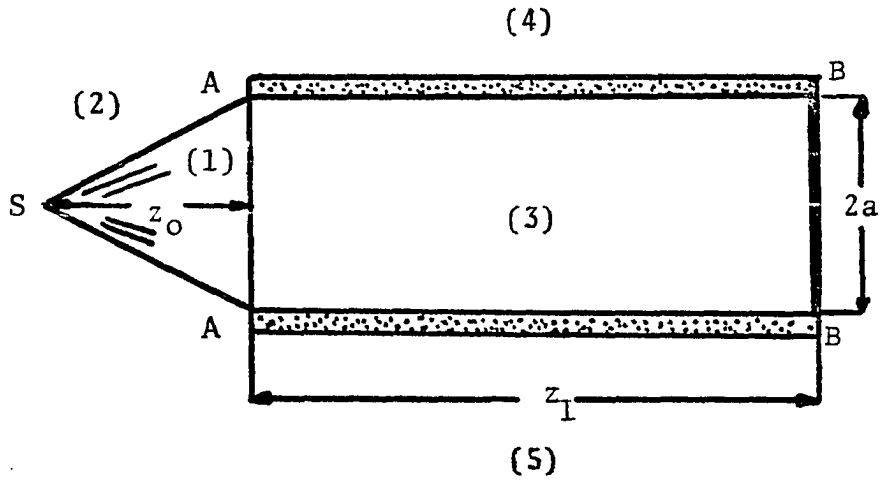

Figure 1.

Fig. 1. Cross-section of the GIMBI interferometer. The source is located at S, the screen at B-B. The device parameters are: 2a, distance between mirrors; z_o, distance from S to boundary A-A of region between mirrors; and z_1, distance from boundary to screen.

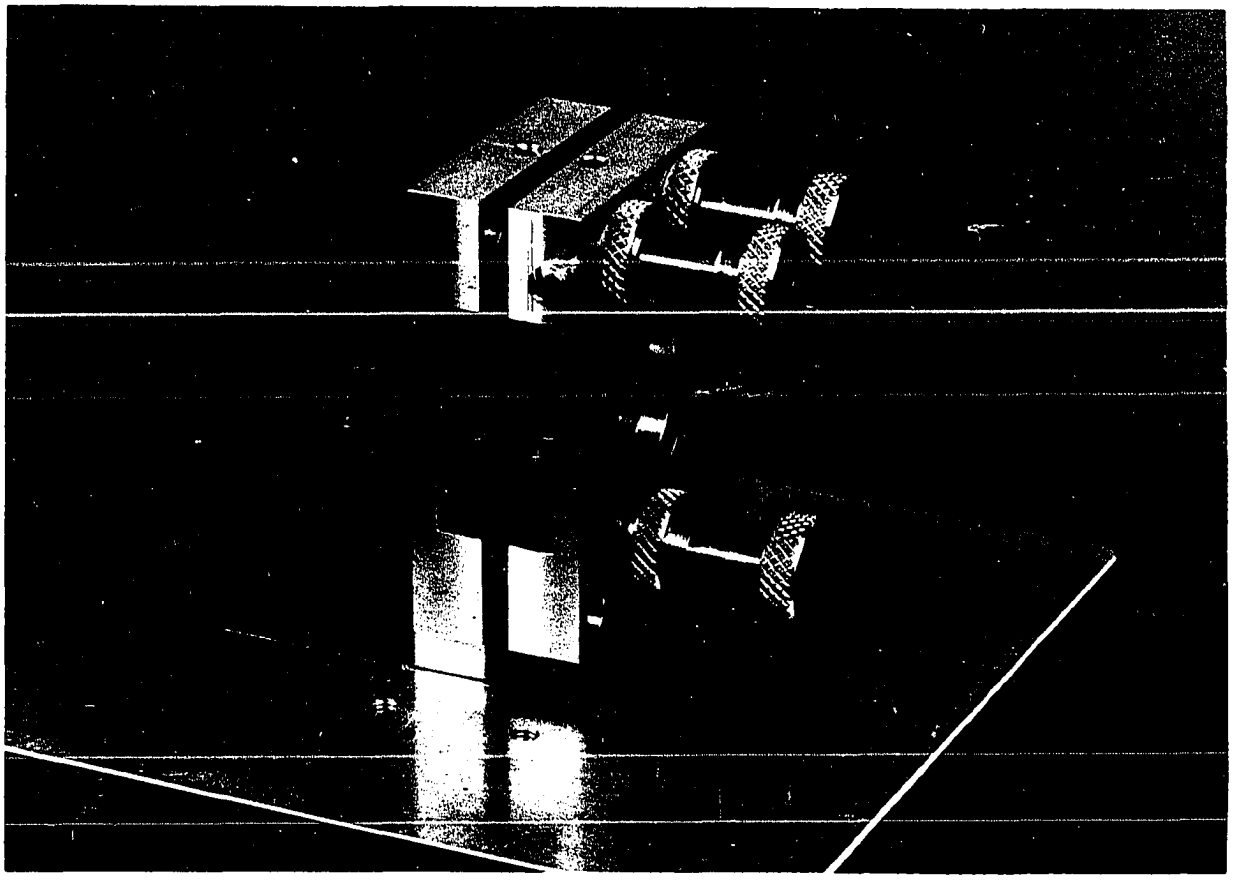

Figure 2

A photograph of two parallel plane interferometer

built by Dr. Day

called

GIMBI*

*Grazing incident multibeam interferometer.

calculations would have to be performed showing the kinds of interference patterns produced for different combinations of the various parameters.

The first theoretical treatment of GIMBI was done by the image method [1]. In this method one considers the light intensity at the screen as due to the interference of a number of beams: one direct from the source; one reflected singly by each mirror; another pair reflected once by both mirrors; and so forth. For a particular polarization, we can replace a reflected beam by a beam from an image source, with a definite phase relationship to the real source. Thus, the radiation field at the screen is the superposition of a number of radiation fields of the various images, and the intensity can be calculated from the absolute value squared of the electric field. Chapter II is devoted to a discussion of the image method.

Since two parallel mirrors actually constitute a kind of waveguide, the GIMBI can also be treated by a completely different method, which we call the mode method or mode solution. In this method we first find all modes of the electromagnetic radiation field in the space between two parallel plane mirrors. We then find the particular linear combination of these modes produced by the source, and evaluate fields and intensity of light at the screen [2]. Full details of this method are given in Chapter III. Similar problems can be found in the literature [3-6].

Chapter IV describes details of the calculations, along with calculated interference patterns using the two different approaches.

CHAPTER II

SOLUTION BY IMAGE METHOD

The image-method treatment of GIMBI has already been described [1]. By this method, the intensity at a given point is found by summing the contributions of all rays (direct and reflected) reaching this point. For radiation of wavelength λ, the published formula for the total field amplitude at point x is the following:

$$\phi(x) = \sum_{n=-N}^{N} r^{|n|} \frac{\exp i(kd_n+\theta_n)}{d_n} , \qquad (1)$$

where

$$k = 2\pi/\lambda , \qquad (2a)$$

$$d_n = [L^2+(nt-x)^2]^{1/2} , \quad -N<n<N, \qquad (2b)$$

$$\theta_n = n\pi , \qquad L = z_0 + z_1 , \qquad (2c)$$

and where the quantity r is related to the reflectivity R of the mirrors by

$$r^2 = R.$$

Parameters z_0, z_1 and x are defined in Fig. 3. Note that when the angle α_0 in Fig. 3a is not close to π, the number of images

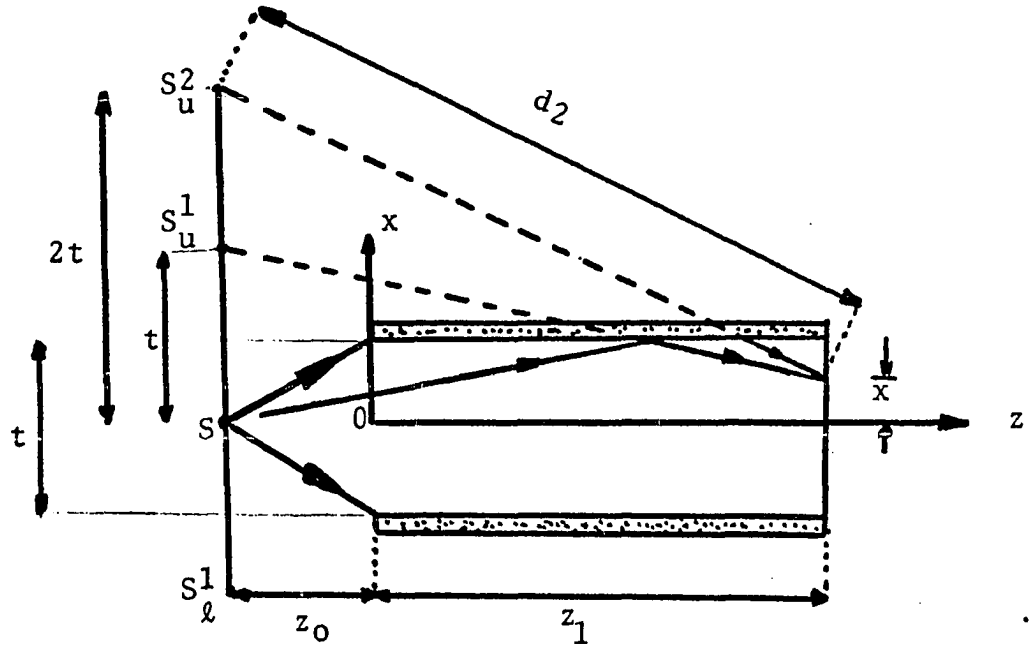

(a)

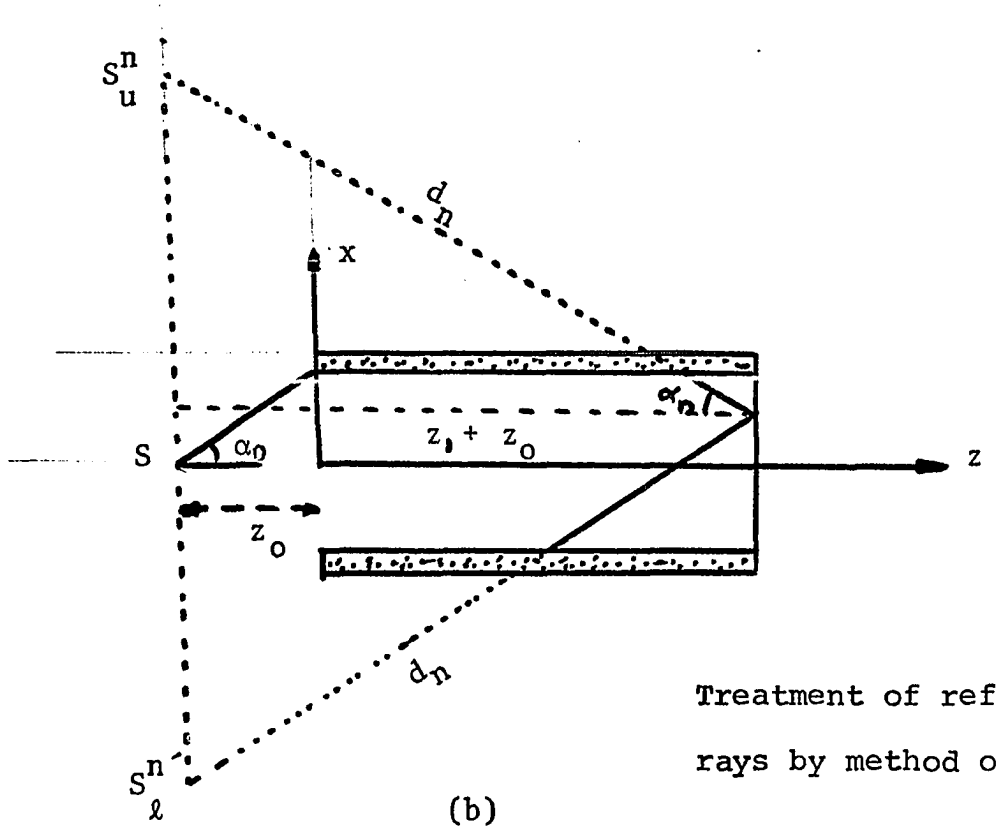

(b)

Treatment of reflected rays by method of images.

Fig. 3

N is finite, and can be deduced from Fig. 3 as follows:

$$\tan \alpha_o = \frac{a}{z_o} \geq \tan \alpha_N \simeq \frac{Nt}{z_o+z_1}. \qquad (3)$$

Actually, for different values of x, we may have different numbers of images above and below the apparatus, contributing to the field at x. Where N_ℓ and N_u are the numbers of images below and above, respectively, we obtain

$$N_\ell(x) = \text{greatest integer in} \quad \frac{z_o+z_1}{2z_o} - \frac{x}{2a} \qquad (4a)$$

$$N_u(x) = \text{greatest integer in} \quad \frac{z_o+z_1}{2z_o} + \frac{x}{2a} \qquad (4b)$$

1. The Image of an Electromagnetic Field.

The image-method treatment of GIMBI is based on the concept of the image of an electromagnetic field in a mirror (perfect conductor). In particular, the image of the $\underset{\sim}{E}$ field can be found as follows: Consider a charge q at a distance d from a perfect conductor. The image of the charge is a charge -q a distance d behind the mirror. As shown in Fig. 4a, consider a field $\underset{\sim}{E}$, parallel to the mirror, acting on q. Because of the resulting acceleration of q and its image, we infer the existence of an "image field" $\underset{\sim}{E}_i$ acting on the image. Since the force $\underset{\sim}{F}_i$ exerted on the image is parallel to the force $\underset{\sim}{F}$ exerted by $\underset{\sim}{E}$ on q, we deduce that $\underset{\sim}{E}_i = -\underset{\sim}{E}$. Thus, the image of an $\underset{\sim}{E}$ field parallel to the mirror has the opposite direction to the original field. As shown in Fig. 4b, the image of a field perpendicular to the mirror must exert a force on the image charge in the <u>opposite</u> direction, and hence the image field is in the <u>same</u> direction.

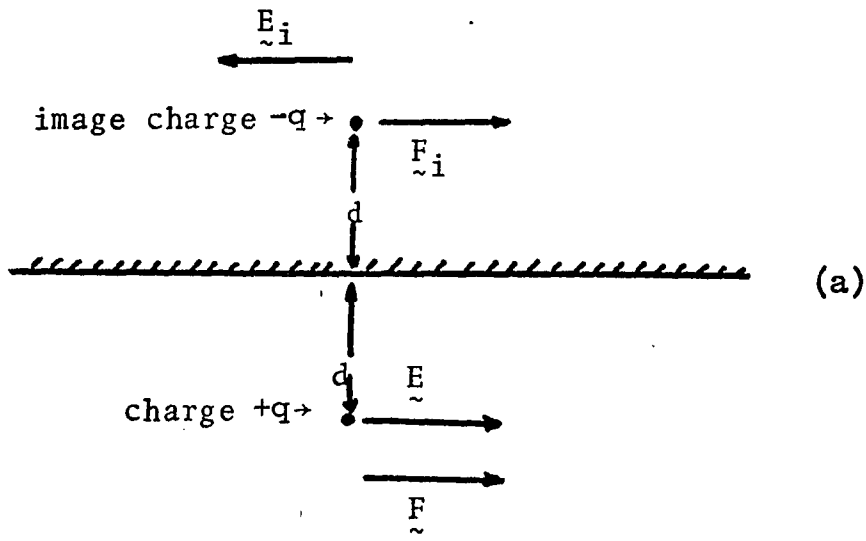

(a)

(a)

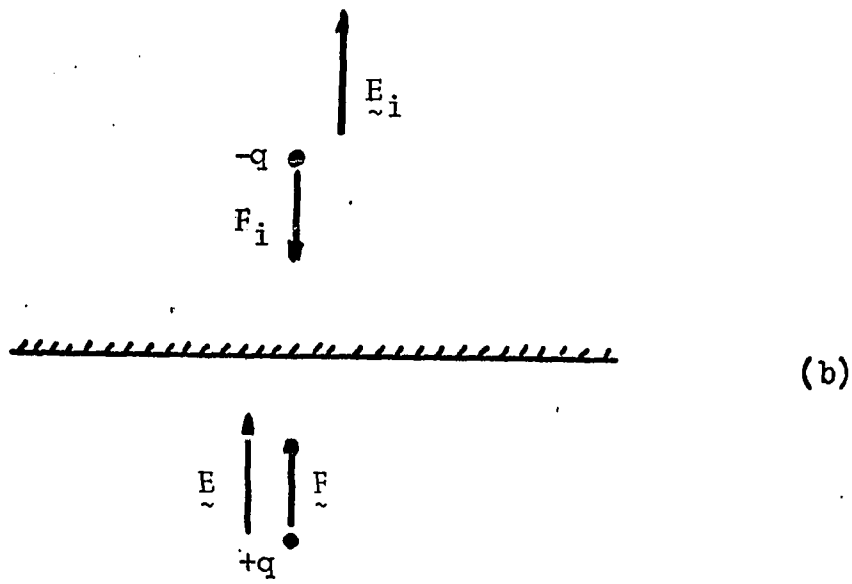

(b)

Fig. 4 Image of a charge, the foce on it, and the $\underset{\sim}{E}$ field producing the force. (a), $\underset{\sim}{E}$ parallel to mirror, (b), $\underset{\sim}{E}$ perpendicular to mirror.

2. Unpolarized and Polarized Light.

Light is an electromagnetic radiation obeying Maxwell's equations, which specifically demand transverse waves. Electromagnetic waves are due to the vibrations of charged particles within the molecules making up the source. The light wave sent out by one molecule may be considered to be plane polarized, since the vibrations occur in only one plane containing the direction of propagation. For a large number of molecules, each of the vibrations is normally in a random direction.

If a beam of light is made up of vibrations in all directions perpendicular to its direction of propagation, so that there is no preponderance of vibrations in any particular transverse direction, the light is said to be unpolarized. But if there is any dissymetry, the beam is said to be polarized.

Since many optical phenomena, such as reflection, depend on polarization, we must express unpolarized light in terms of polarized light. The correct procedure is to consider unpolarized light as an <u>incoherent</u> mixture of two beams of equal amplitudes and orthogonal polarizations. To find the resulting intensity, we find the intensity due to each polarized beam separately, and add the intensities. Where reflection of light is concerned, it is convenient to choose polarization directions parallel to and perpendicular to the <u>plane of incidence</u>: this is the plane defined by the incident and reflected rays.

3. Derivation of Image Method Treatment of GIMBI.

In light of the above discussion, we find intensities for two kinds of polarized light, which must be added to find the intensity for unpolarized light.

(i) Polarization perpendicular to the plane of incidence. The expression for the radiation field originating from the source with this kind of polarization is .

$$\underset{\sim}{E}_1 = \hat{\underset{\sim}{y}} \frac{\exp(ikr)}{r} , \tag{5}$$

where $r = [(z_0+z)^2+x^2]^{\frac{1}{2}}$ and, as shown in Fig. 5, $\hat{\underset{\sim}{y}}$ is a unit vector perpendicular to the plane of the figure.

An image field will have a phase difference of 180°, and may be considered to have originated from the image of the source. We designate subscripts u and ℓ (upper and lower) for the mirrors, and use superscripts to denote the order of an image. Thus, S_u^1 stands for the first image of the source located above the upper mirror. From these source images, image fields may be said to originate, with successive phase differences of 180°. Thus, we can obtain equations like the following from Fig. 5:

$$\underset{\sim}{E}_u^1 = (-1)^1 \underset{\sim}{E}_1 = \hat{\underset{\sim}{y}} (-1)^1 \frac{\exp(ikd_1)}{d_1},$$

$$\underset{\sim}{E}_u^2 = (-1)^2 \underset{\sim}{E}_1 = \hat{\underset{\sim}{y}} (-1)^2 \frac{\exp(ikd_2)}{d_2},$$

$$\underset{\sim}{E}_\ell^1 = (-1)^1 \underset{\sim}{E}_1 = \hat{\underset{\sim}{y}} (-1)^1 \frac{\exp(ikd_1)}{d_1},$$

$$\underset{\sim}{E}_\ell^2 = (-1)^2 \underset{\sim}{E}_1 = \hat{\underset{\sim}{y}} (-1)^2 \frac{\exp(ikd_2)}{d_2}, \text{ etc.}$$

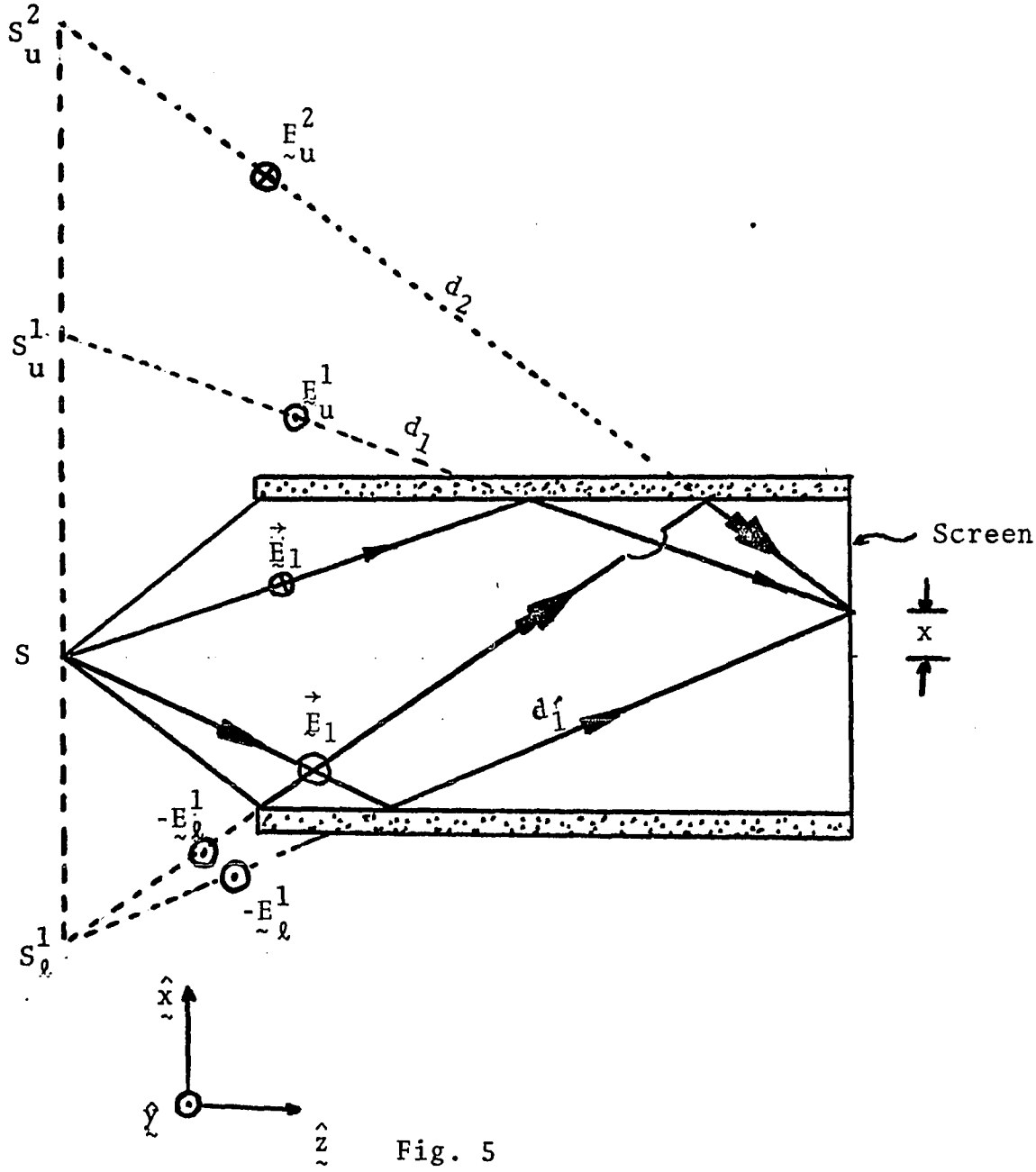

Fig. 5

Fig. 5. Image method for light polarized perpendicular to the plane of incidence.

Each reflection diminishes a field by a factor $r_\perp = R_\perp^{1/2}$, where $R_\perp$ is the reflectivity of the mirrors. Thus, the n-th order reflected field is reduced by the factor $r_\perp^n$. The sum of fields at a point x on the screen can be written

$$\underset{\sim}{E}_\perp(x) = \hat{\underset{\sim}{y}} \sum_{n=N_\ell(x)}^{N_u(x)} (-r_\perp)^{|n|} \frac{\exp(ikd_n)}{d_n}, \qquad (6)$$

where d_n and the N's were defined previously. The reflectivity quantity $r_\perp$ is discussed further in the Appendix.

(ii) Polarization parallel to the incident plane. For this case, the $\underset{\sim}{E}$ field of the source has the following form:

$$\underset{\sim}{E}_2 = (\hat{\underset{\sim}{x}} \cos\alpha - \hat{\underset{\sim}{z}} \sin\alpha) \frac{\exp(ikr)}{r} \qquad (7)$$

where r has already been defined, and the angle α is defined in Fig. 6. Calling the z- and x-components of this field CA and CB, as shown in the figure, we note that the image of CA is -CA, while the image of CB is CB. In other words, images of horizontal components change sign alternatively, while images of vertical components are unchanged. As in case (i), we add image fields, appropriately diminished by reflections, to find the total field at a point, obtained the following:

$$\underset{\sim}{E}_{||}(x) = \sum_{n=-N_\ell(x)}^{N_u(x)} [\hat{\underset{\sim}{x}} \cos\alpha_n - (-1)^n \hat{\underset{\sim}{z}} \sin d_n] r_{||}^{|n|}(\alpha_n) \frac{\exp(ikd_n)}{d_n} . \qquad (8)$$

Here, $r_{||}(\alpha_n)$ is the appropriate quantity for describing reflection of light polarized parallel to the plane of incidence, which quantity is discussed in the Appendix.

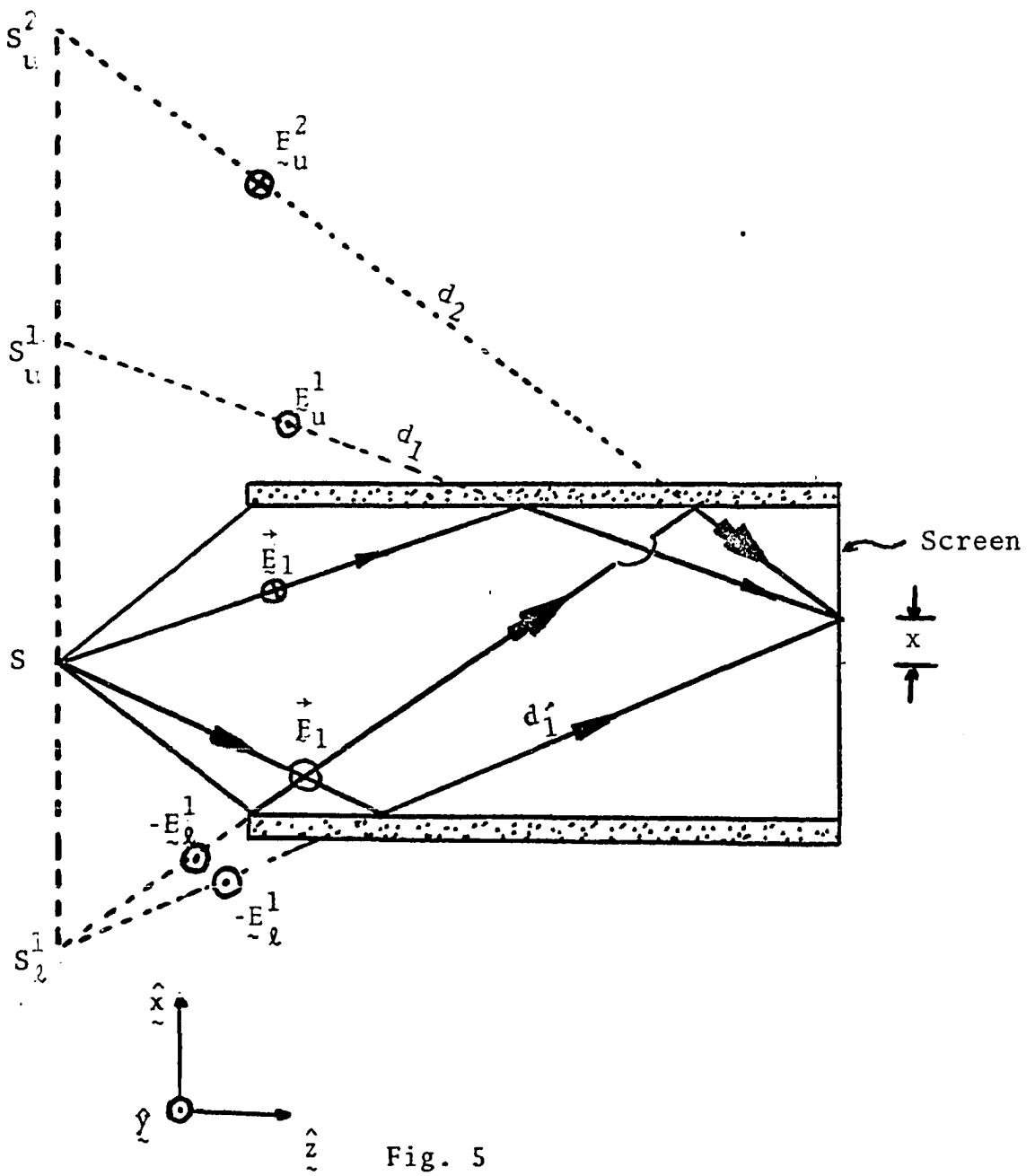

Fig. 5

Fig. 5. Image method for light polarized perpendicular to the plane of incidence.

Each reflection diminishes a field by a factor $r_\perp = R_\perp^{\frac{1}{2}}$, where $R_\perp$ is the reflectivity of the mirrors. Thus, the n-th order reflected field is reduced by the factor $r_\perp^n$. The sum of fields at a point x on the screen can be written

$$\underset{\sim}{E}_\perp(x) = \hat{\underset{\sim}{y}} \sum_{n=N_\ell(x)}^{N_u(x)} (-r_\perp)^{|n|} \frac{\exp(ikd_n)}{d_n}, \qquad (6)$$

where d_n and the N's were defined previously. The reflectivity quantity $r_\perp$ is discussed further in the Appendix.

(ii) Polarization parallel to the incident plane. For this case, the $\underset{\sim}{E}$ field of the source has the following form:

$$\underset{\sim}{E}_2 = (\hat{\underset{\sim}{x}} \cos\alpha - \hat{\underset{\sim}{z}} \qquad (7)$$

where r has already bee e α is defined in Fig. 6. Calling the z s field CA and CB, as shown in the fi age of CA is -CA, while the image of CB i images of horizontal components change sig ile images of vertical components are uncha in case (i), we add image fields, appropriately diminished by reflections, to find the total field at a point, obtained the following:

$$\underset{\sim}{E}_{||}(x) = \sum_{n=-N_\ell(x)}^{N_u(x)} [\hat{\underset{\sim}{x}} \cos\alpha_n - (-1)^n \hat{\underset{\sim}{z}} \sin d_n] r_{||}^{|n|}(\alpha_n)$$

$$\frac{\exp(ikd_n)}{d_n} . \qquad (8)$$

Here, $r_{||}(\alpha_n)$ is the appropriate quantity for describing reflection of light polarized parallel to the plane of incidence, which quantity is discussed in the Appendix.

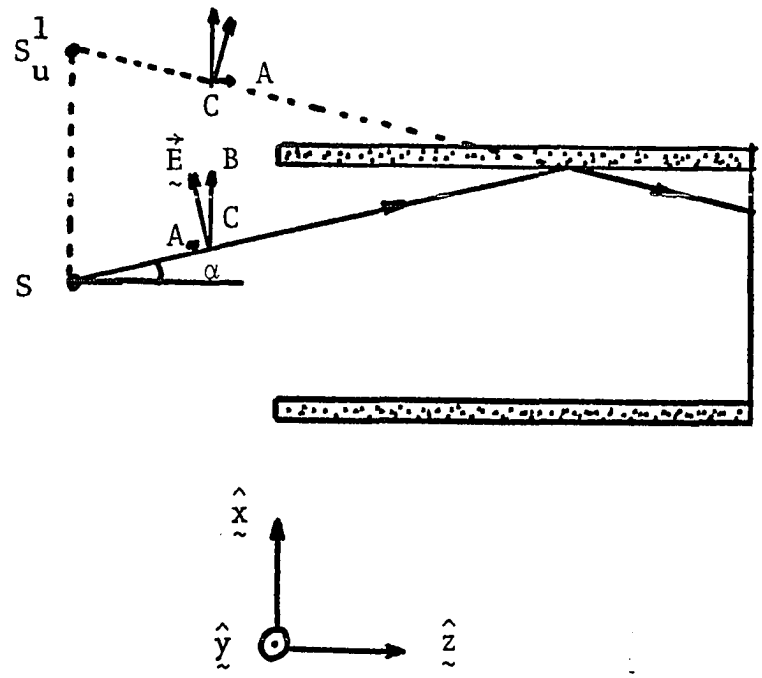

Fig. 6. Image method for light polarized parallel to the plane of incidence.

The resulting interference pattern at the screen is found from Eqs. (6) and (8) by the following expression for intensity I(x):

$$I(x) \propto |\underset{\sim}{E}_{11}(x)|^2 + |E_{\perp}(x)|^2. \qquad (9)$$

We recognize that Day's formula, Eq. (1), is essentially the same as Eq. (6), obtained for light polarized perpendicular to the plane of incidence. As shown in the Appendix, $r_{||}$ is very nearly zero for grazing incidence, so the contribution from parallel-polarized light is negligible (except for the unreflected ray, which produces uniform intensity over the screen).

Remark: It should now be clear that, in the image method, reflected fields are replaced by image fields. The combination of original field plus image fields must satisfy the following boundary conditions at the mirrors:

$$\hat{\underset{\sim}{n}} \times \underset{\sim}{E} = 0, \qquad \hat{\underset{\sim}{n}} \cdot \underset{\sim}{B} = 0,$$

where $\hat{\underset{\sim}{n}}$ is a unit vector perpendicular to the mirrors. Thus, it is clear that the tangential components of incident and image E fields must add to zero. For polarization of type (ii), the B field is parallel to the mirror, as is its image. For case (i) the B field lies in the plane of Fig. 5, and we find that the x-component of the image B field is reversed.

CHAPTER III

MODE THEORY TREATMENT OF GIMBI

The theory of partial differential equations informs us that the radiation field in a source-free region of space with given boundary conditions is a superposition of a set of special solutions, or modes, which are a complete and orthogonal set of eigenfunctions matching the boundary conditions. Considering the space between the mirrors in GIMBI to be such a region, we can obtain the GIMBI interference pattern by a procedure involving three steps: (i) obtaining the complete set of orthogonal functions for the radiation field between the mirrors; (ii) determining the coefficients of the linear combination of modes produced by a particular source; (iii) calculating the field and intensity at the location of the screen.

1. Modes in Rectangular Coordinates

For light of a definite frequency $\nu = 2\pi\omega$, electric and magnetic fields are considered to have time dependence $e^{-i\omega t}$, whereupon Maxwell's equations in free space take the form

$$\nabla\cdot\underset{\sim}{E} = 0, \tag{10a}$$

$$\nabla\cdot\underset{\sim}{B} = 0, \tag{10b}$$

$$\nabla\times\underset{\sim}{E} = -i\omega\underset{\sim}{B}, \tag{10c}$$

$$\nabla\times\underset{\sim}{B} = i\omega\mu_o\varepsilon_o\underset{\sim}{E}. \tag{10d}$$

Taking the curl of Eqs. (10c) and (10d), using a vector identity, and substituting various of Eqs. (10) in the resulting expressions, one can show that $\underset{\sim}{E}$ and $\underset{\sim}{B}$ both satisfy the vector Helmholtz equation:

$$(\nabla^2 + \mu_0\varepsilon_0\omega^2)\underset{\sim}{E} = 0; \tag{11a}$$

$$(\nabla^2 + \mu_0\varepsilon_0\omega^2)\underset{\sim}{B} = 0. \tag{11b}$$

Plane-wave solutions in free space for plane-polarized radiation have the form

$$\underset{\sim}{E}(\underset{\sim}{r}) = \underset{\sim}{E}_0\, e^{i\,\underset{\sim}{k}\,\cdot\,\underset{\sim}{r}}, \tag{12a}$$

$$\underset{\sim}{B}(\underset{\sim}{r}) = c\,\underset{\sim}{k} \times \underset{\sim}{E}(\underset{\sim}{r}), \tag{12b}$$

where the magnitude of $\underset{\sim}{k}$ is

$$|\underset{\sim}{k}| = \omega/c, \tag{13}$$

where c is the velocity of light [$c = (\mu_0\varepsilon_0)^{-\frac{1}{2}}$], and the direction of $\underset{\sim}{k}$ is the direction of propagation of the wave. The direction of $\underset{\sim}{E}_0$ is parallel to the plane of polarization, and must be perpendicular to $\underset{\sim}{k}$.

In the space between two parallel mirrors, consider radiation propagating in the z direction (parallel to the mirrors). We can think of "rays" bouncing back and forth from one mirror to the other, traveling in this direction. Clearly, it is possible for $\underset{\sim}{E}$ and $\underset{\sim}{B}$ to have z-components, and for the z-components of the propagation vector $\underset{\sim}{k}$ to be smaller than the magnitude of $\underset{\sim}{k}$. Letting a wave propagate in this manner, with propagation constant (eigenvalue) k_n, and defining a vector differential operator

$$\nabla_t^2 = \nabla^2 - \frac{\partial^2}{\partial z^2}, \tag{14}$$

we can write Eq. (11a) in the form

$$(\nabla_t^2 + \frac{\partial^2}{\partial z^2} + k^2)E(x,y)\, e^{i\,k_n z} = 0.$$

Evaluating the partial with respect to z, we find the x,y

dependence satisfies

$$(\nabla_t^2 + \gamma_n^2)E(x,y) = 0, \tag{15a}$$

where $\gamma_n^2 = k^2 - k_n^2$.

In similar fashion, we can obtain

$$(\nabla_t^2 + \gamma_n^2)\, B(x,y) = 0. \tag{15b}$$

Defining longitudinal (z) and transverse components of $\underset{\sim}{E}$ by

$$\underset{\sim}{E}_z = (\hat{\underset{\sim}{z}} \cdot \underset{\sim}{E})\hat{\underset{\sim}{z}}, \qquad \underset{\sim}{E}_t = (\hat{\underset{\sim}{z}} \times \underset{\sim}{E}) \times \hat{\underset{\sim}{z}},$$

where $\hat{\underset{\sim}{z}}$ is a unit vector in the z direction, and similarly for components of $\underset{\sim}{B}$, we can show that the longitudinal and transverse components are related by [7]

$$\underset{\sim}{E}_t = \frac{1}{\gamma_n^2}\left[\underset{\sim}{\nabla}_t \left(\frac{\partial E_z}{\partial z}\right) - i\,\frac{\omega}{c}\,\hat{\underset{\sim}{z}} \times \underset{\sim}{\nabla}_t B_z\right], \tag{16a}$$

$$\underset{\sim}{B}_t = \frac{1}{\gamma_n^2}\left[\underset{\sim}{\nabla}_t \left(\frac{\partial B_z}{\partial z}\right) + i\,\frac{\omega}{c^2}\,\hat{\underset{\sim}{z}} \times \underset{\sim}{\nabla}_t E_z\right]. \tag{16b}$$

The boundary conditions on the mirrors will be taken as those for a perfect conductor, namely

$$\hat{\underset{\sim}{n}} \cdot \underset{\sim}{B} = 0\ , \tag{17a}$$

$$\hat{\underset{\sim}{n}} \times \underset{\sim}{E} = 0\ , \tag{17b}$$

where $\hat{\underset{\sim}{n}}$ is a unit vector normal to the surface of the mirrors.

If propagation is in the z direction parallel to the mirrors, the relation (17b) means the y- and z-components of $\underset{\sim}{E}$ vanish at the mirrors. Equation (17a) means that the x-component of $\underset{\sim}{B}$ vanishes at the mirrors.

The various normal modes obtained are of three types. First, there is a mode with $E_z = B_z = 0$, known as the TEM (Transverse Electric and Magnetic) mode, given by

$$\underset{\sim}{E}(x,y) = \hat{\underset{\sim}{x}}, \qquad \underset{\sim}{B}(x,y) = \hat{\underset{\sim}{y}}, \; k_z = k. \tag{18}$$

This is simply a part of a plane, plane-polarized wave. Second, there are modes obtained by setting $E_z = 0$, $B_z \neq 0$, known as TE (Transverse Electric) modes. Third, there are modes obtained by setting $B_z = 0$, $E_z \neq 0$, known as TM (Transverse Magnetic) modes.

The different TE eigenfunctions are found by assuming that

$$B_z = X(x)e^{i k_n z}, \tag{19}$$
$$E_z = 0.$$

The infinite extension of mirrors in the y direction implies the independence of B_z on y in this direction. The wave equation for B_z reduces to

$$\left(\frac{d^2}{dx^2} + \gamma_n^2\right) X(x) = 0. \tag{20}$$

The boundary condition to apply is that $E_y = 0$ at $x = \pm a$. From Eqs. (16a) and (19), we obtain

$$\frac{dX}{dx} = 0 \text{ at } x = \pm a. \tag{21}$$

The solutions of Eq. (20), subject to the boundary condition (21), are

$$X(x) \propto \begin{cases} \sin \gamma_n x, & n \text{ odd}; \\ \cos \gamma_n x, & n \text{ even}, \end{cases} \tag{22}$$

where $\gamma_n = n\pi/2a$. The eigenvalue k_n thus has the value

$$k_n = \left[k^2 - \left(\frac{n\pi}{2a}\right)^2\right]^{\frac{1}{2}}. \tag{23}$$

The complete expression for the $\underset{\sim}{E}$ field for the n-th TE mode, propagation in the $\hat{\underset{\sim}{z}}$ direction is

$$\underset{\sim}{E}_{TE(n)} = \begin{cases} \hat{\underset{\sim}{y}} \cos \gamma_n x \, e^{i k_n z}, & n \text{ odd}; \\ \hat{\underset{\sim}{y}} \sin \gamma_n(x) \, e^{i k_n z}, & n \text{ even}. \end{cases} \tag{24}$$

In similar fashion, the TM modes are found by assuming

$$\begin{aligned} E_z &= X(x) \, e^{i k_n z}, \\ B_z &= 0. \end{aligned} \tag{25}$$

Again, $X(x)$ in a solution of Eq. (20), and since E_z must vanish at the mirrors, we have

$$X(x) = 0 \quad \text{at } x = \pm 1.$$

Accordingly, we find

$$X(x) \propto \begin{cases} \cos \gamma_n x, & n \text{ odd}; \\ \sin \gamma_n x, & n \text{ even}, \end{cases} \tag{26}$$

where γ_n and k_n are the same as for the TE mode. The $\underset{\sim}{E}$ field corresponding to the n-th TM mode can be written

$$\underset{\sim}{E}_{TM(n)} \begin{cases} [\sin \gamma_n x \, \hat{\underset{\sim}{x}} + i \frac{\gamma_n}{k_n} \cos \gamma_n x \, \hat{z}] e^{i k_n z}, & n \text{ odd}; \\ [\cos \gamma_n x \, \hat{\underset{\sim}{x}} - c \quad \sin \gamma_n x \, \hat{z}] e^{i k_n z}, & n \text{ even}. \end{cases} \tag{27}$$

Note that the TEM mode can be considered as a special case of the TM mode with $n = 0$.

Also, attention is drawn to the fact that n cannot take a value larger than n_{max}, where

$$n_{max} = \frac{2t}{\lambda}.$$

Here t is the separation of mirrors and λ the wavelength of the light source. If this condition is violated, the eigenvalue k_n in Eq. (23) will be imaginary, $k_n = i\kappa_n$, and the z-dependence will be $e^{-\kappa_n z}$, which does not describe a propagating wave.

It is also instructive to consider the modes in cylindrical coordinates, for the case of azimuthal symmetry. Letting x be the axial, r the radial, and θ the azimuthal coordinate, we have cylindrical coordinates (r,θ,x). For fields independent of θ and bounded by mirrors at $x = \pm a$, we obtain the same modes as for rectangular coordinates with $e^{i k_n z}$ replaced by $H^+(k_n r)$, where H^+ is the Hänkel function for expanding waves [8]. In the region of large $k_n r$, the Hänkel function can be replaced by its asymptotic form, so that we can make the replacement

$$e^{i k_n z} \rightarrow \frac{e^{i k_n r}}{\sqrt{r}} \quad . \tag{28}$$

2. Coefficients of the Expansion in Modes for a Given Source

We consider a point source of unpolarized radiation of wave number k halfway between the mirrors and a distance z_0 out from their edges, as shown in Fig. 1. As explained in Chapter II, we treat unpolarized radiation by adding intensities for the two kinds of polarized light: light polarized parallel to, and perpendicular to, the mirrors. (In chapter II we referred to these polarizations as perpendicular to and parallel to the plane of incidence, respectively.)

Considering an infinitesimally thin wedge of rays of angle $d\theta$ traveling in the z direction, as shown in the radiation field for the parallel kind of polarization:

$$\underset{\sim}{E}_1(\underset{\sim}{r}) = \hat{\underset{\sim}{y}} \frac{e^{ikr}}{r} , \tag{29a}$$

For the other kind of polarization, we see from Fig.7b that

$$\underset{\sim}{E}_2(\underset{\sim}{r}) = [\hat{\underset{\sim}{x}} \frac{z_o+z}{r} - \hat{\underset{\sim}{z}} \frac{x}{r}] \frac{e^{ikr}}{r} . \tag{29b}$$

Note that $\underset{\sim}{E}_1(\underset{\sim}{r})$, having only a y-component, contributes only to TE modes, while $\underset{\sim}{E}_2(\underset{\sim}{r})$ contributes only to TEM and TM modes.

The evaluation of mode coefficients is performed by matching the fields (29a) and (29b) to linear combinations of modes at the boundary formed by the edges of the mirrors. Since both radiation fields and all modes involve propagation in the same sense across the boundary, we need only match the fields themselves, as their normal derivatives will then coincide.

Considering the wedge of Fig. 7a to be part of a cylindrically symmetric situation with negligible azimuthal variation, we match at a "surface" of length 2a in the x-direction, and infinitesimal width $dy = z_0 d\theta$ in the y-direction. The problem, as in the image method, is two dimensional and the variation of intensity in the y-direction is not considered. We express the expansions of source in terms of modes in the form

$$\underset{\sim}{E}_1(x) = \sum_{n=1} C_{TE(n)} \underset{\sim}{E}_{TE(n)}(x), \tag{30a}$$

$$\underset{\sim}{E}_2(x) = \sum_{n=1} C_{TM(n)} \underset{\sim}{E}_{TM(n)}(x), \tag{30b}$$

where $\underset{\sim}{E}_{TE(n)}(x)$ and $\underset{\sim}{E}_{TM(n)}(x)$ are given by Eqs. (24) and (28) with

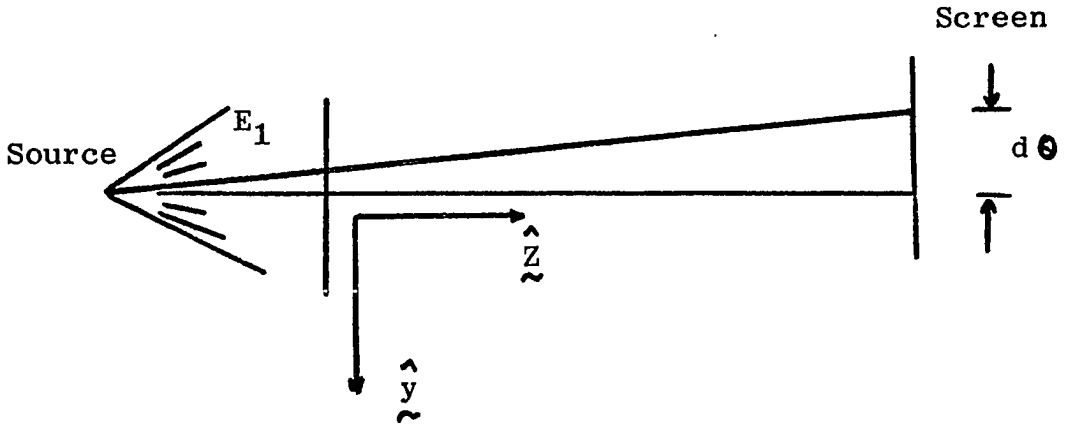

(a)

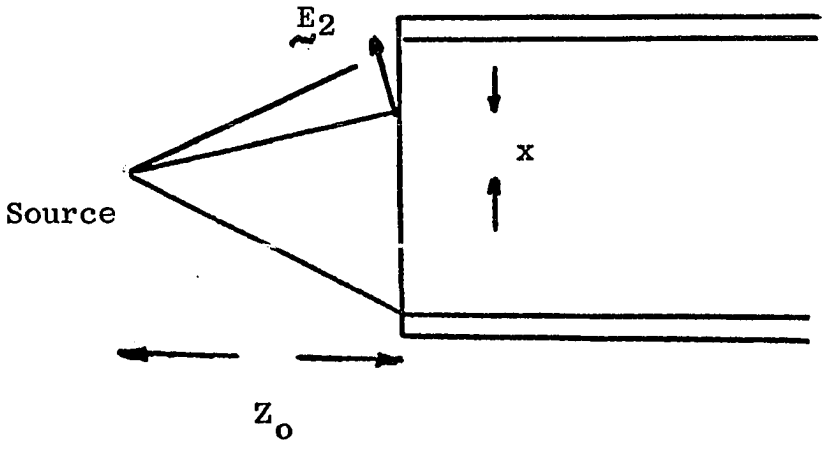

(b)

Fig. 7. Schematics for the mode method treatment of GIMBI (a) shows the thin wedge of rays treated, seen from above. (b) shows the direction of the $\underset{\sim}{E}$ vector for polarization of type $\underset{\sim}{E}2$ [Eq. (29b)].

$z = 0$. The coefficients $C_{TE(n)}$ and $C_{TM(n)}$ are found by single integrations:

$$C_{TE(n)} = \frac{1}{N_1(n)} \int_{-a}^{a} \underset{\sim}{E}^{*}_{TE(n)}(x) \cdot \underset{\sim}{E}_1(x)\,dx, \tag{31a}$$

$$C_{TM(n)} = \frac{1}{N_2(n)} \int_{-a}^{a} \underset{\sim}{E}^{*}_{TM(n)}(x) \cdot \underset{\sim}{E}_2(x)\,dx, \tag{31b}$$

where the normalization constants are defined by

$$N_1(n) = \int_{-a}^{a} |\underset{\sim}{E}_{TE(n)}(x)|^2 dx, \tag{32a}$$

$$N_2(n) = \int_{-a}^{a} |\underset{\sim}{E}_{TM(n)}(x)|^2 dx. \tag{32b}$$

For the TE modes, the normalization is especially simple:

$$N_1(n) = a. \tag{33}$$

3. Propagation of Modes and Intensity of the Interference Pattern

Having determined the coefficients of the expansions (31a) and (31b), the next step in obtaining the interference pattern is to evaluate the radiation fields at the screen. Considering Eq. (28) we write

$$\underset{\sim}{E}_1(x,z_1) = \sqrt{\frac{z_o}{z_1+z_o}} \sum_{n=1} C_{TE(n)}\, \underset{\sim}{E}_{TE(n)}(x)\, e^{i k_n z_1}, \tag{34a}$$

$$\underset{\sim}{E}_2(x,z_1) = \sqrt{\frac{z_o}{z_1+z_o}} \sum_{n=1} C_{TM(n)}\, \underset{\sim}{E}_{TM(n)}(x)\, e^{i k_n z_1}. \tag{34b}$$

The intensity $I(x)$ is then given by the sum of the intensities for the two kinds of polarization:

$$I(x) \propto |\underset{\sim}{E}_1(x,z)|^2 + |\underset{\sim}{E}_2(x,z)|^2. \tag{35}$$

Actually, there is absorption of energy in the transmission of various modes through the space between the mirrors. This phenomenon, related to the reflectivity loss mentioned in the previous chapter, is also discussed in the Appendix. For reasonable geometries, frequencies, and mirror materials, the TM modes are so much diminished that we can safely ignore their contribution to the interference pattern. This can be demonstrated experimentally by allowing only light plane-polarized perpendicular to the mirrors to enter the device, whereupon a negligible amount of light reaches the screen.

For our calculations, we assumed that the TE modes propagated without losses, just as we assumed that there was perfect reflectivity in the image method for light plane-polarized parallel to the mirrors. Actually, one should multiply the n-th term of Eq. (34) by the factor $e^{-\kappa_n z}$, where κ_n is nearly linear in n, as shown in the Appendix. Since the n-th mode corresponds roughly to light reflecting back and forth in a ray inclined at an angle α_n to the planes of the mirrors, where $\tan \alpha_n = \gamma_n / k_n$, the dependence of the mode calculation on losses should be nearly the same as for the image method.

The details of the computer calculations are given in Chapter IV, along with results and conclusions.

CHAPTER IV

CALCULATIONS, RESULTS, AND CONCLUSIONS

Calculations using the image method were performed by a computer program which essentially involves substitution in Eq. (6). Calculations were made only for light polarized parallel to the mirrors, as reflectivity is very low for the other kind of polarization. We considered only the case of perfectly reflecting mirrors, with $r_{\perp} = 1$. The calculations are exact, in that no approximations other than machine round-off (which is negligible) are involved.

Calculations for the mode method were performed for the analogous case: light polarized parallel to the mirrors (which involved only TE modes); and perfect transmission of TE modes. Unlike the image-method calculations, the mode-method calculations involve important approximations. First, in the evaluation of the integrals of Eq. (31a) to determine the coefficients $C_{TE(n)}$, we used numerical integration (Simpson's rule) to approximate the integrals. Second, it is necessary to terminate the sum over modes in Eq. (34a). A discussion of the significance of these approximations is presented in the following section.

The various parameters which may be varied are as follows: z_0, fidysnvr gtom doutvr yo mittotd; 2a, separation of mirrors; $z_0 + z_1$, distance from source to screen; and λ, wavelength of the radiation. The first three parameters are defined in Fig. 1. It should be noted that, if all four parameters are changed by the same factor, the resulting interference patterns are simply expanded by the same factor.

1. Details of Mode-Method Calculation

The integral of Eq. (31a) has the form

$$C_{TE(n)} = \frac{1}{a}\int_{-a}^{a} \frac{\exp ik(z_o+x^2)^{\frac{1}{2}}}{(z_o^2+x^2)^{\frac{1}{2}}} \begin{Bmatrix} \cos \frac{n\pi x}{2a} \\ \sin \frac{n\pi x}{2a} \end{Bmatrix} dx \begin{matrix} n \text{ odd} \\ n \text{ even} \end{matrix} . \qquad (36)$$

Note that this is a type of Fourier series expansion, relating to the Fourier sine series. Since the first factor of the integrand is an even function of x, and since the interval $-a \leq x \leq a$ is symmetric, integrals for even n vanish, and we obtain

$$C_{TE(n)} = \begin{cases} \frac{2}{a}\int_{-a}^{a} \frac{\exp ik(z_o^2+x^2)^{\frac{1}{2}}}{(z_o^2+x^2)^{\frac{1}{2}}} \cos \frac{n\pi x}{2a}\, dx, & n \text{ odd}; \\ 0, & n \text{ even}. \end{cases} \qquad (37)$$

We evaluated the above integrals using Simpson's rule [9], which involves dividing the interval $0 \leq x \leq a$ into an even number 2N of cells, of width n = a/2N. With this method, the integral

$$I = \int_{o}^{a} f(x)dx$$

is approximated by the sum

$$I \approx \frac{h}{3}\left[f(o)+4\sum_{n=1}^{N}[(2n-1)h] + 2\sum_{n=1}^{N-1} f(2nh)+f(a)\right]. \qquad (38)$$

This method is equivalent to fitting the integrand f(x) by a quadratic polynomial over two adjacent cells. For an oscillatory integrand such as that of Eq. (37), one must have several cells for each cycle of the oscillation. Thus, the number of cells required depends on the various parameters. Since for $x^2 << z_0^2$ the factor expik $(z_0^2+x^2)^{\frac{1}{2}}$ is approximately given by

$$\text{expik}(z_0^2+x^2)^{\frac{1}{2}} \approx \text{expik } z_0 \text{ expik } \frac{x^2}{2z_0} \quad , \tag{39}$$

As a function of x, this has a decreasing cycle length with increasing x. Thus, the shortest cycle will be at x=a. The approximate length of this last cycle can be estimated as follows:

Choose Δx so that varying x from $a-\Delta x$ to $a+\Delta x$ changes the argument of exp $(ik \frac{x^2}{2z_0})$ by 2π:

$$\frac{k}{2z_0} \left| (a+\Delta x)^2 - (a-\Delta x)^2 \right| = 2\pi,$$

$$2\Delta x = \frac{\lambda z_0}{a} = \text{length of last cycle.}$$

This is a fraction $\lambda z_0/a^2$ of the interval $0 \leq x \leq a$.

f we want at least four cells in this last cycle, we must have

$$2N > \frac{4a^2}{\lambda z_0} .$$

The factor cos $\gamma_n x$ also affects the number of cells needed. Since this function has $\frac{1}{2}n$ cycles in the interval, we again multiply by four and obtain

$$2N(n) > 4\left|\frac{a^2}{\lambda z_0} + \tfrac{1}{2}n\right|$$

as a rough guess as to the number of cells needed. Table I shows values of $|C_{TE(n)}|$ calculated with varying numbers of Simpson's rule cells for a case with $4a^2/\lambda z_o = 5$.

Noting that the absolute values of the coefficients are monotone decreasing functions of n (see table I) we used the rule-of-thumb that a series can be terminated when the absolute value of a coefficient was less than 1/10 that of the leading coefficient. For the cases of columns 1 and 2 in Table II, Figs. 8a and 8b show how well the terminated Fourier series fits the real part of $\frac{1}{r} e^{ikr}$. In general, we would expect the accuracy of the fit at z_o+z_1, at the screen to be about the same as at z=0, since only the relative phase of the "Fourier coefficients" $C_{TE(n)} e^{ik_n z}$ will vary.

We can also use the Bessel inquality [10] to determine the accuracy of our Fourier expansion. To be explicit, at the matching boundary we are attempting to fit

$$\sum C_{TE(n)} \cos \gamma_n x = \frac{e^{ikr}}{r} , \qquad (40)$$

where $r = [x^2+z_o^2]^{\frac{1}{2}}$. For this case, the Bessel inequality has the form

$$\int_0^a \left| \frac{e^{ikr}}{r} \right|^2 dx \geq \frac{2}{a} \sum \left| C_{TE(n)} \right|^2 . \qquad (41)$$

If the series is terminated, the difference in the two sides of Eq. (41) is the mean square error. Integrating the left-hand-side, we obtain

TABLE I. Effect Of Using Various Numbers Of Cells On The Simpson's Rule Calculation) $|C_{TE(n)}|$.

NO.0f cells	6	12	18	24	30	36
n = 1	.18809469	.18812759	.18812923	.18812951	.18812958	.18812961
3	.16092597	.16090766	.16090703	.16090694	.16090691	.16090690
5	.09930241	.09909094	.09908170	.09908020	.09907980	.09907965
7	.05953936	.05906599	.05904661	.05904350	.05904267	.05904237
9	.04000368	.03911407	.03908122	.03907603	.03907464	.03907415
11	.03050786	.02888261	.02883039	.02882228	.02882013	.02881937
13	.02598270	.02298847	.02290869	.02289658	.02289338	.02289225
15	.02491707	.01920731	.01908914	.01907163	.01906705	.01906544
17	.02801662	.01658904	.01641833	.01639377	.01638740	.01638516
19	.03770294	.01468210	.01444029	.01440663	.01439800	.01439498
21	.05376421	.01325236	.01291500	.01286984	.01285839	.01285441
23	.06162733	.01216804	.01170240	.01164284	.01162792	.01162277

Table I. Continued.

No. of Cells	42	48	54	60	66	72
n = 1	.18812962	.18812963	.18812963	.18812963	.18812963	.18812963
3	.16090690	.16090690	.16090690	.16090690	.16090690	.16090690
5	.09907959	.09907956	.09907954	.09907953	.09907953	.09907953
7	.05904224	.05904218	.05904214	.05904212	.05904211	.05904211
9	.03907394	.03907383	.03907378	.03907375	.03907373	.03907372
11	.02881904	.02881888	.02881880	.02881875	.02881872	.02881870
13	.02289177	.02289154	.02289142	.02289135	.02289131	.02289128
15	.01906476	.01906443	.01906425	.01906415	.01906409	.01906405
17	.01638422	.01638377	.01638353	.01638339	.01638331	.01638326
19	.01439371	.01439310	.01439278	.01439259	.01439248	.01439241
21	.01285274	.01285193	.01285151	.01285127	.01285112	.01285103
23	.01162061	.01161957	.01161903	.01161872	.01161853	.01161841

Table II. Values of $|C_{TE(n)}|$ for Several Sets of Parameters

	$\frac{a}{2} \times |C_{TE(n)}| \times 100$		
Parameter Set	1	2	3
z_o (mm)	5	5	5
t (mm)	0.1	0.1	0.1
λ (Å)	2000	4000	3990
n			
1	.3114	.4703	.4697
3	.3224	.4023	.4025
5	.3468	.2477	.2482
7	.2908	.1476	.1480
9	.2066	.0976	.0978
11	.1395	.0720	.0721
13	.0968	.0572	.0572
15	.0713	.0477	.0477
17	.0558	.0410	.0410
19	.0458	.0360	.0360
21	.0390	.0321	.0321
23	.0340	.0290	.0291

Fig. 8. Graphical Comparisons of the function $\frac{e^{ikr}}{r}$ and its Fourier expansion (real parts only) for two sets of parameters. Parameters are given in Table II, column 2 (for Fig. 8a) and column 1 (for Fig. 8b). Asterisks are points of the function and dots of the expansion. Where both coincide, a dot is used.

OPTICS AND MODES AT MATCHING BOUNDARY

MIRR.SEP.	SOURCE LOC.	WAVELENGTH	SCREEN LOC.	POINTS	CELLMODES
0.10	5.00	4000.00	170.00	40.00	150.00

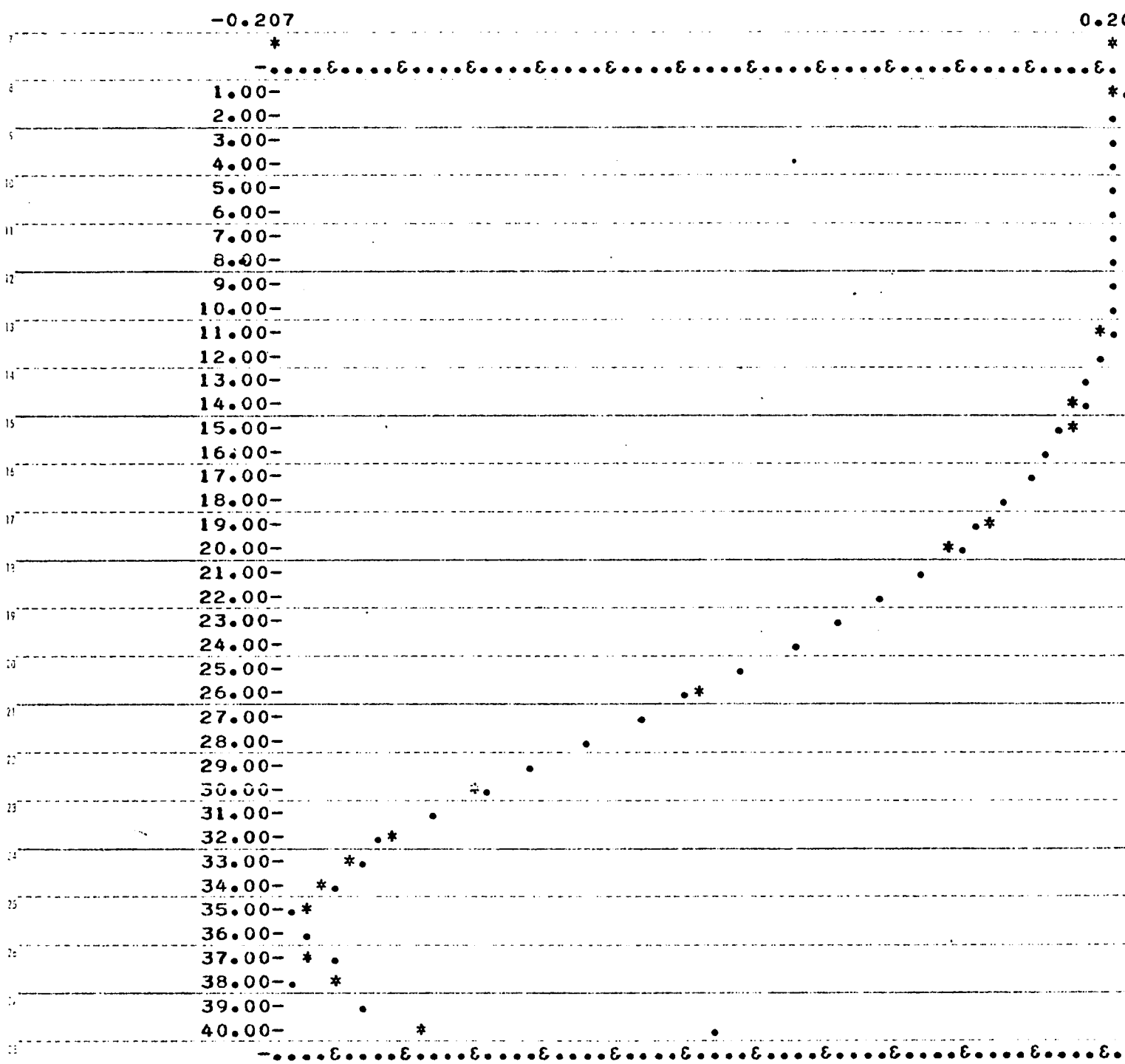

THE SCALING FACTOR IS... 0.00681

Fig. 8a

OPTICS AND MODES AT MATCHING BOUNDARY

MIRR.SEP.	SOURCE LOC.	WAVELENGTH	SCREEN LOC.	POINTS	CELLMODES
0.10	5.00	2000.00	170.00	40.00	215.00

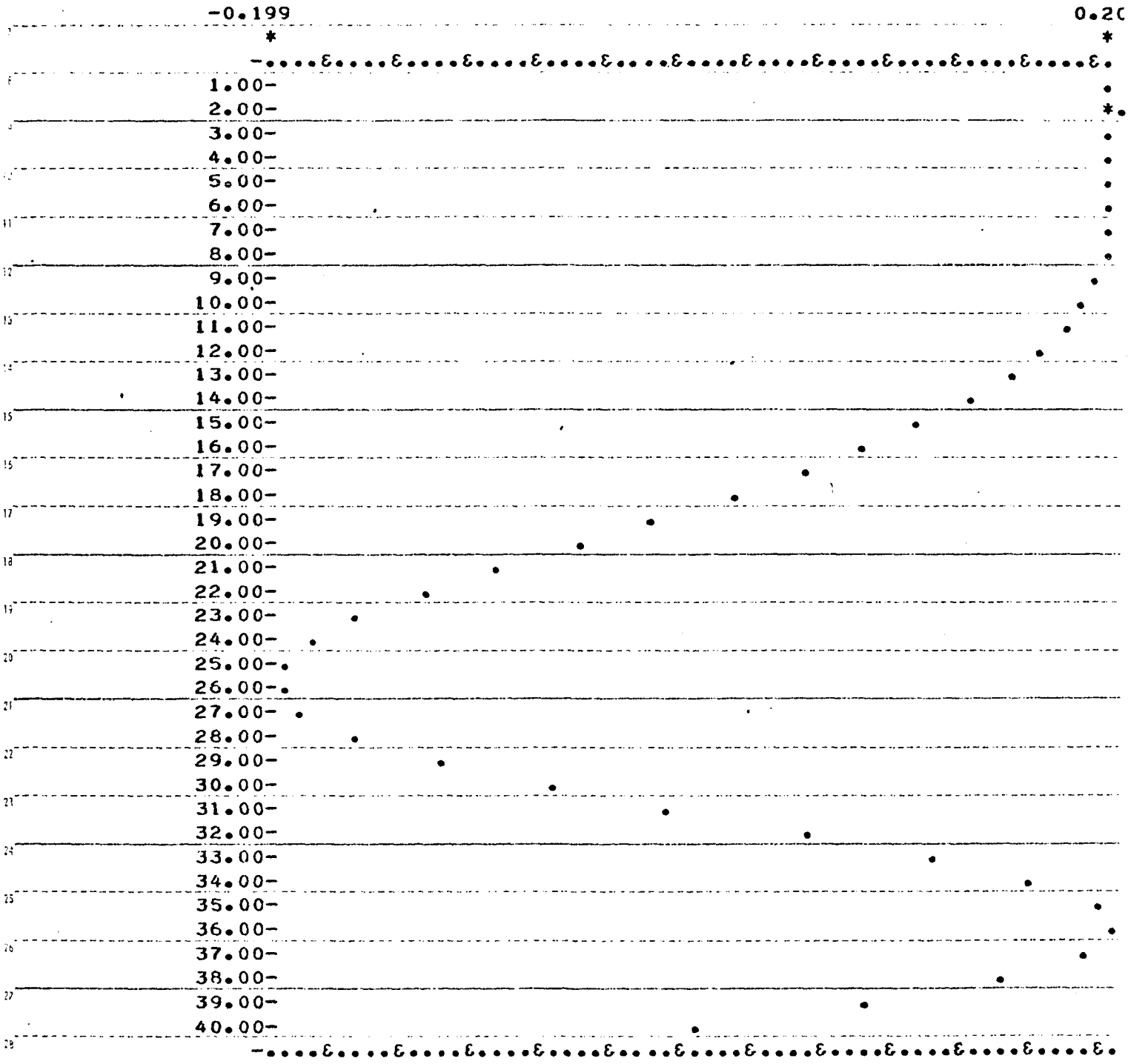

THE SCALING FACTOR IS... 0.00665

Fig. 8b

$$\int_0^a \left|\left(\frac{e^{ikr}}{r}\right)\right|^2 dx = \int_0^a \frac{1}{z_o^2+x^2}\, dx = 1/z_0 \tan^{-1}\frac{a}{z_o}$$

which, for the data of Table II column 2 , is 2×10^{-3}. For the same data, values of $\sum_{n=1}^{N} | C_{TE(n)} |^2$ are plotted in Table III for various values of N.

2. Results. They consist of various computer outputs of two types: one obtained from the image method, and the other from the mode method.

The output gives a plot of the intensity along the x-axis on the screen. The data is printed on the top of the plots, where lengths are in millimeters. The intensity is a function of the separation of the mirrors, the wavelength of the source, its location and the screen distance. The outputs are grouped to show the influence of above parameters. From Table IV, one can easily find the intensity plot correspond to a specified data. In each group of the outputs one parameter varies while the others remain unchanged. We have considered the variation of screen distance, in this regard large and small variation of this dimension is considered. Two central wavelength 2000 Å and 4000Å areconsidered, the variation of wavelength around these central wavelength have been worked out. The separation of the mirrors was taken to be .1 mm, which is unusually small. The reason for this choise is the restraint concerning computer time, involving the modes method. For example, it takes 15 minutes to process one set of data with the above separation of

TABLE III. Accuracy of Truncated Fourier Series, Using Bessel's Inequality [Eq. (41)]. With increasing n, the quantity $\frac{a}{2} \sum_{i=1}^{n} \left|C_{TE(i)}\right|^2$ should approach 2×10^{-3}. Data taken from Table II, column 2.

n	$\left\|C_{TE(n)}\right\|$	$\frac{a}{2} \sum_{i=1}^{n} \left\|C_{TE(n)}\right\|^2$
1	.18812963	.00088482
3	.16090690	.00153209
5	.09907952	.00177751
7	.05904210	.00186466
9	.03907371	.00190283
11	.02881869	.00192359
13	.02289126	.00193669
15	.01906403	.00194578
17	.01638322	.00195249
19	.01439236	.00195767
21	.01285097	.00196180
23	.01161833	.00196517

TABLE IV. Parameters Used in Calculating Figures.9-27

Fig. No.	t mm.	z_o mm.	λ A°	z_1 mm.	Fig. No.	t mm.	z_o mm.	λ A°	z_1 mm.
9a, b	·1	5	2000	150	19a, b	·1	5	4000	150
10a, b	·1	5	2000	170	20a, b	·1	5	4000	169
11a, b	·1	5	2000	169	21a, b	·1	5	4000	200
12a, b	·1	5	2000	200	22a, b	·1	5	4005	170
13a, b	·1	5	2005	170	23a, b	·1	5	4010	170
14a, b	·1	5	2010	170	24a, b	·1	5	3995	170
15a, b	·1	5	1990	170	25a, b	·1	5	3990	170
16a, b	·1	5	1995	170	26a, b	·1	4	4000	170
17a, b	·1	4	2000	170	27	·5	5	4000	170
18	·5	5	2000	170					

Figs. 9-27. Plots of Intensity as a function of distance from the center of the screen for the GIMBI interferometer. Graphs were calculated using the image method (Figs. 9a-17a, 18, 19a-26a, 27) and the mode method (Figs. 9b-17b, 19b-26b), using sets of parameters listed in Table IV.

SOLUTION BY IMAGE METHOD

FOLLOWINGS ARE MIRR.SEP.,SOURCE LOC.,WAVELENGTH AND SCREEN LOC.

0.100 5.000 2000.000 155.000 40.000 15.000 14.000

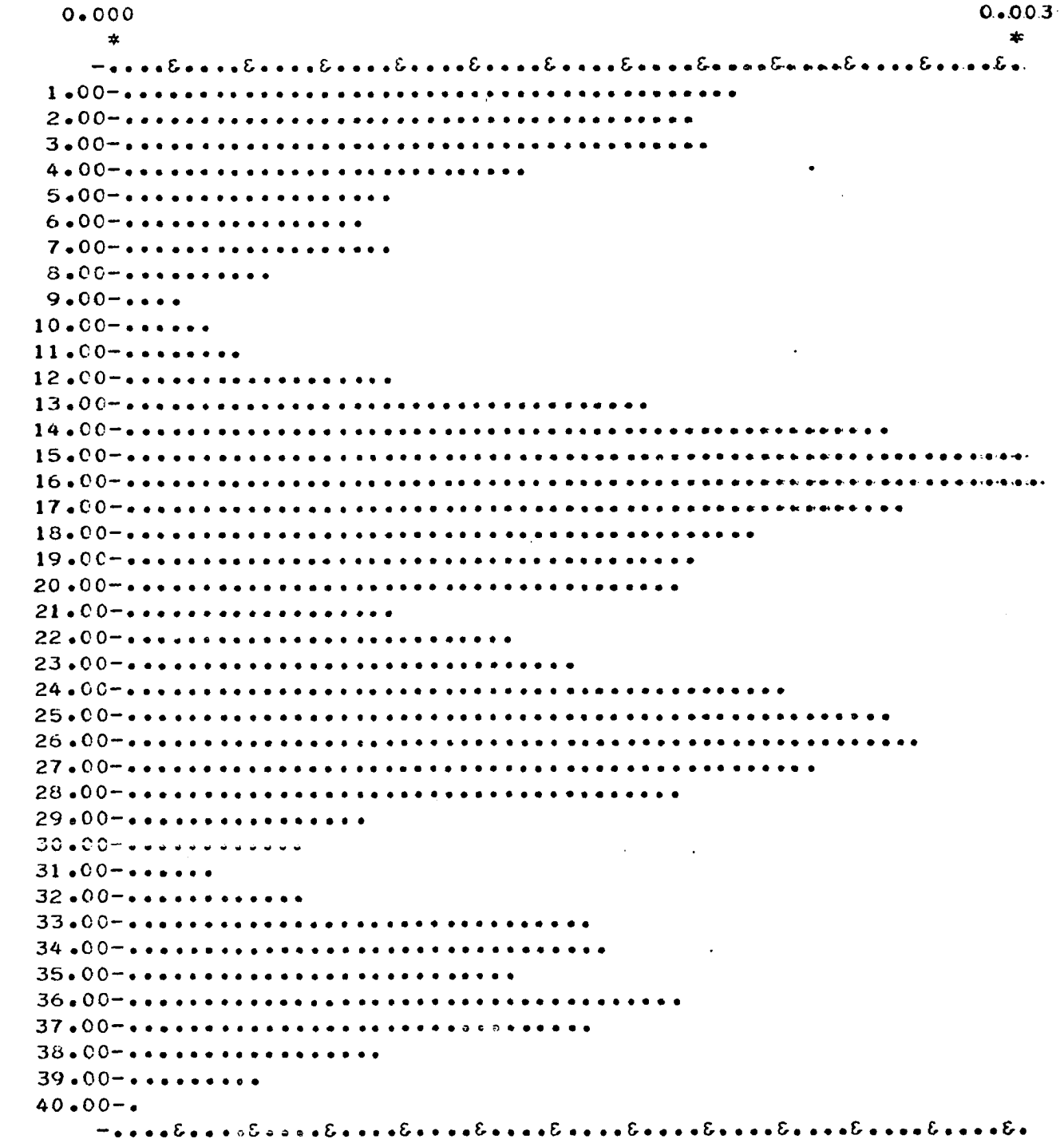

THE SCALING FACTOR IS... 0.00005

Fig. 9a

NUMBER OF RAYS CONTRIBUTE TO THE INTENSITY ARE NN# 30& 14& 15&1

```
      SCLUTICN     BY     MCDE     METHCC


FCLLCWINGS ARE MIRR.SEP.,SOURCE LCC.,WAVELENGTH AND SCREEN LOC.,NC.CELL AND NC.
    0.100      5.000  2000.000   150.000    40.000   250.000    24.000


    C.000                                                          C.003
      *                                                              *
       -....&....&....&....&....&....&....&....&....&....&....&....&....&.
    1.00-.....................................
    2.CC-.....................................
    3.CC-.....................................
    4.00-.....................................
    5.CC-.....................
    6.CC-.....
    7.00-.....
    8.CC-.....
    9.00-.....
   10.00-.....
   11.CC-.....
   12.00-.....
   13.CC-.....
   14.CC-.....
   15.00-.....
   16.00-.....
   17.CC-.....
   18.00-.....
   19.CC-.....
   20.CC-.....
   21.CC-.....
   22.CC-.....
   23.00-.....
   24.CC-.....
   25.CC-.....
   26.00-.....
   27.CC-.....
   28.CC-.....
   29.00-.....
   30.CC-.....
   31.CC-.....
   32.00-.....
   33.CC-.....
   34.CC-.....
   35.CC-.....
   36.CC-.....
   37.CC-.....
   38.00-.....
   39.CC-.....
   40.00-.
       -....&....&....&....&....&....&....&....&....&....&....&....&....&.


THE SCALING FACTCR IS... 0.00005
```

Fig. 9b

SOLUTION BY IMAGE METHOD

FOLLOWINGS ARE MIRR.SEP.,SOURCE LOC.,WAVELENGTH AND SCREEN LOC.

0.100 5.000 2000.000 175.000 40.000 17.000 16.000

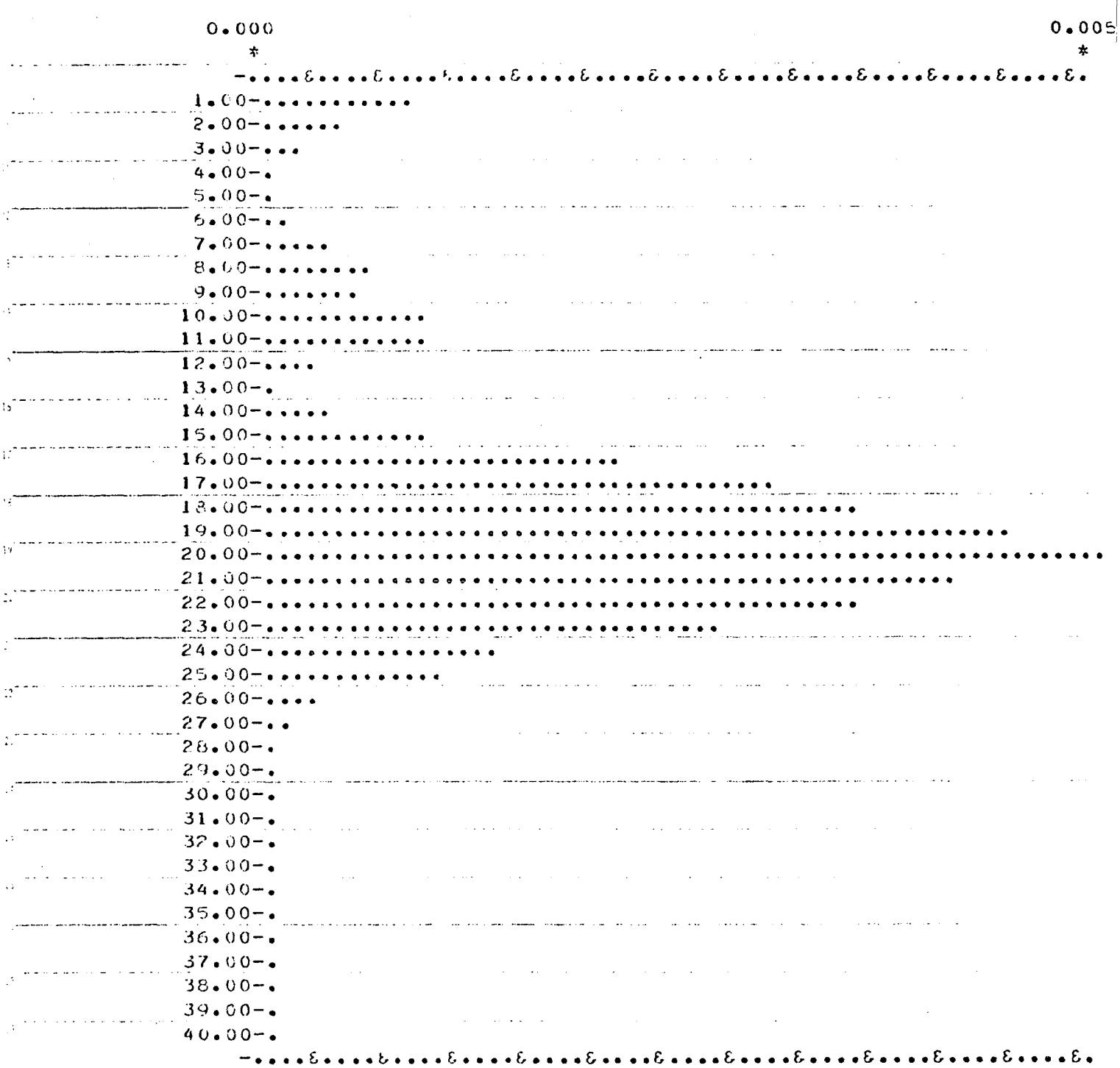

Fig. 10a

SCLUTION BY MODE METHOD

FOLLOWINGS ARE MIRR.SEP..SOURCE LOC..WAVELENGTH AND SCREEN LOC..NO.CE
0.100 5.000 2000.000 170.000 40.000 250.000 24.000

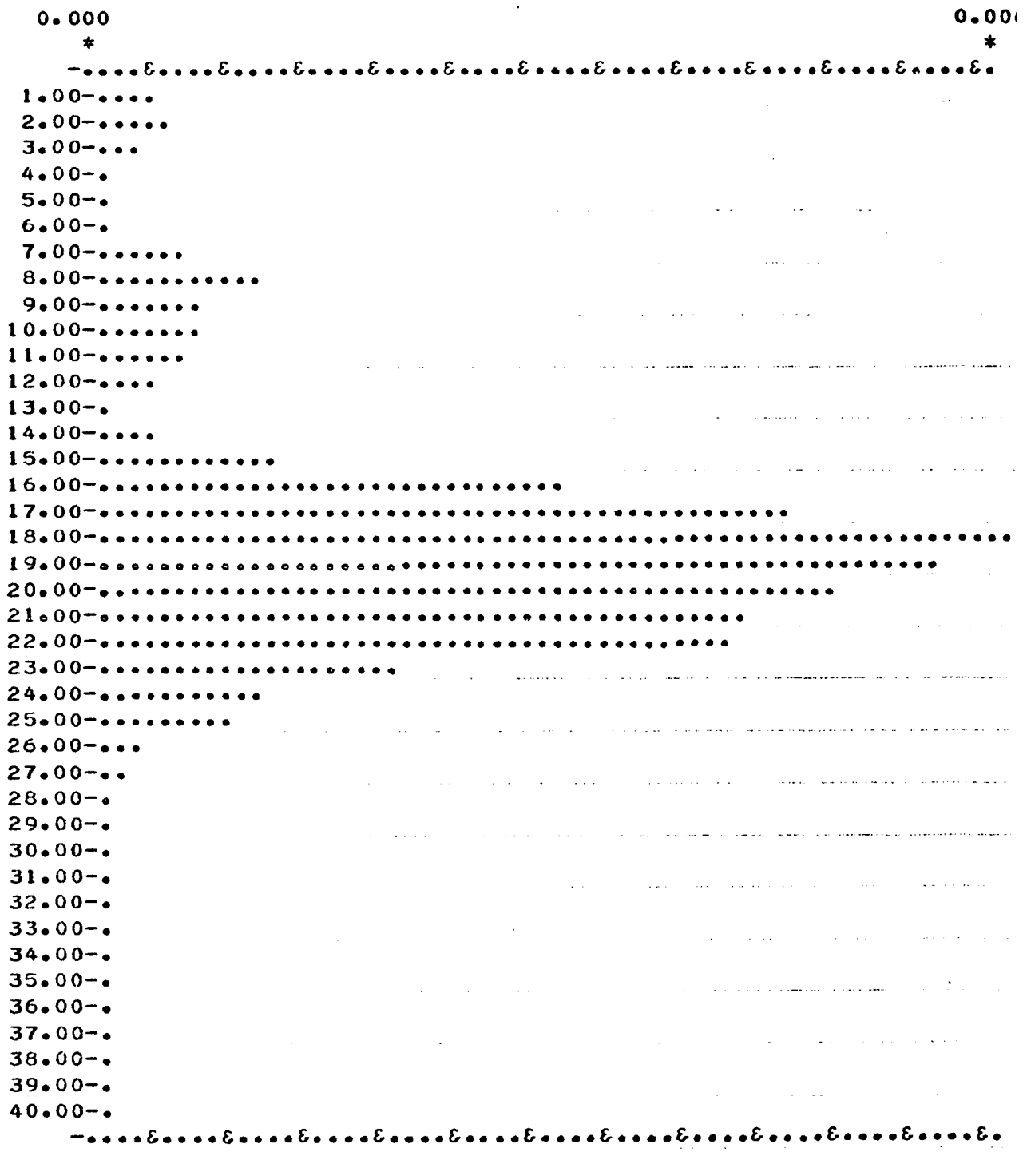

Fig. 10b

SCLUTICN BY MCDE METHCC

FCLLCWINGS ARE MIRR.SEP.,SCURCE LCC.,WAVELENGTH AND SCREEN LOC.,NC.CELL AND NC.
C.100 5.0C0 2000.CCC 165.0C0 40.000 250.000 24.000

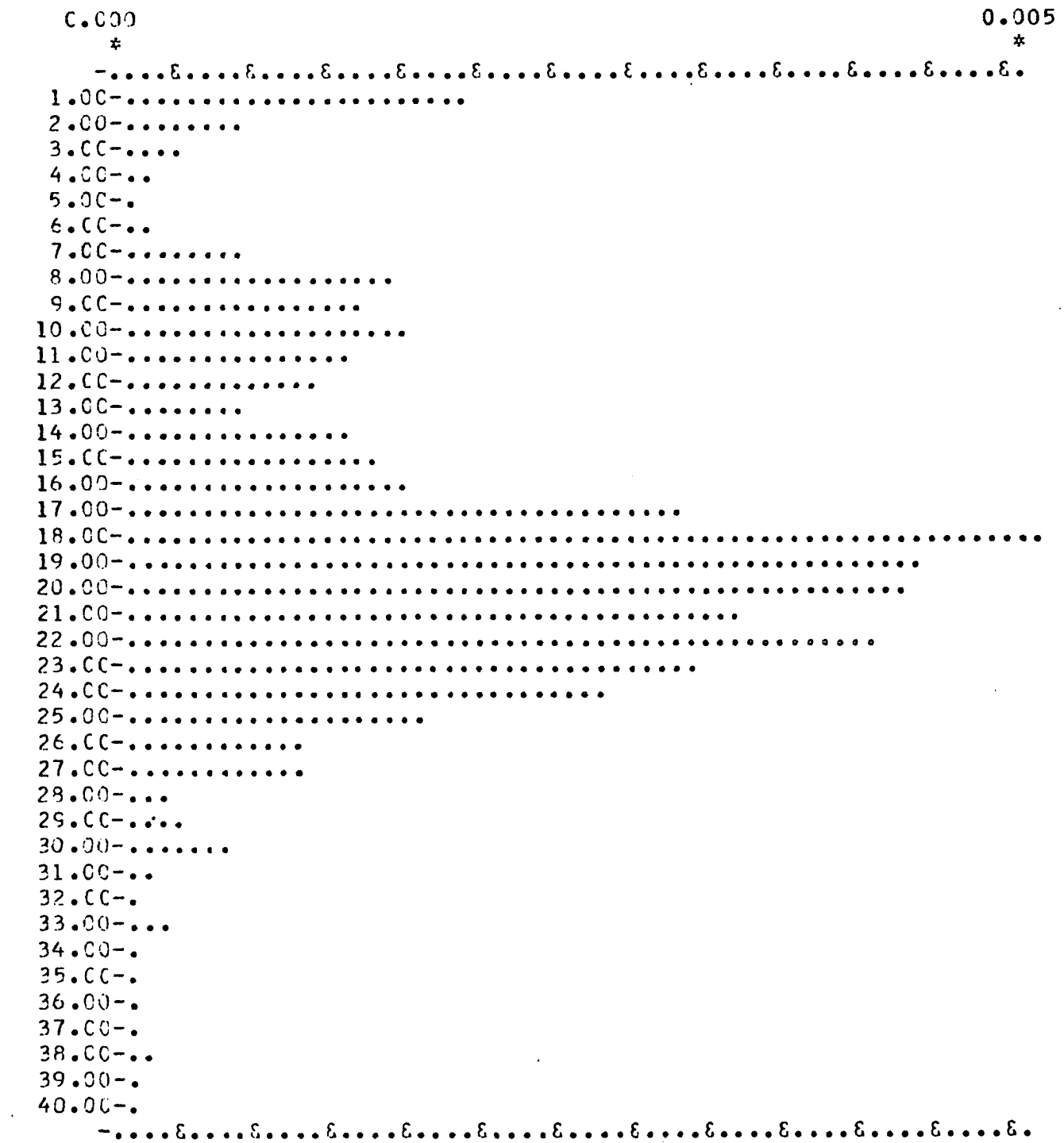

THE SCALING FACTOR IS... C.COCC8

Fig. 11a

SOLUTION BY IMAGE METHOD

FOLLOWINGS ARE MIRR.SEP.,SOURCE LOC.,WAVELENGTH AND SCREEN LOC.
0.100 5.000 2000.000 174.000 40.000 17.000 16.000

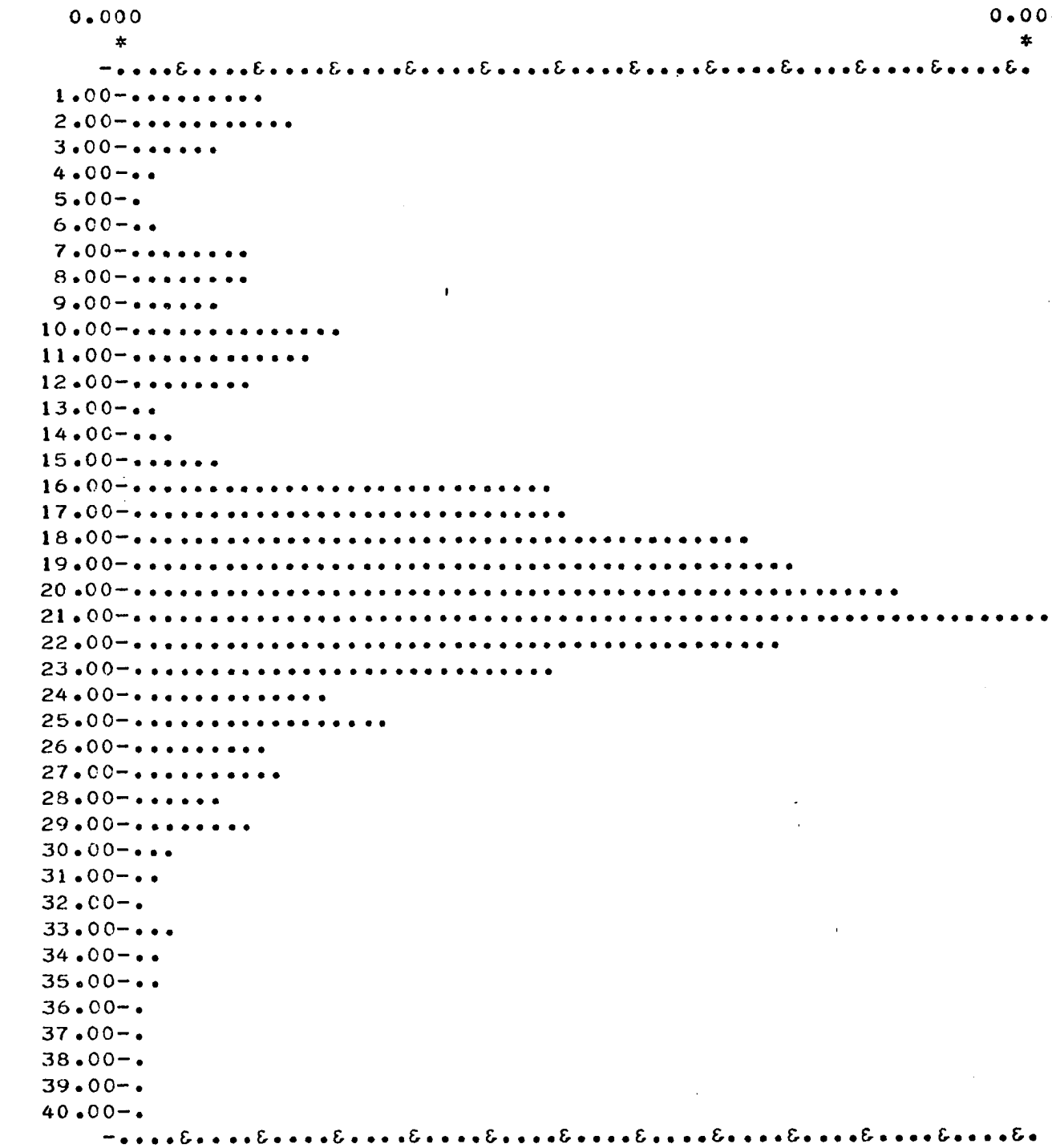

THE SCALING FACTOR IS... 0.00010

Fig. 11b

NUMBER OF RAYS CONTRIBUTE TO THE INTENSITY ARE NN# 34& 16& 17&1

SOLUTION BY IMAGE METHOD

FOLLOWINGS ARE MIRR.SEP.,SOURCE LOC.,WAVELENGTH AND SCREEN LOC.
0.100 5.000 2000.000 205.000 40.000 20.000 19.000

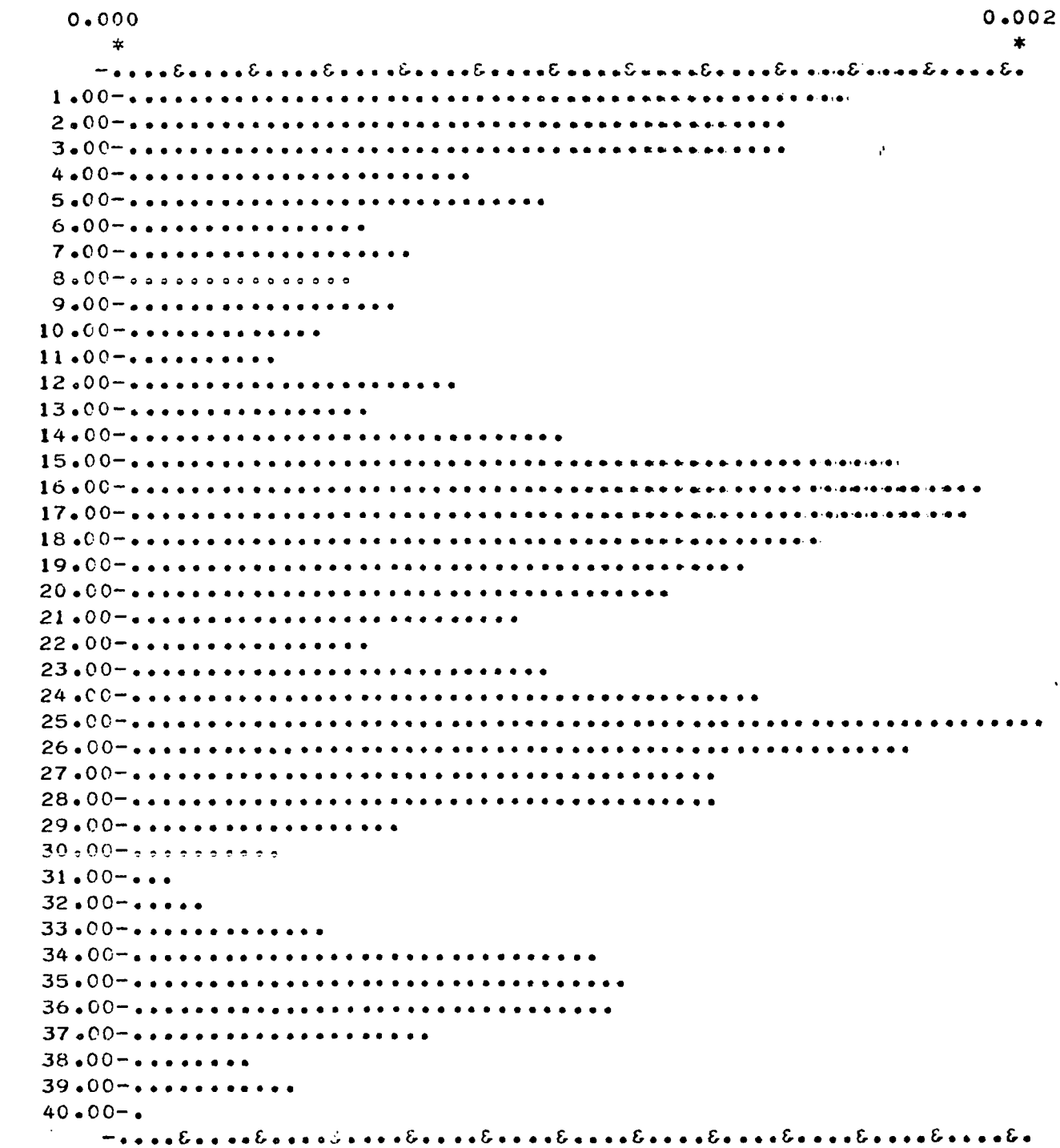

THE SCALING FACTOR IS... 0.00004

Fig. 12a

NUMBER OF RAYS CONTRIBUTE TO THE INTENSITY ARE NN# 40& 19& 20&1

SOLUTION BY MODE METHOD

FOLLOWINGS ARE MIRR.SEP.,SOURCE LOC.,WAVELENGTH AND SCREEN LOC.,NO.CELL AND NO.
0.100 5.000 2000.000 200.000 40.000 250.000 24.000

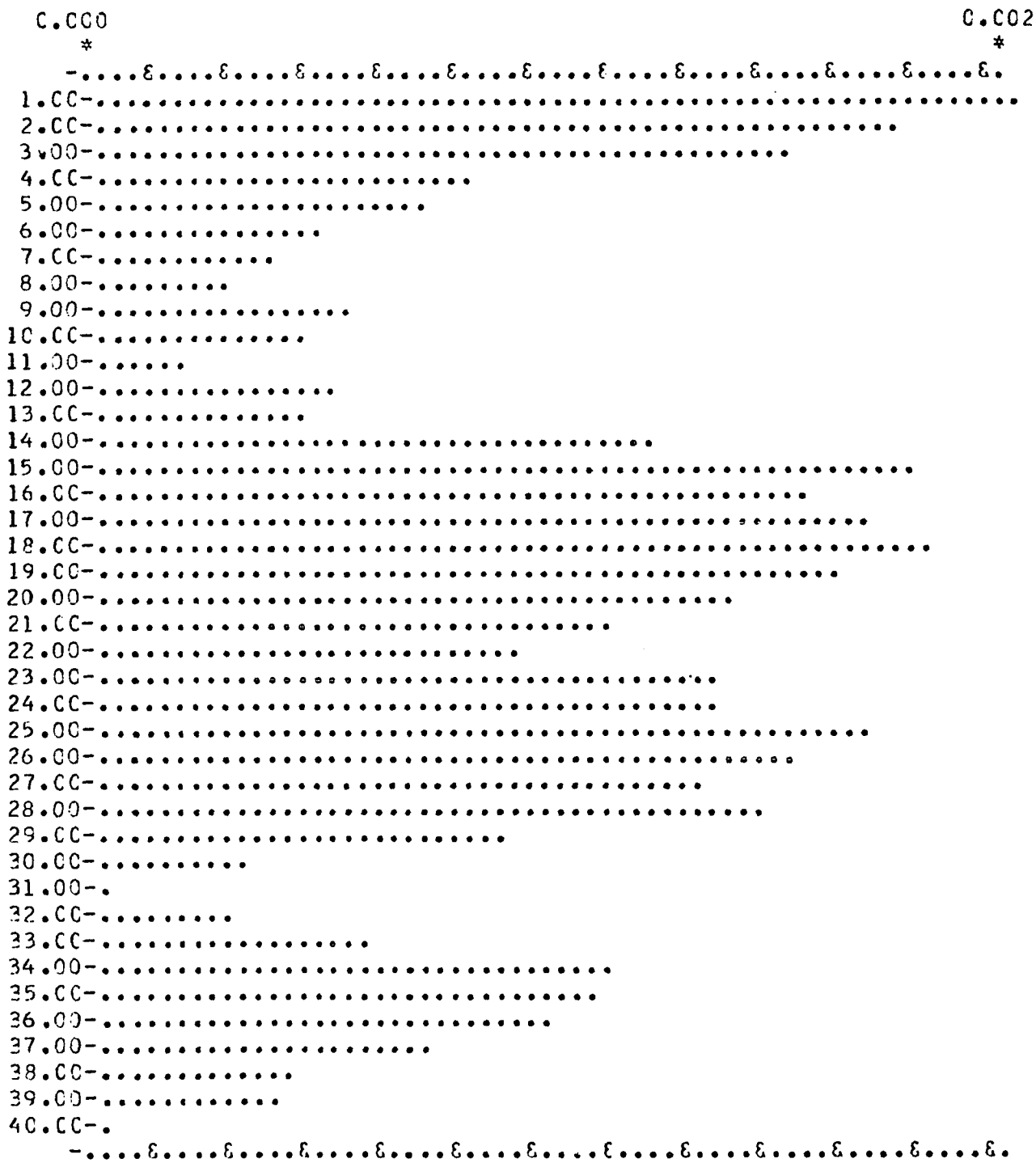

THE SCALING FACTOR IS... 0.00004

Fig. 12b

SOLUTION BY IMAGE METHOD

FOLLOWINGS ARE MIRR.SEP..SOURCE LOC..WAVELENGTH AND SCREEN LOC.

0.100 5.000 2005.000 175.000 40.000 17.000 16.000

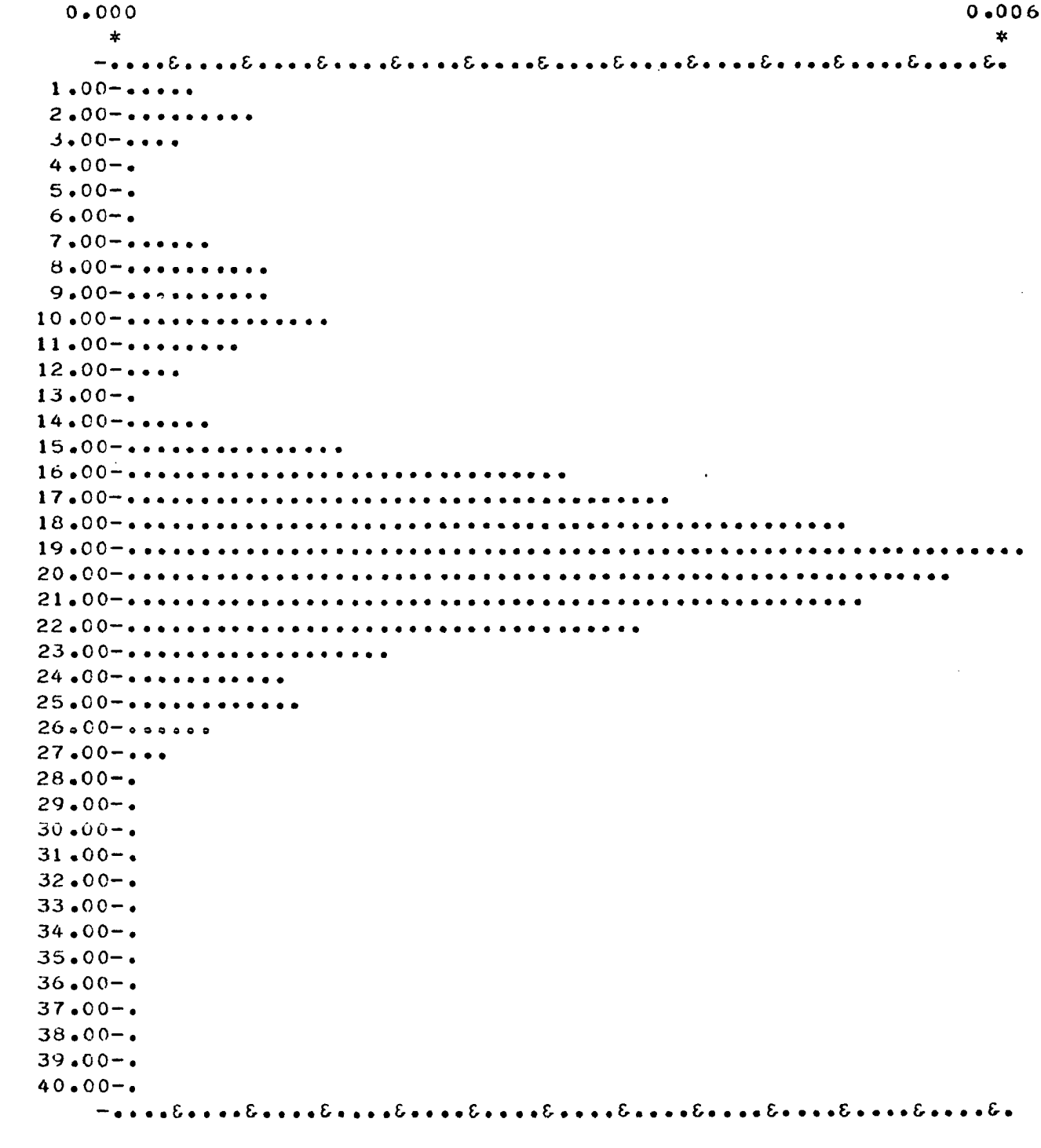

Fig. 13a

THE SCALING FACTOR IS... 0.00010

NUMBER OF RAYS CONTRIBUTE TO THE INTENSITY ARE NN# 34& 16& 17&1

SCLUTICN BY MCDE METHCC

FCLLCWINGS ARE MIRR.SEP.,SCURCE LCC.,WAVELENGTH AND SCREEN LOC.,NC.CELL AND NC.
C.100 5.000 2305.000 170.000 40.000 250.000 24.000

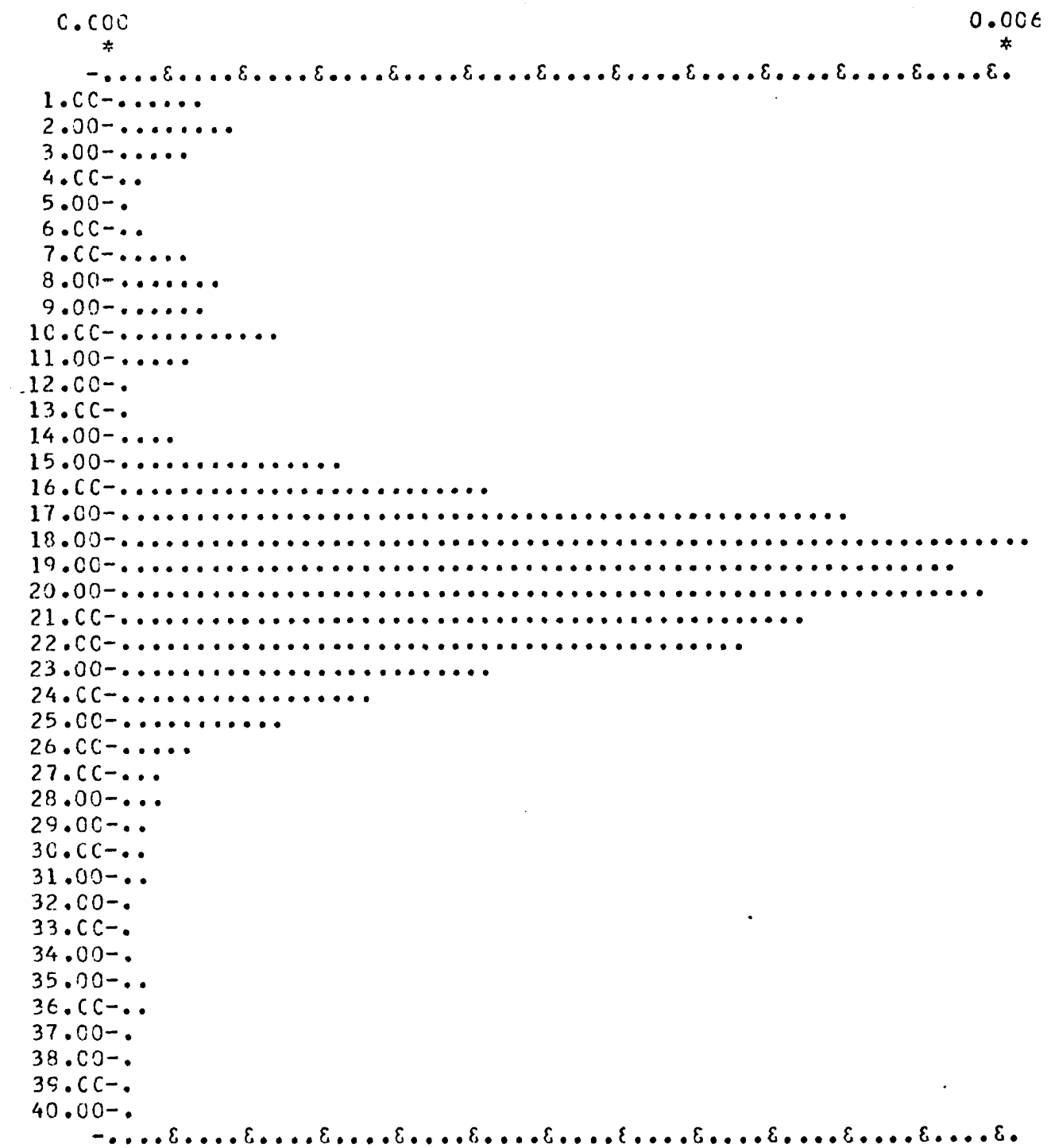

Fig. 13b

THE SCALING FACTCR IS... C.00009

SOLUTION BY IMAGE METHOD

FOLLOWINGS ARE MIRR.SEP.,SOURCE LOC.,WAVELENGTH AND SCREEN LOC.
0.100 5.000 2010.000 175.000 40.000 17.000 16.000

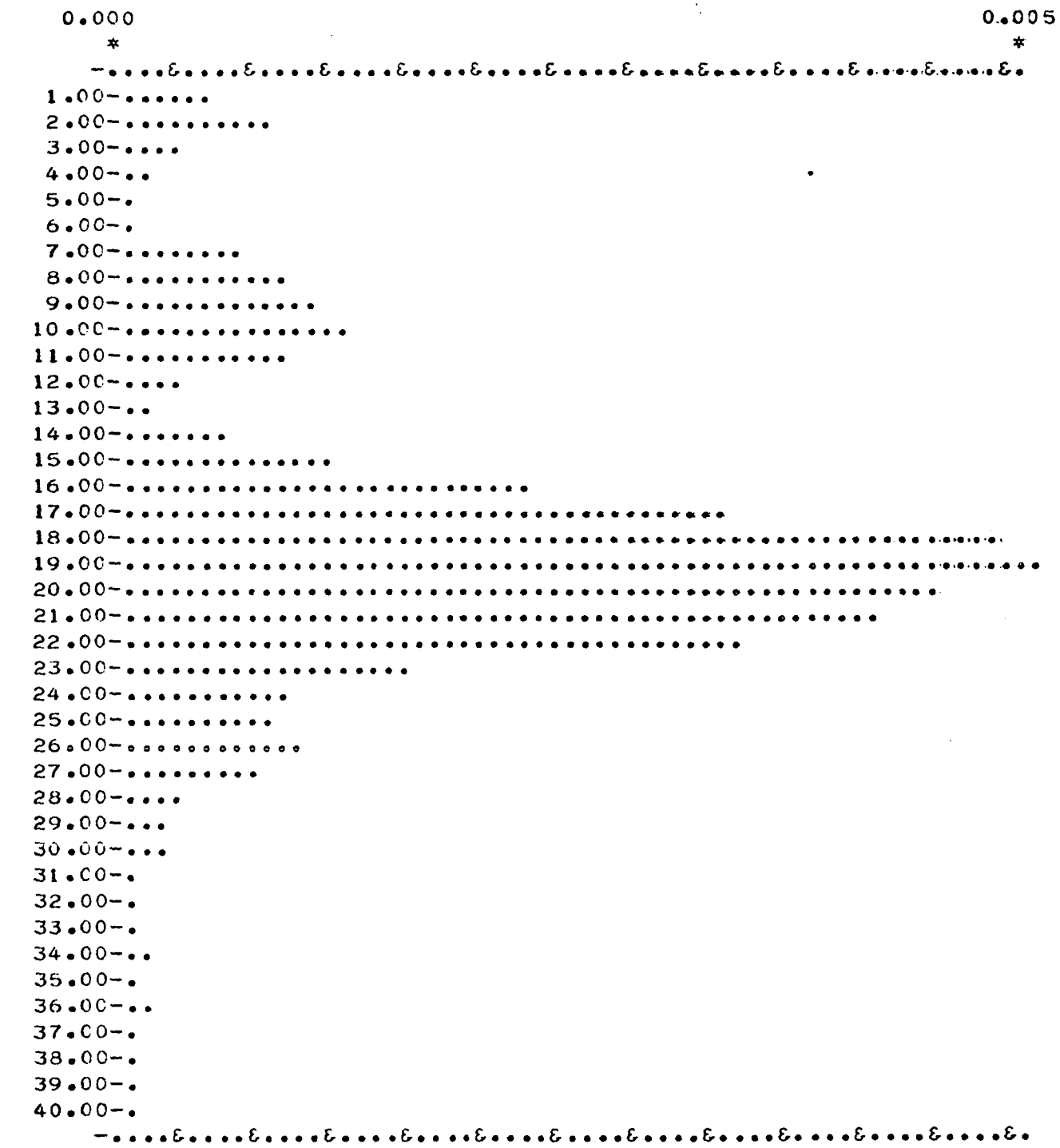

Fig. 14a

THE SCALING FACTOR IS... 0.00009

NUMBER OF RAYS CONTRIBUTE TO THE INTENSITY ARE NN# 34& 16& 17&1

SOLUTION BY MODE METHOD

FOLLOWINGS ARE MIRR.SEP.,SOURCE LOC.,WAVELENGTH AND SCREEN LOC.,NO.CELL AND NO.
0.100 5.000 2010.000 170.000 40.000 250.000 24.000

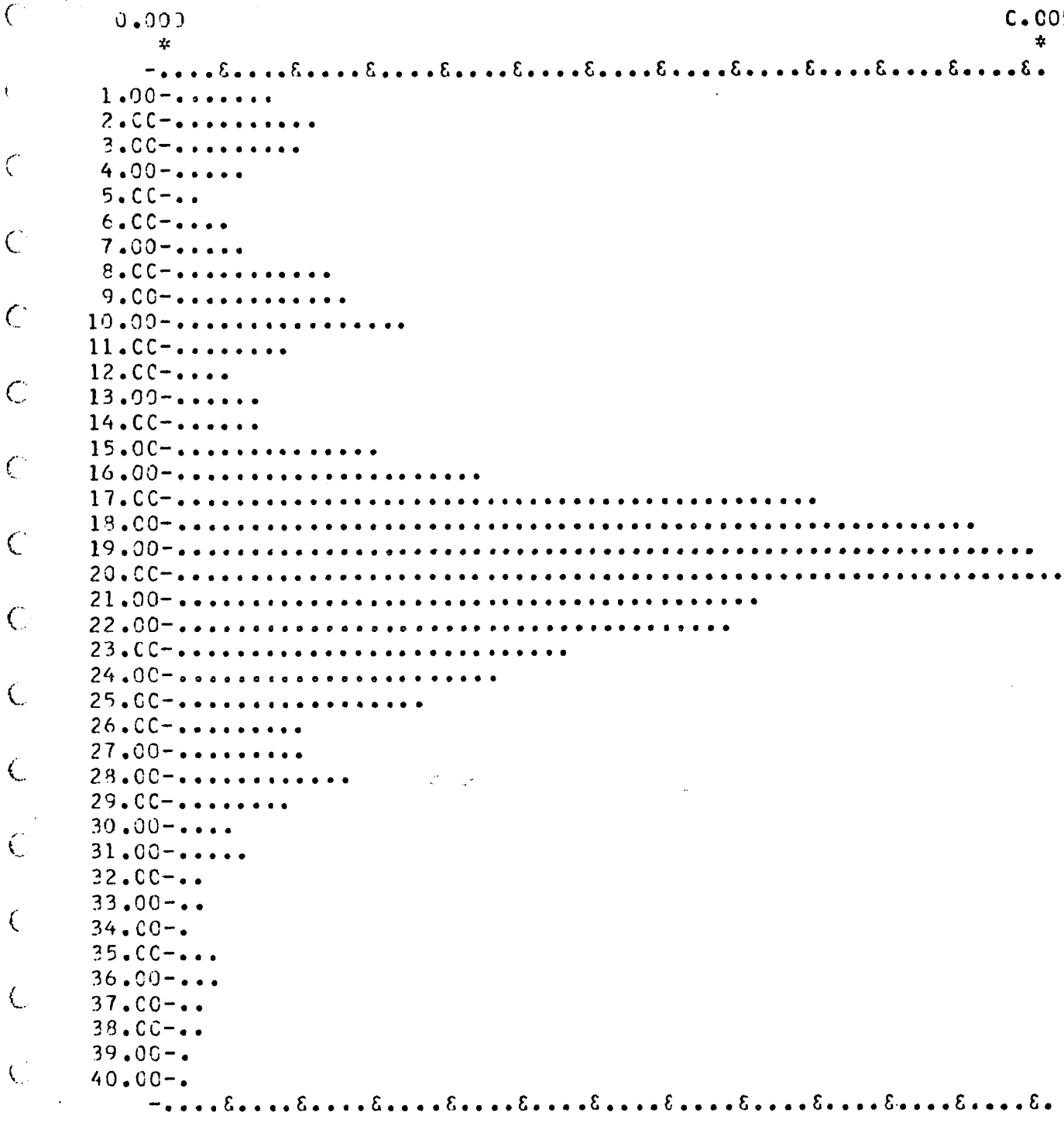

Fig. 14b

THE SCALING FACTOR IS... 0.00008

NORMALIZED INTENSITY

SOLUTION BY IMAGE METHOD

FOLLOWINGS ARE MIRR.SEP.,SOURCE LOC.,WAVELENGTH AND SCREEN LOC.
0.100 5.000 1990.000 175.000 40.000 17.000 16.000

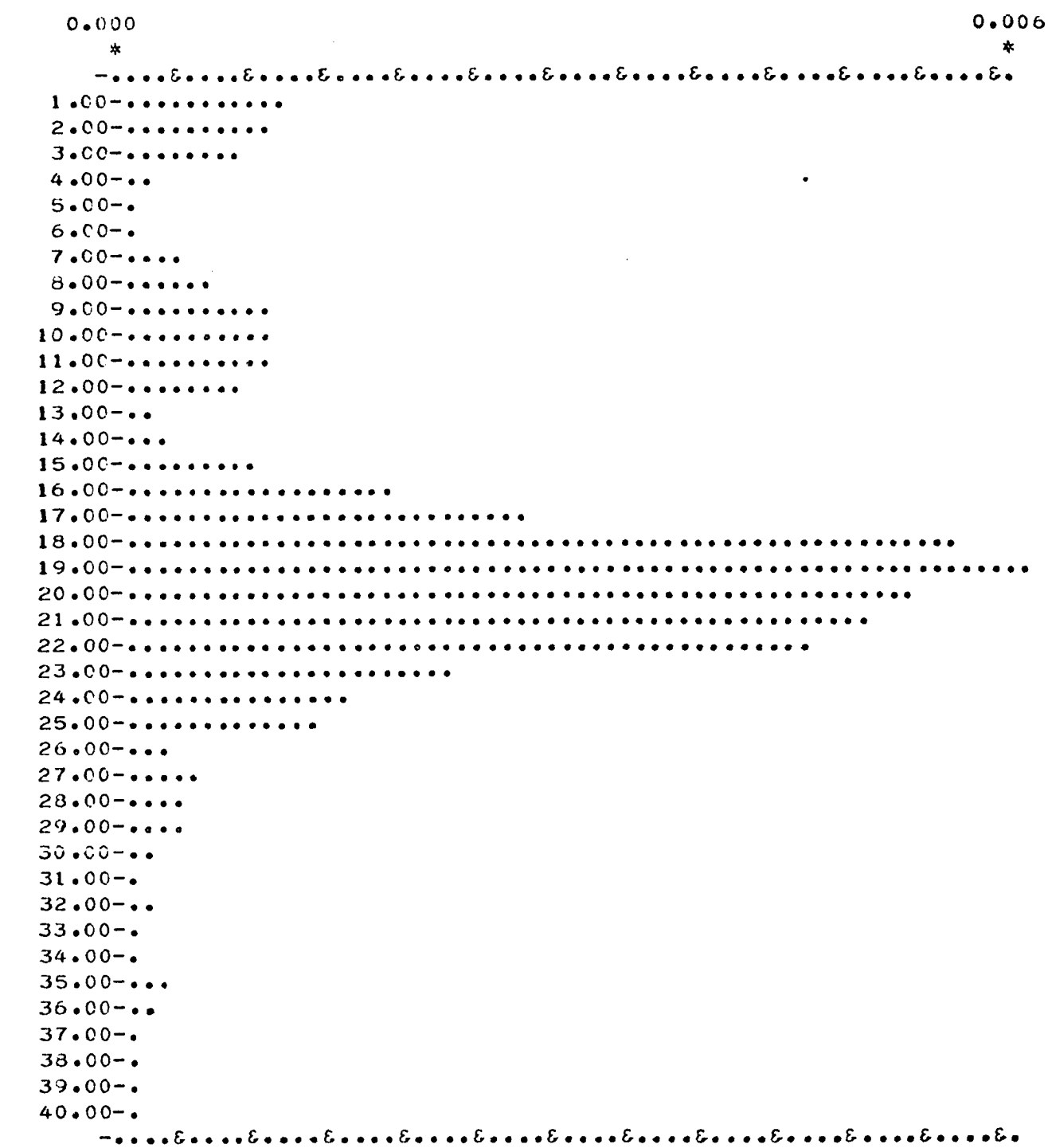

Fig. 15a

THE SCALING FACTOR IS... 0.00010

NUMBER OF RAYS CONTRIBUTE TO THE INTENSITY ARE NN# 346 166 1761

SOLUTION BY MODE METHOD

FOLLOWINGS ARE MIRR.SEP.,SOURCE LOC.,WAVELENGTH AND SCREEN LOC.,NO.CELL AND NO.

0.100	5.000	1990.000	170.000	40.000	250.000	24.000

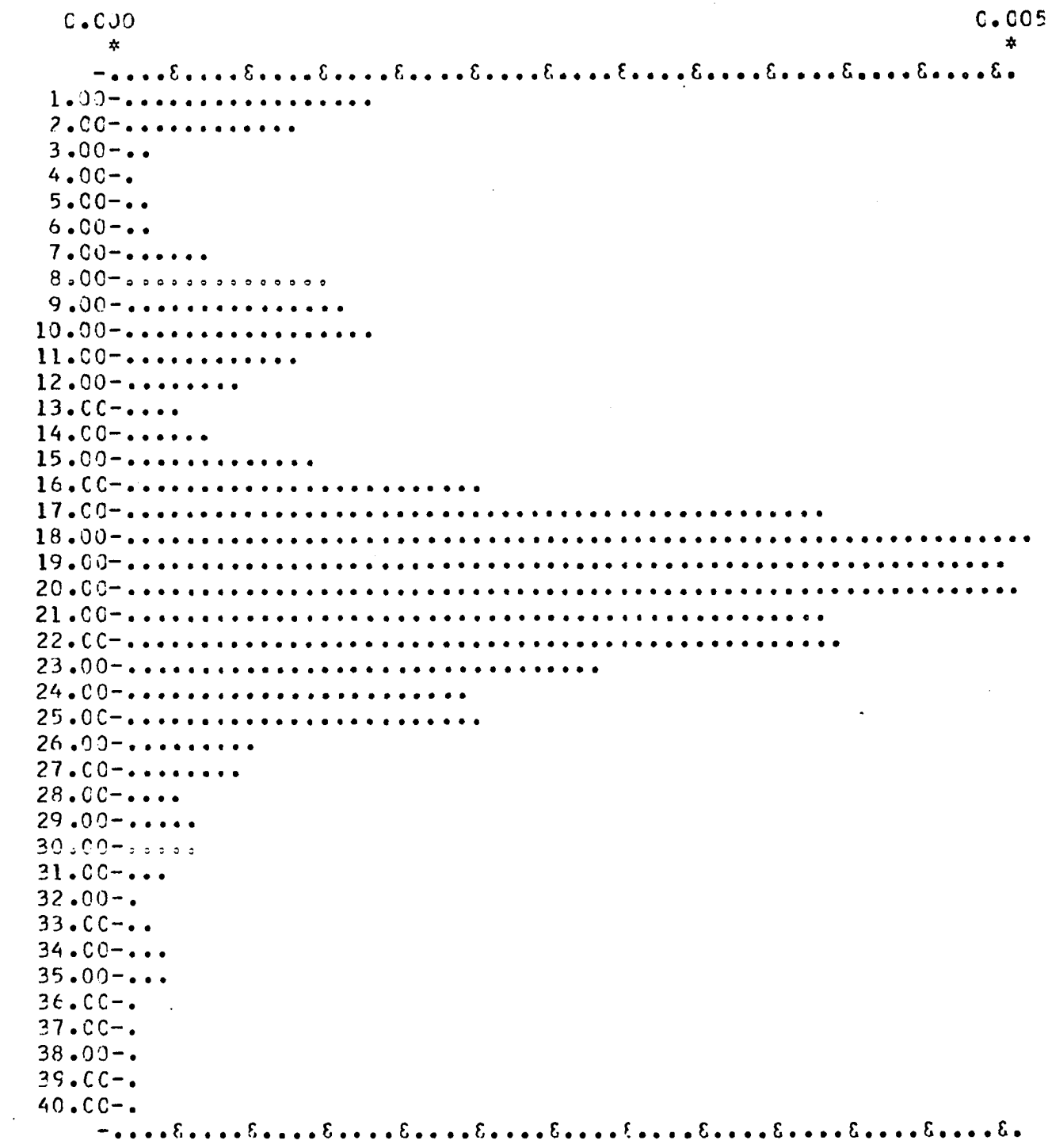

THE SCALING FACTOR IS... 0.00008

Fig. 15b

SOLUTICN BY IMAGE METHOD

FOLLOWINGS ARE MIRR.SEP..SOURCE LOC..WAVELENGTH AND SCREEN LOC.
0.100 5.000 1995.000 175.000 40.000 17.000 16.000

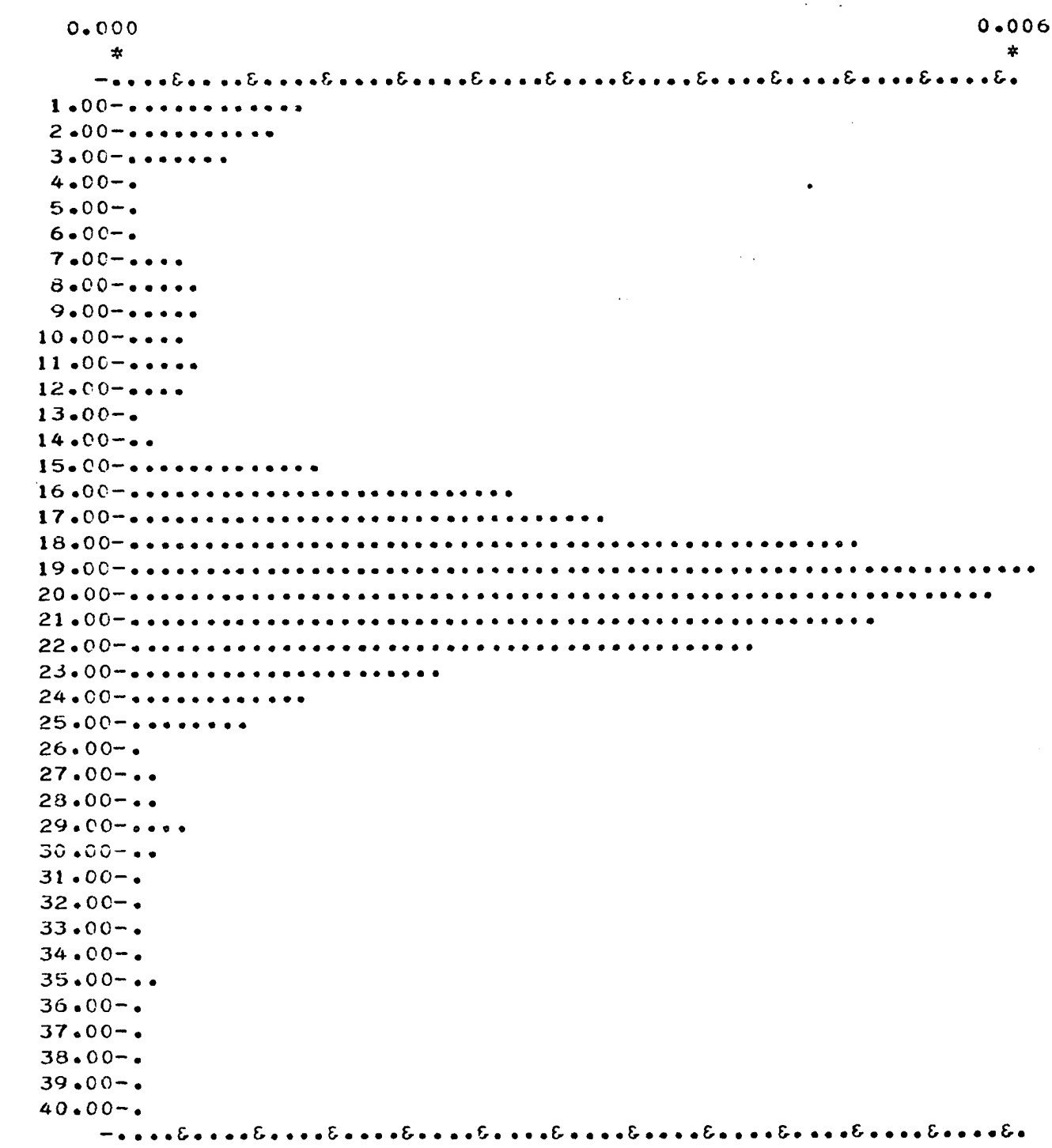

Fig. 16a

THE SCALING FACTOR IS... 0.00010

NUMBER OF RAYS CONTRIBUTE TO THE INTENSITY ARE NN# 34& 16& 17&1

SCLUTICN BY MCDE METHCC

FCLLCWINGS ARE MIRR.SEP.,SCURCE LCC.,WAVELENGTH AND SCREEN LOC.,NO.CELL AND NO.
C.100 5.000 1995.CCC 17C.000 40.000 250.000 24.000

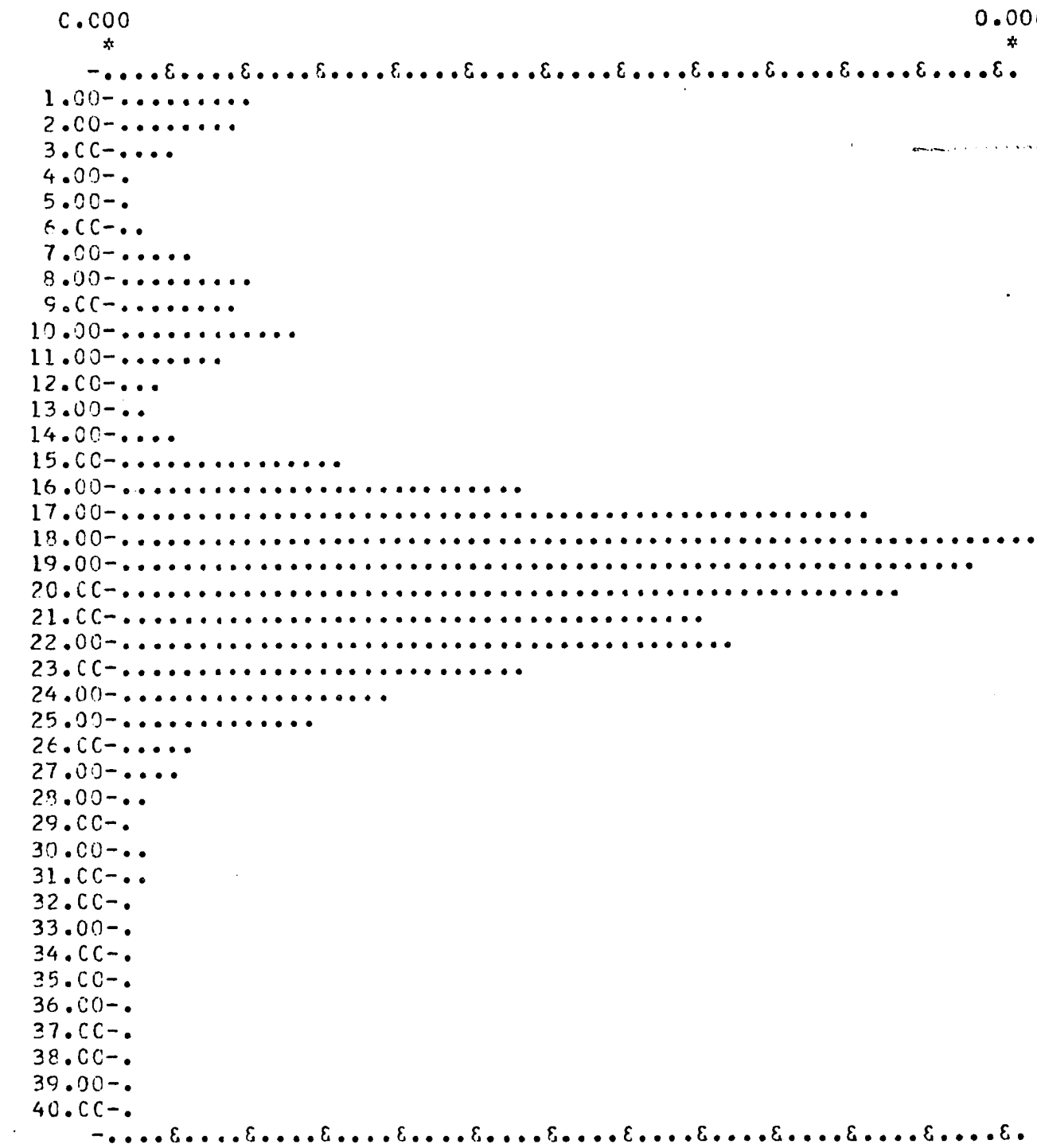

Fig. 16b

THE SCALING FACTOR IS... C.COC1C

SOLUTION BY IMAGE METHOD

FOLLOWINGS ARE MIRR.SEP.,SOURCE LOC.,WAVELENGTH AND SCREEN LOC.
0.100 4.000 2000.000 174.000 40.000 22.000 21.000

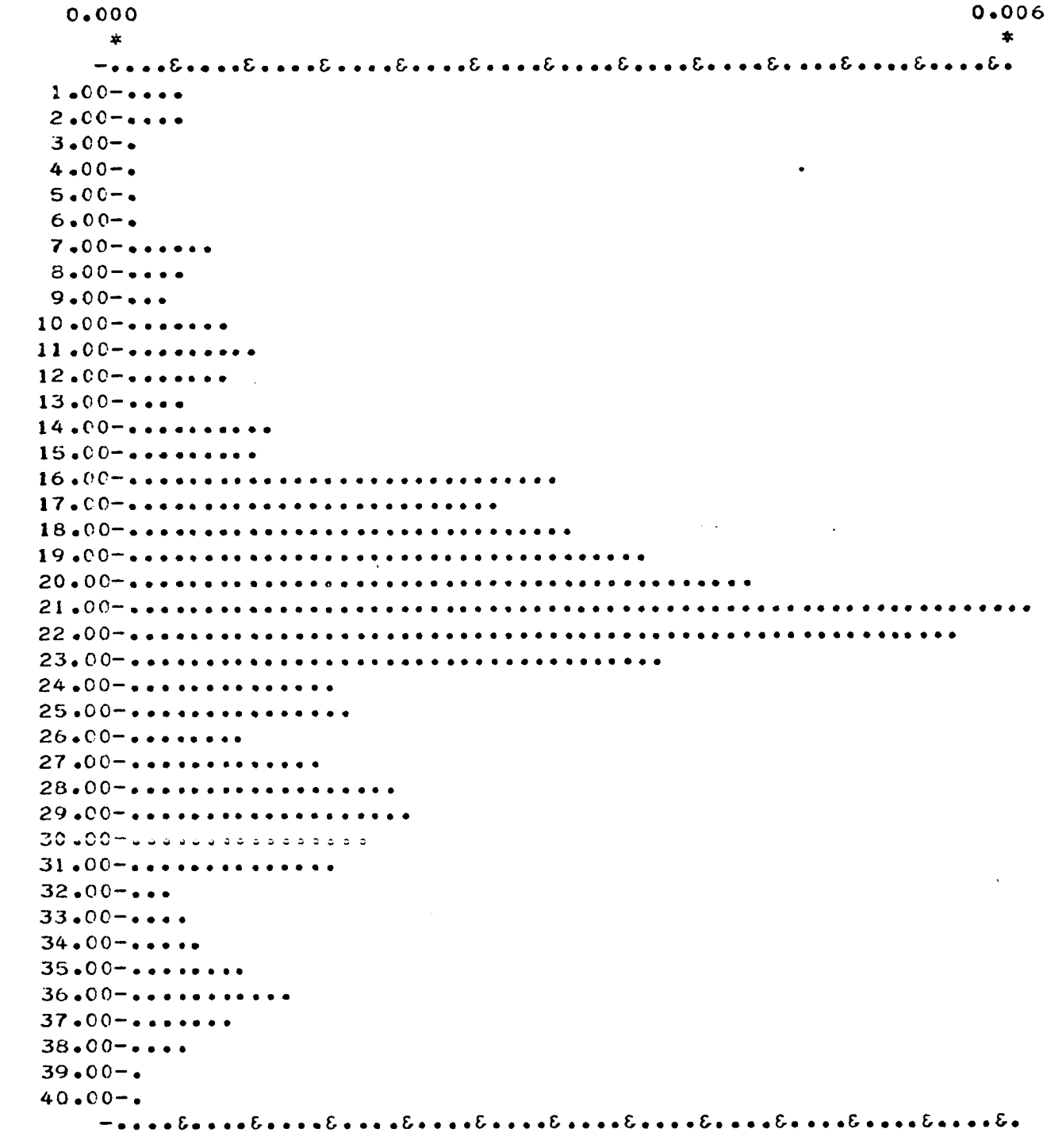

Fig. 17a

THE SCALING FACTOR IS... 0.00011

NUMBER OF RAYS CONTRIBUTE TO THE INTENSITY ARE NN# 446 216 2261

```
SOLUTION      BY      MODE      METHOD


FOLLOWINGS ARE MIRR.SEP.,SOURCE LOC.,WAVELENGTH AND SCREEN LOC.,NO.CELL AND NO.
   0.100      4.000   2000.000    170.000     40.000    250.000     24.000


   0.000                                                                0.005
      *                                                                   *
     -....&....&....&....&....&....&....&....&....&....&....&....&.
  1.00-.......
  2.00-.
  3.00-.
  4.00-.
  5.00-..
  6.00-.
  7.00-...
  8.00-...........
  9.00-....
 10.00-...........
 11.00-........
 12.00-.........
 13.00-..............
 14.00-..............................
 15.00-................
 16.00-.................
 17.00-....................................
 18.00-.................................................
 19.00-.........................................
 20.00-.........................................
 21.00-...........................................
 22.00-.............................................................
 23.00-.............................................
 24.00-...................................
 25.00-...................
 26.00-...............
 27.00-...........
 28.00-.............
 29.00-...................
 30.00-........................
 31.00-..........
 32.00-....
 33.00-..
 34.00-..
 35.00-....
 36.00-.........
 37.00-.......
 38.00-........
 39.00-..
 40.00-.
     -....&....&....&....&....&....&....&....&....&....&....&....&.


THE SCALING FACTOR IS... 0.00009
```

Fig. 17b

SOLUTION BY IMAGE METHOD

FOLLOWINGS ARE MIRR.SEP.,SOURCE LOC.,WAVELENGTH AND SCREEN LOC.

0.500 5.000 2000.000 175.000 40.000 17.000 17.000

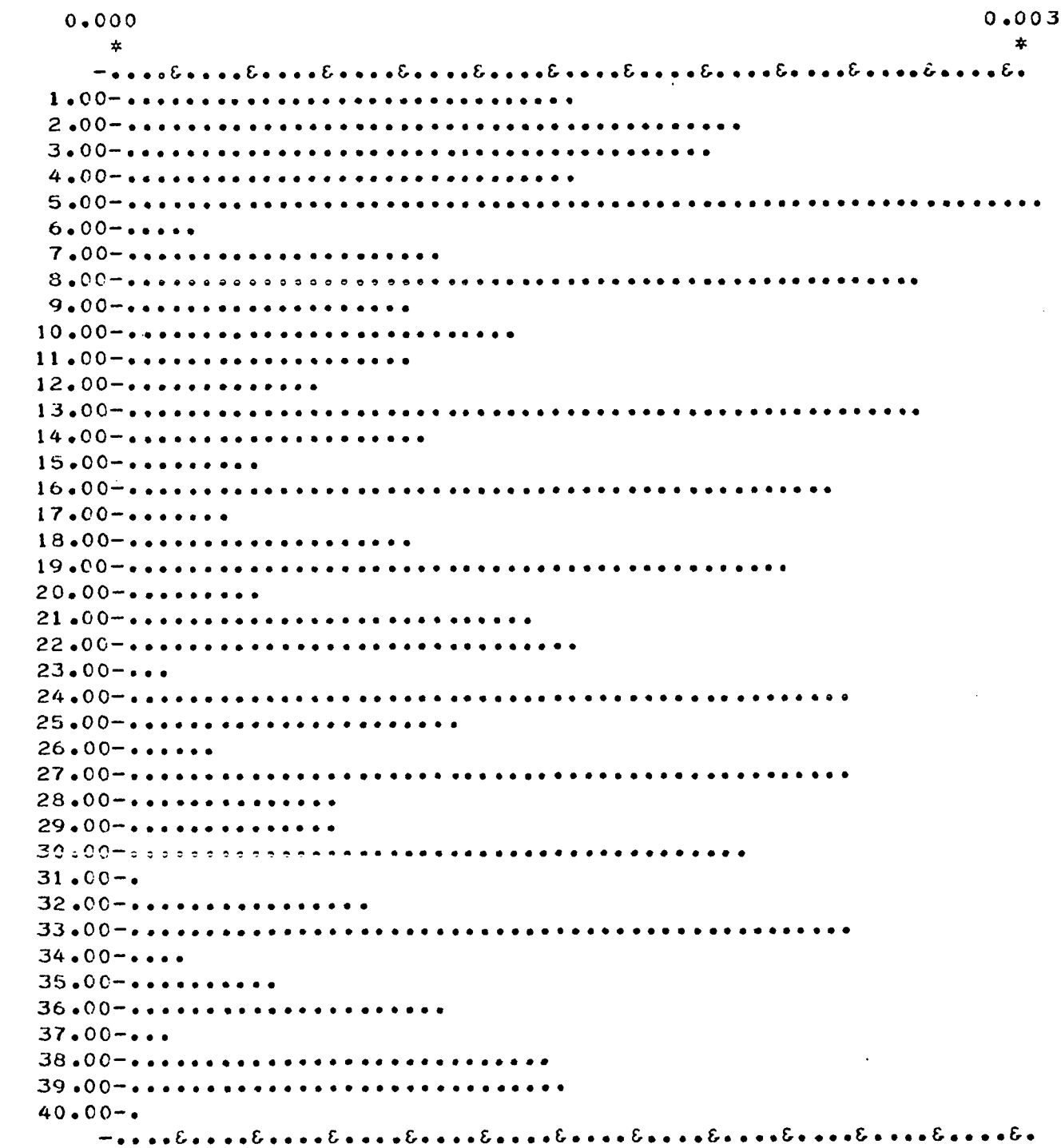

Fig. 18

THE SCALING FACTOR IS... 0.00004

NUMBER OF RAYS CONTRIBUTE TO THE INTENSITY ARE NN# 356 176 1761

SOLUTION BY IMAGE METHOD

FOLLOWINGS ARE MIRR.SEP.,SOURCE LOC.,WAVELENGTH AND SCREEN LOC.

0.100 5.000 4000.000 155.000 40.000 15.000 14.000

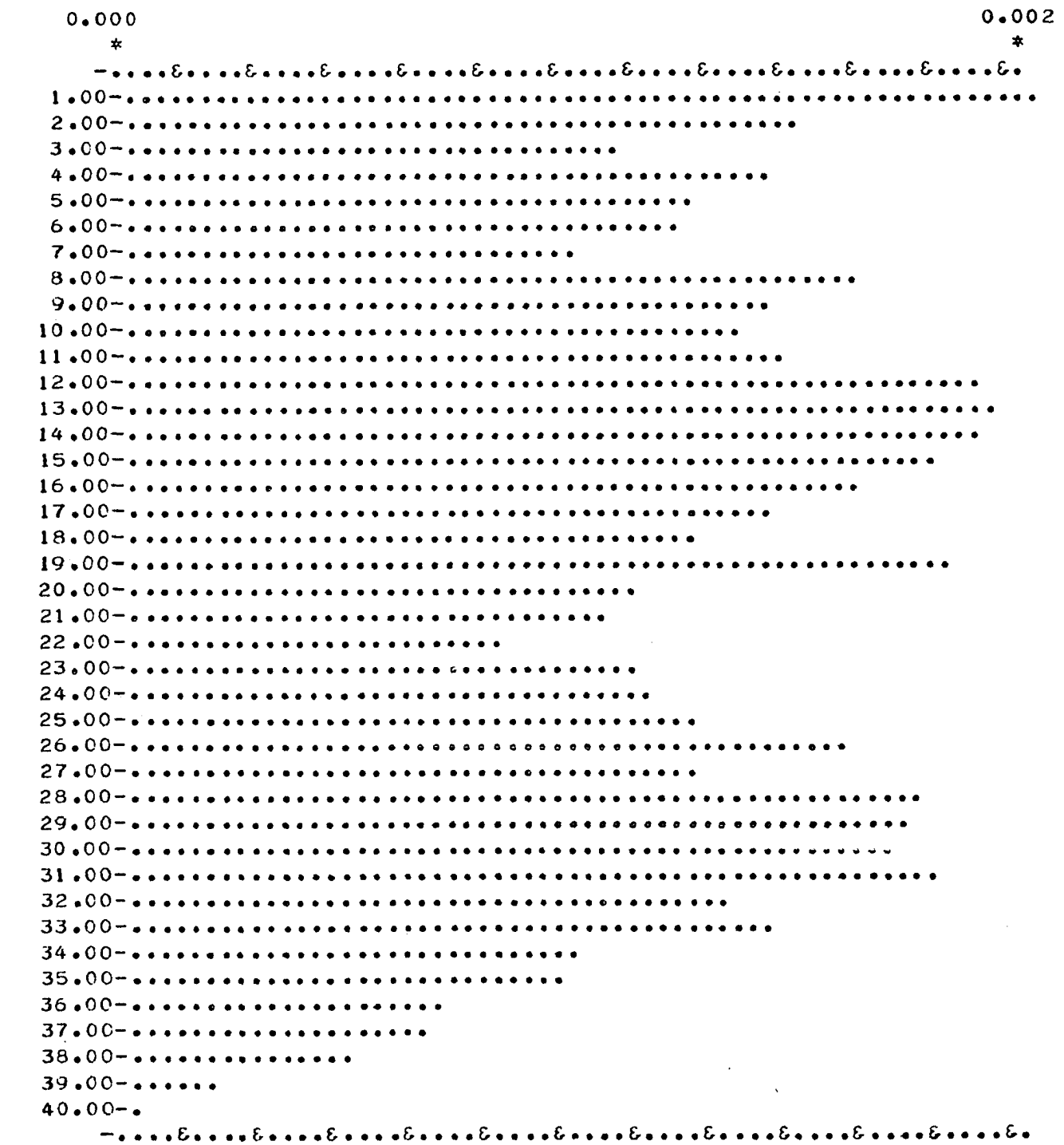

Fig. 19a

THE SCALING FACTOR IS... 0.00003

NUMBER OF RAYS CONTRIBUTE TO THE INTENSITY ARE NN# 30& 14& 15&1

SCLUTICN BY MCDE METHCD

FCLLCWINGS ARE MIRR.SEP.,SCURCE LCC.,WAVELENGTH AND SCREEN LOC.,NC.CELL AND NC.
C.100 5.000 4000.000 150.000 40.000 250.000 24.000

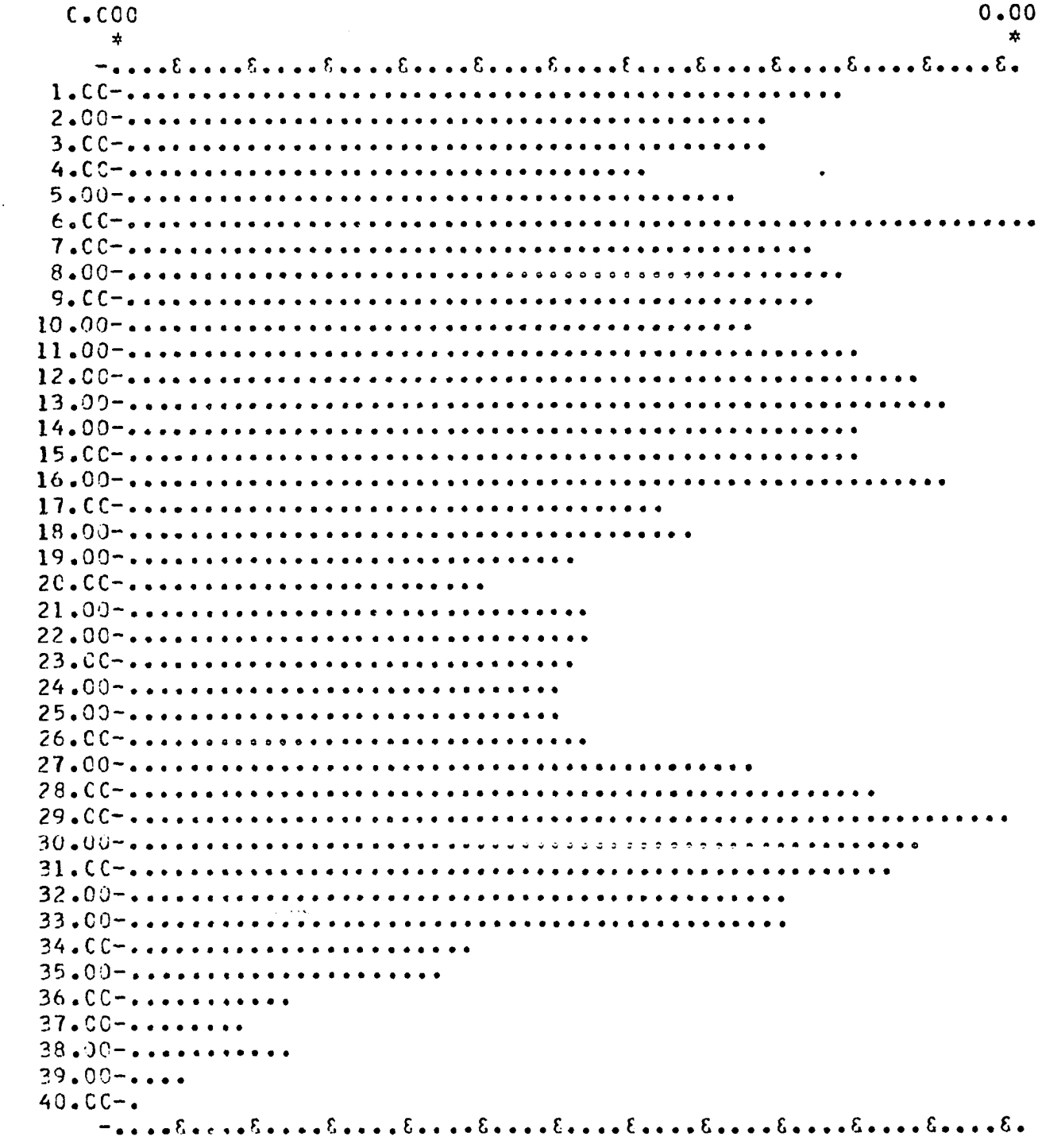

Fig. 19b

THE SCALING FACTCR IS... 0.00003

SOLUTION BY IMAGE METHOD

FOLLOWINGS ARE MIRR.SEP.,SOURCE LOC..WAVELENGTH AND SCREEN LOC.

0.100 5.000 4000.000 174.000 40.000 17.000 16.000

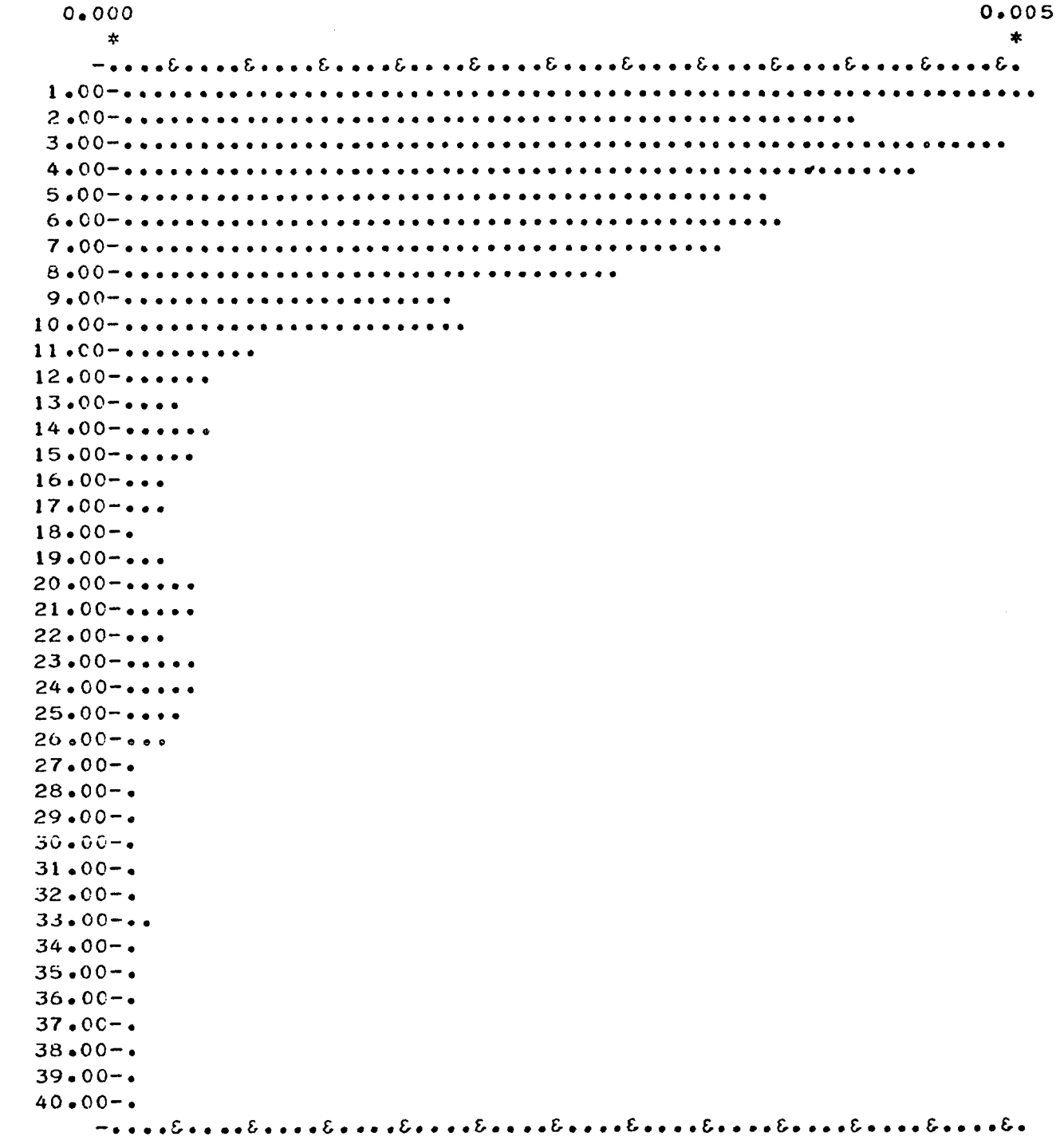

Fig. 20a

THE SCALING FACTOR IS... 0.00009

NUMBER OF RAYS CONTRIBUTE TO THE INTENSITY ARE NN# 346 166 1761

SCLUTICN BY MCDE METHCC

FCLLCWINGS ARE MIRR.SEP.,SOURCE LCC.,WAVELENGTH AND SCREEN LOC.,NC.CELL AND NC.
0.100 5.000 4000.000 169.000 40.000 250.000 24.000

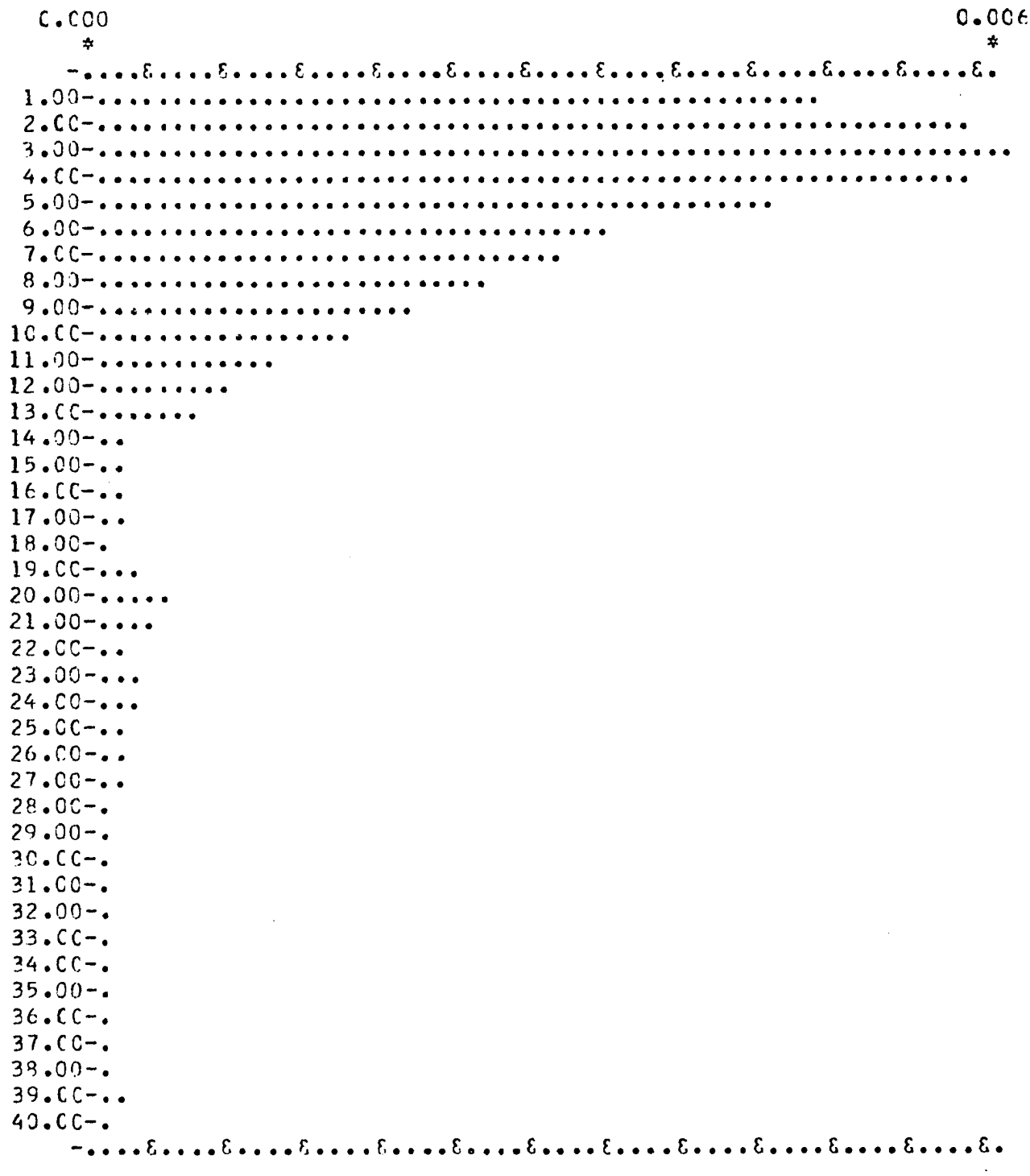

Fig. 20b

THE SCALING FACTCR IS... C.00C09

SOLUTION BY IMAGE METHOD

FOLLOWINGS ARE MIRR.SEP.,SOURCE LOC.,WAVELENGTH AND SCREEN LOC.

0.100 5.000 4000.000 205.000 40.000 20.000 19.000

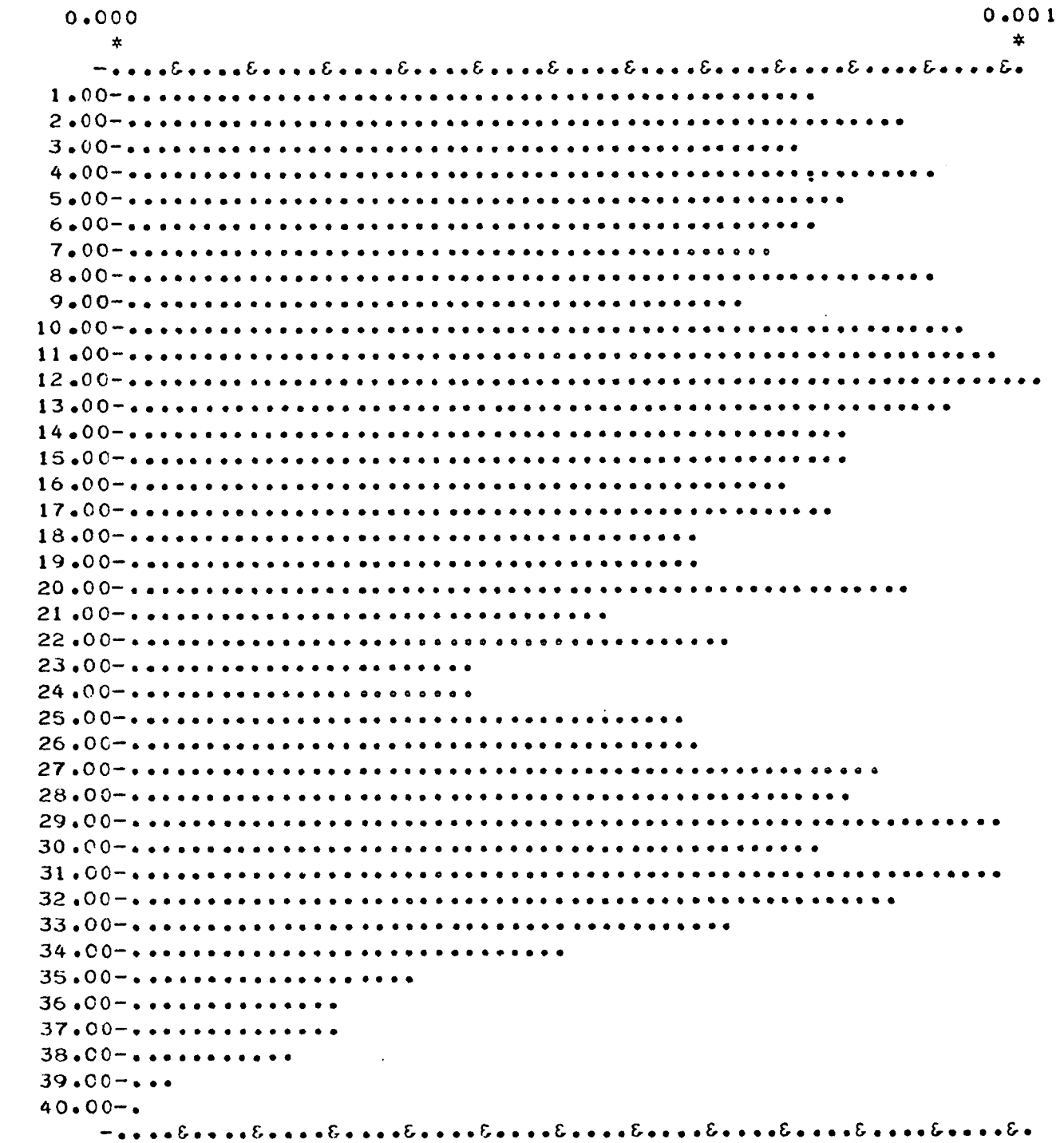

Fig. 21a

THE SCALING FACTOR IS... 0.00002

NUMBER OF RAYS CONTRIBUTE TO THE INTENSITY ARE NN# 40& 19& 20&1

SOLUTION BY MODE METHOD

FOLLOWINGS ARE MIRR.SEP.,SOURCE LOC.,WAVELENGTH AND SCREEN LOC.,NO.CELL AND NO.
0.100 5.000 4000.000 200.000 40.000 250.000 24.000

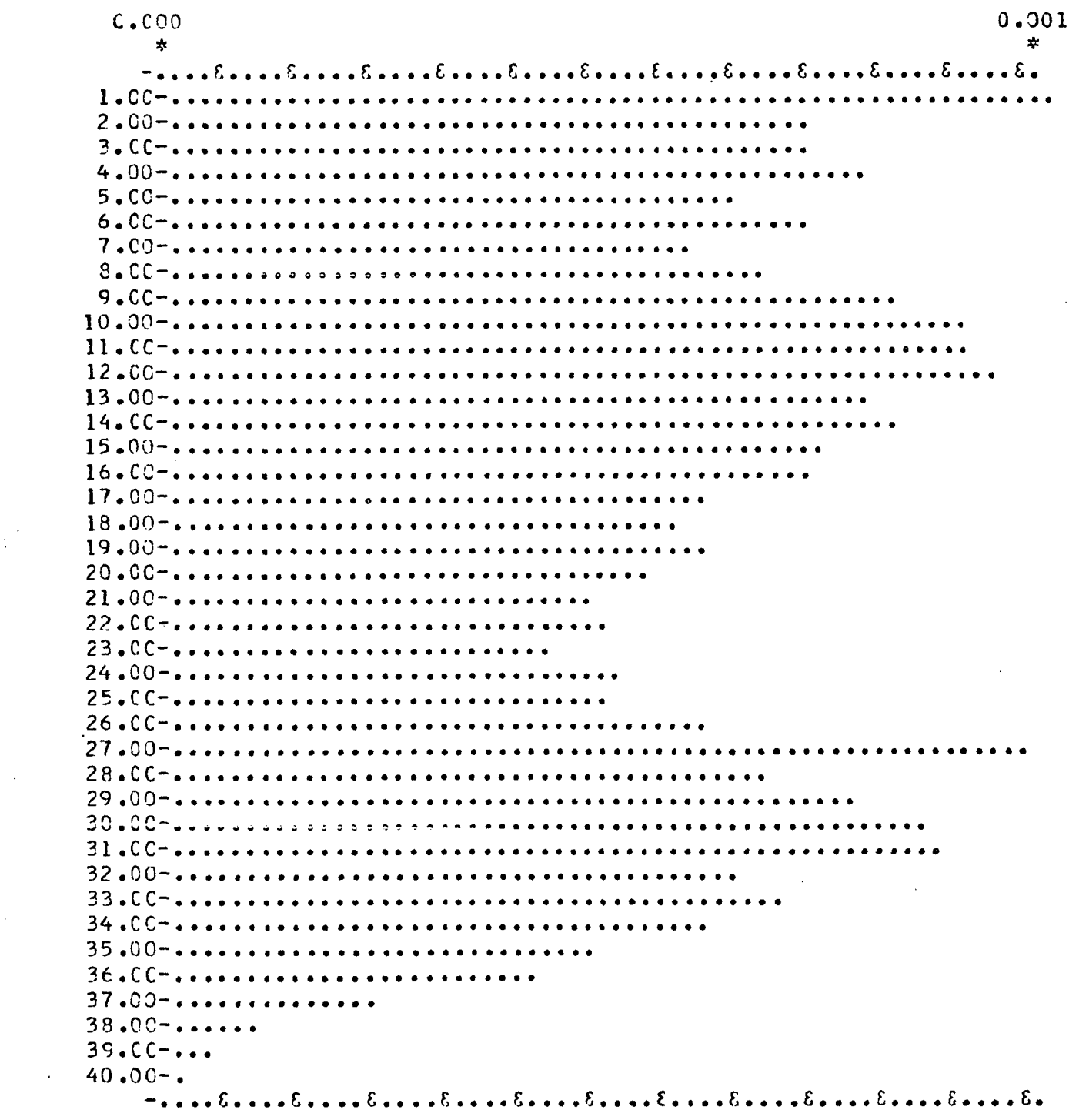

Fig. 21b

THE SCALING FACTOR IS... 0.00002

SOLUTION BY IMAGE METHOD

FOLLOWINGS ARE MIRR.SEP.,SOURCE LOC.,WAVELENGTH AND SCREEN LOC.

0.100 5.000 4005.000 175.000 40.000 17.000 16.000

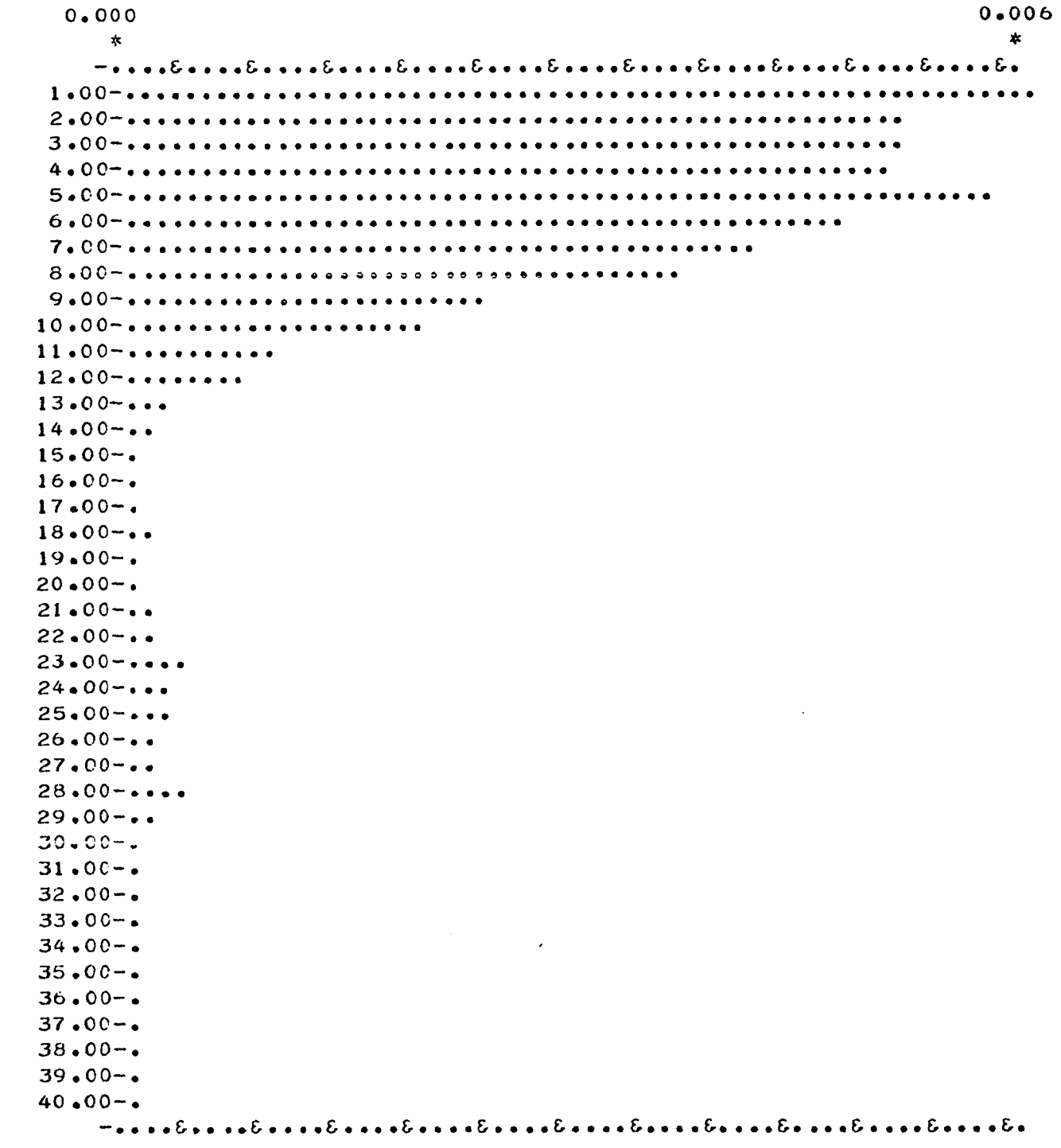

Fig. 22a

THE SCALING FACTOR IS... 0.00010

NUMBER OF RAYS CONTRIBUTE TO THE INTENSITY ARE NN# 34& 16& 17&1

SCLUTICN BY MCDE METHCD

FCLLCWINGS ARE MIRR.SFF.,SCURCE LCC.,WAVELENGTH AND SCREEN LOC.,NC.CELL AND NC.
C.100 5.CCC 4CC5.CCC 17C.0C0 4C.000 250.000 24.000

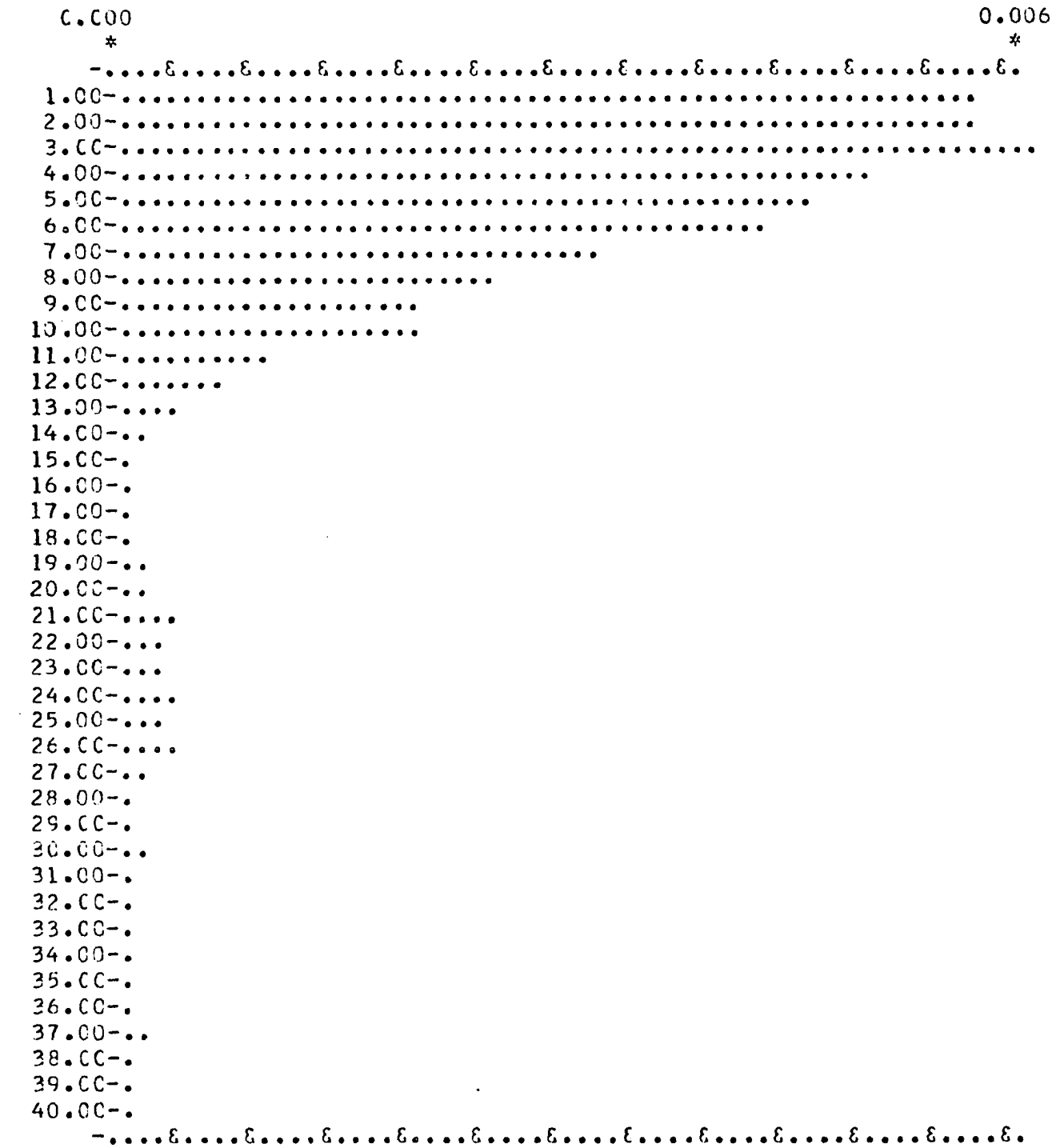

Fig. 22b

THE SCALING FACTCR IS... C.COC10

SOLUTION BY MODE METHOD

FOLLOWINGS ARE MIRR.SEP.,SOURCE LOC.,WAVELENGTH AND SCREEN LOC.,NO.CELL AND NO.
0.100 5.000 4010.000 170.000 40.000 250.000 24.000

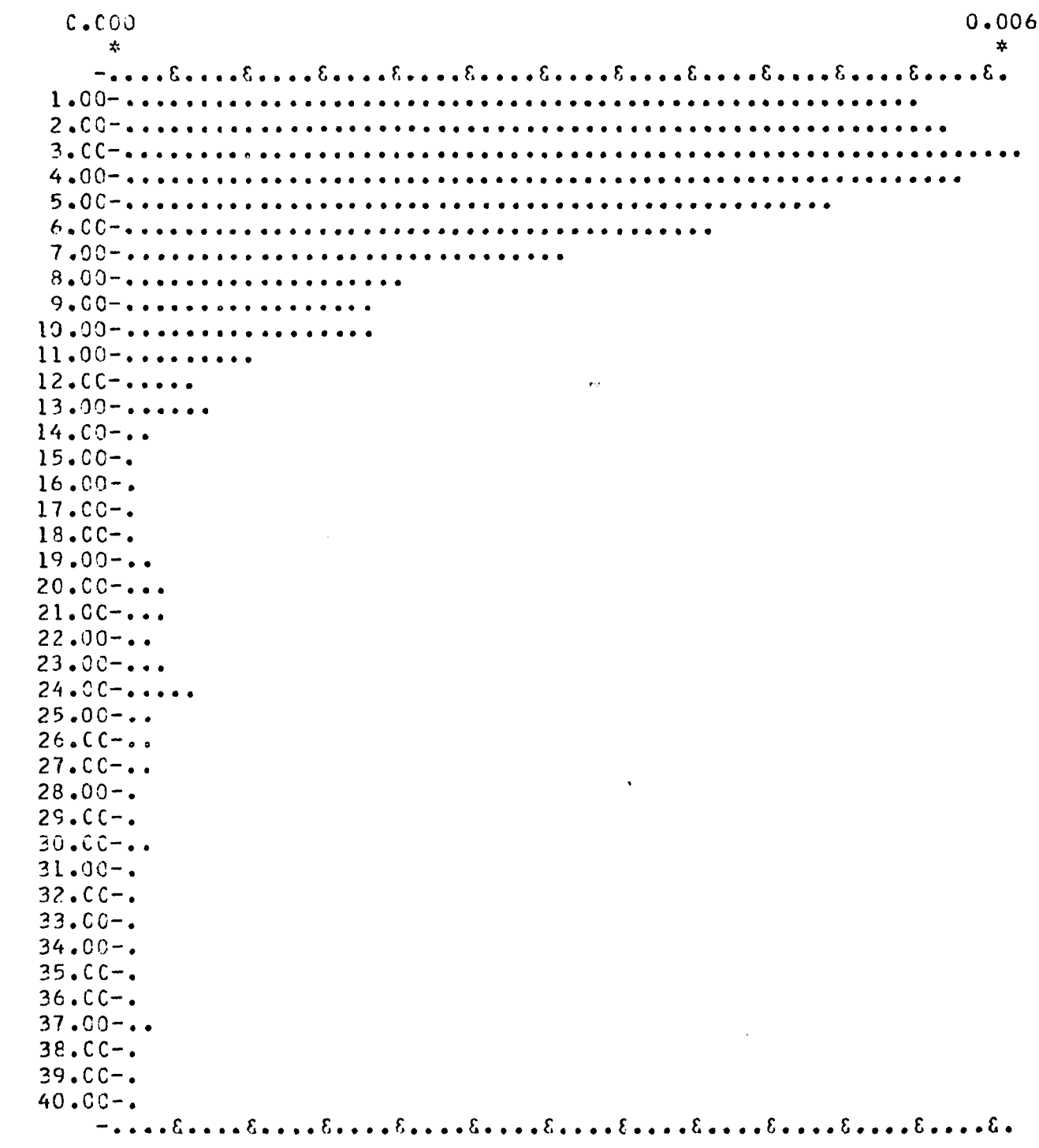

Fig. 23a

THE SCALING FACTOR IS... 0.00010

SOLUTION BY IMAGE METHOD

FOLLOWINGS ARE MIRR.SEP..SOURCE LOC..WAVELENGTH AND SCREEN LOC.

0.100 5.000 4010.000 175.000 40.000 17.000 16.000

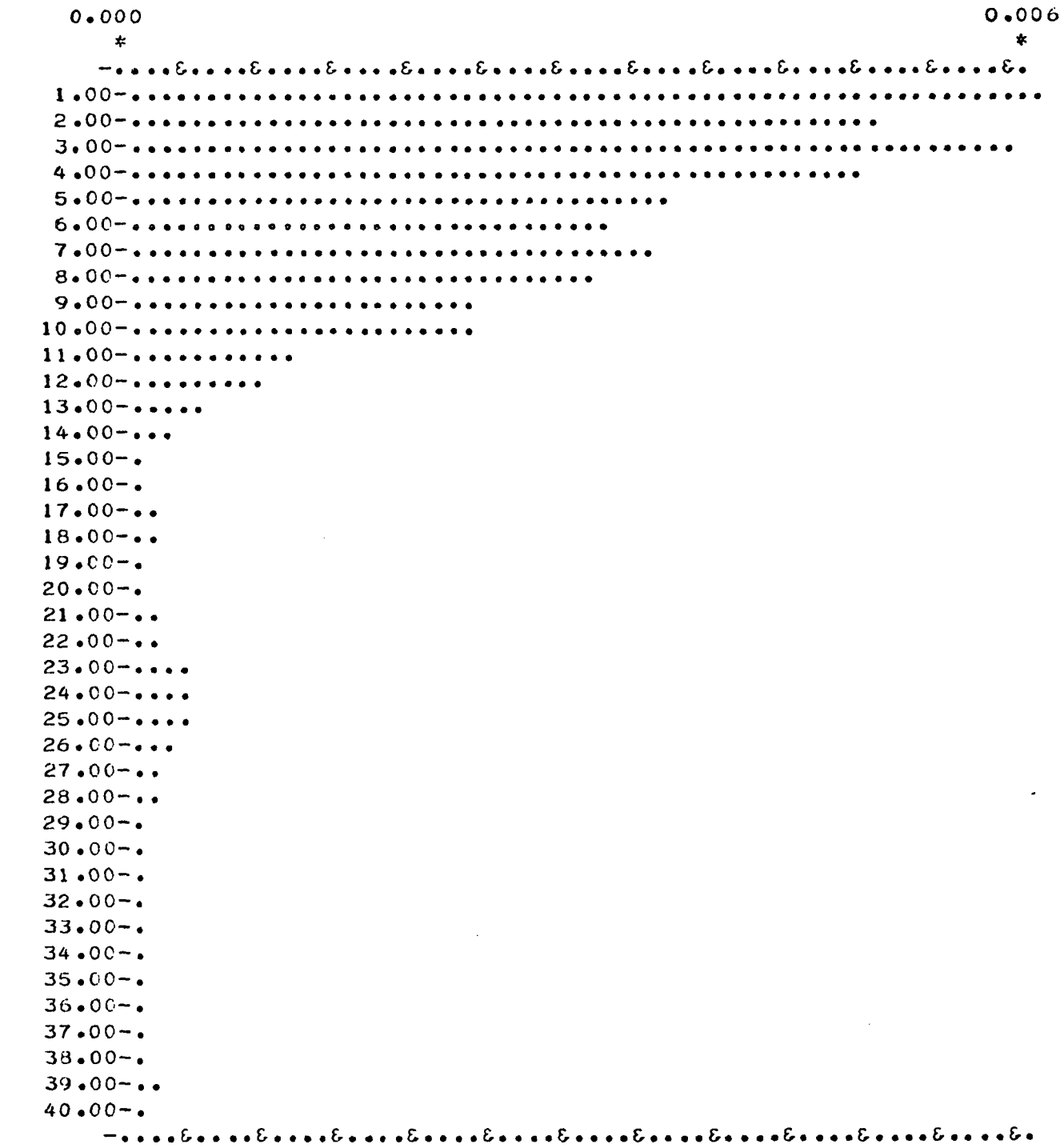

Fig. 23a

THE SCALING FACTOR IS... 0.00010

NUMBER OF RAYS CONTRIBUTE TO THE INTENSITY ARE NN# 34& 16& 17&1

SOLUTION BY IMAGE METHOD

FOLLOWINGS ARE MIRR.SEP.,SOURCE LOC.,WAVELENGTH AND SCREEN LOC.

0.100 5.000 3995.000 175.000 40.000 17.000 16.000

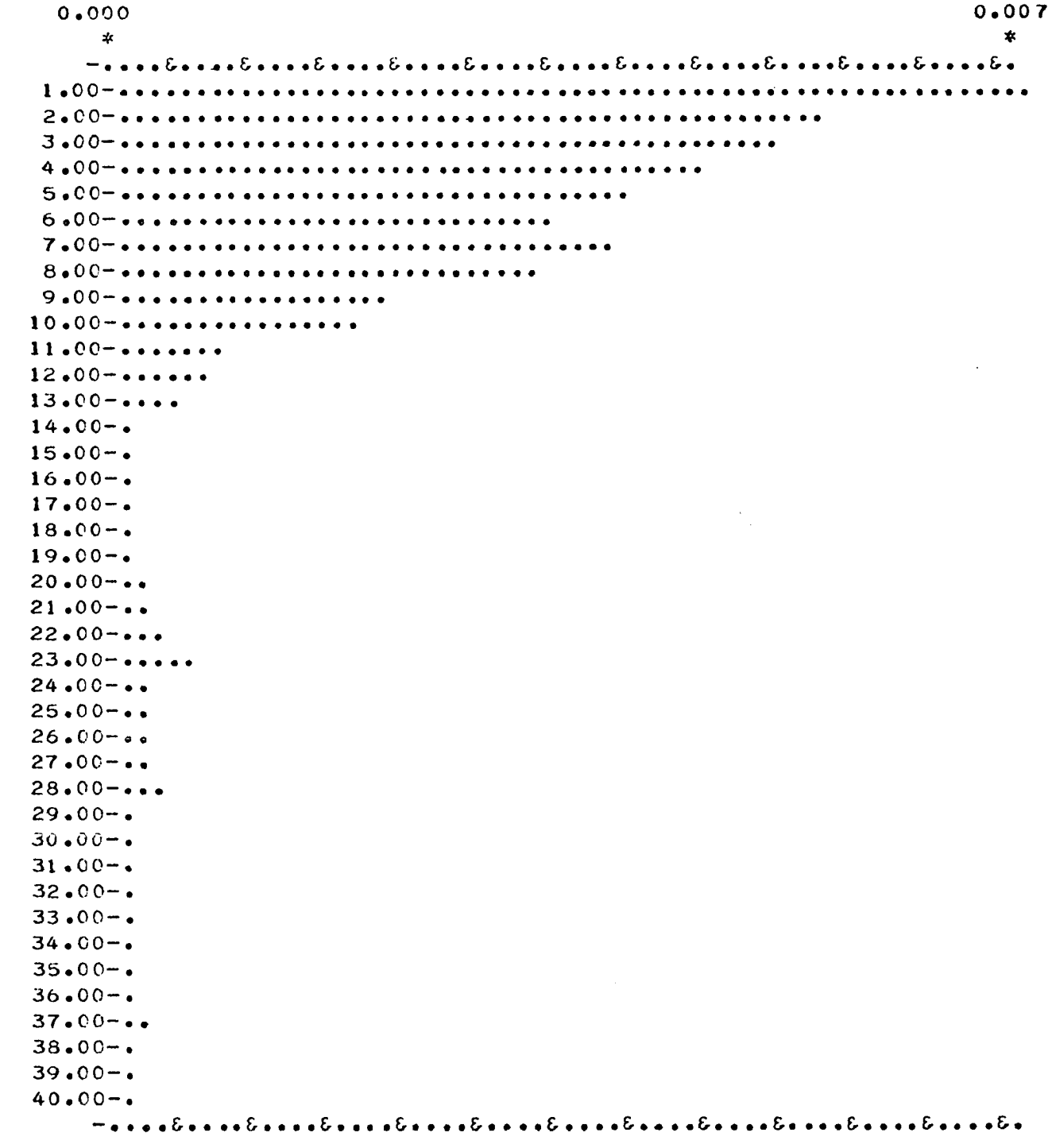

Fig. 24a

THE SCALING FACTOR IS... 0.00011

NUMBER OF RAYS CONTRIBUTE TO THE INTENSITY ARE NN# 346 166 1761

SOLUTION BY MODE METHOD

FOLLOWINGS ARE MIRR.SEP.,SOURCE LOC.,WAVELENGTH AND SCREEN LOC.,NO.CELL AND NO.
0.100 5.000 3995.000 170.000 40.000 250.000 24.000

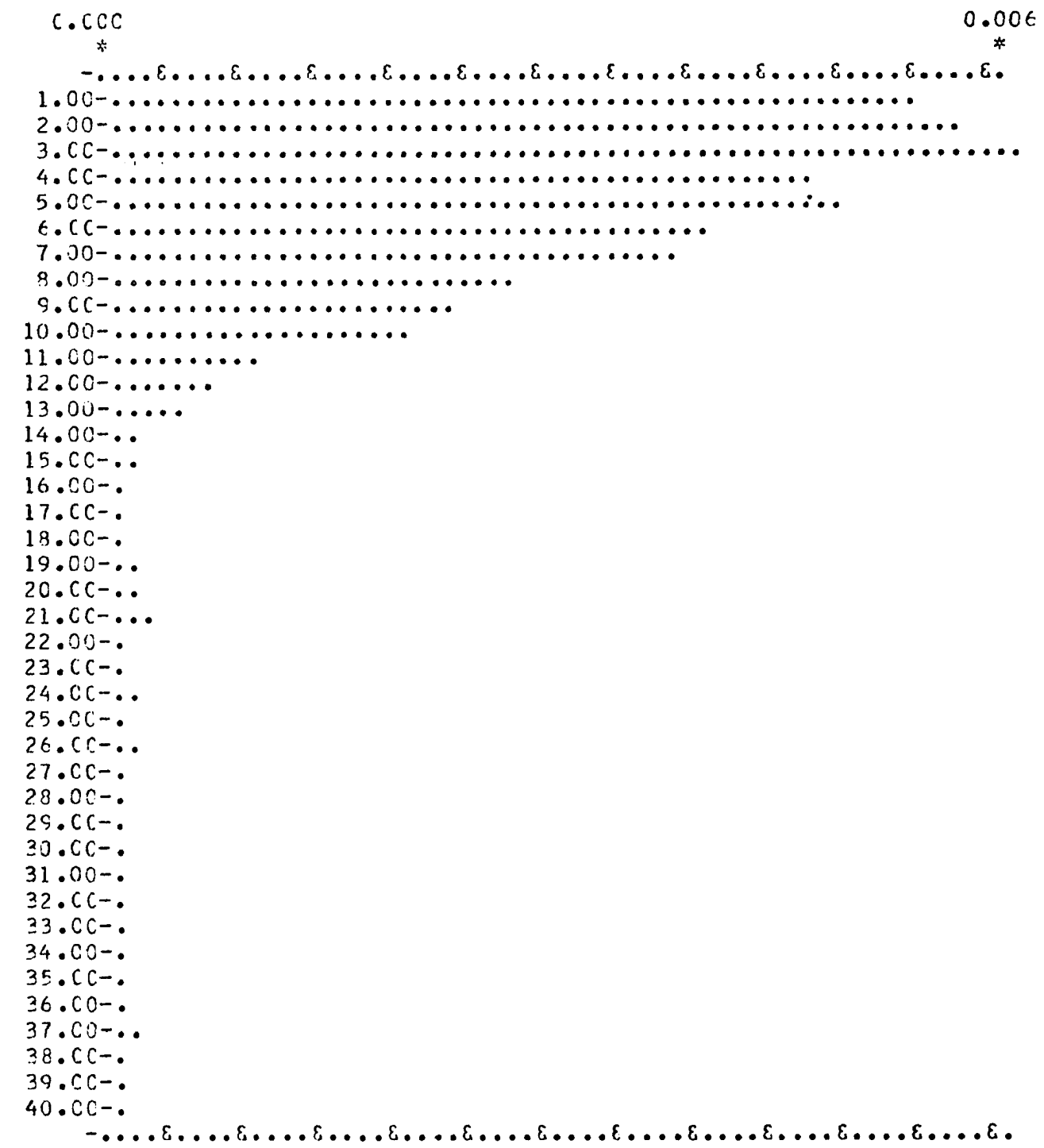

Fig. 24b

THE SCALING FACTOR IS... 0.00010

SOLUTION BY IMAGE METHOD

FOLLOWINGS ARE MIRR.SEP.,SOURCE LOC.,WAVELENGTH AND SCREEN LOC.

0.100 5.000 3990.000 175.000 40.000 17.000 16.000

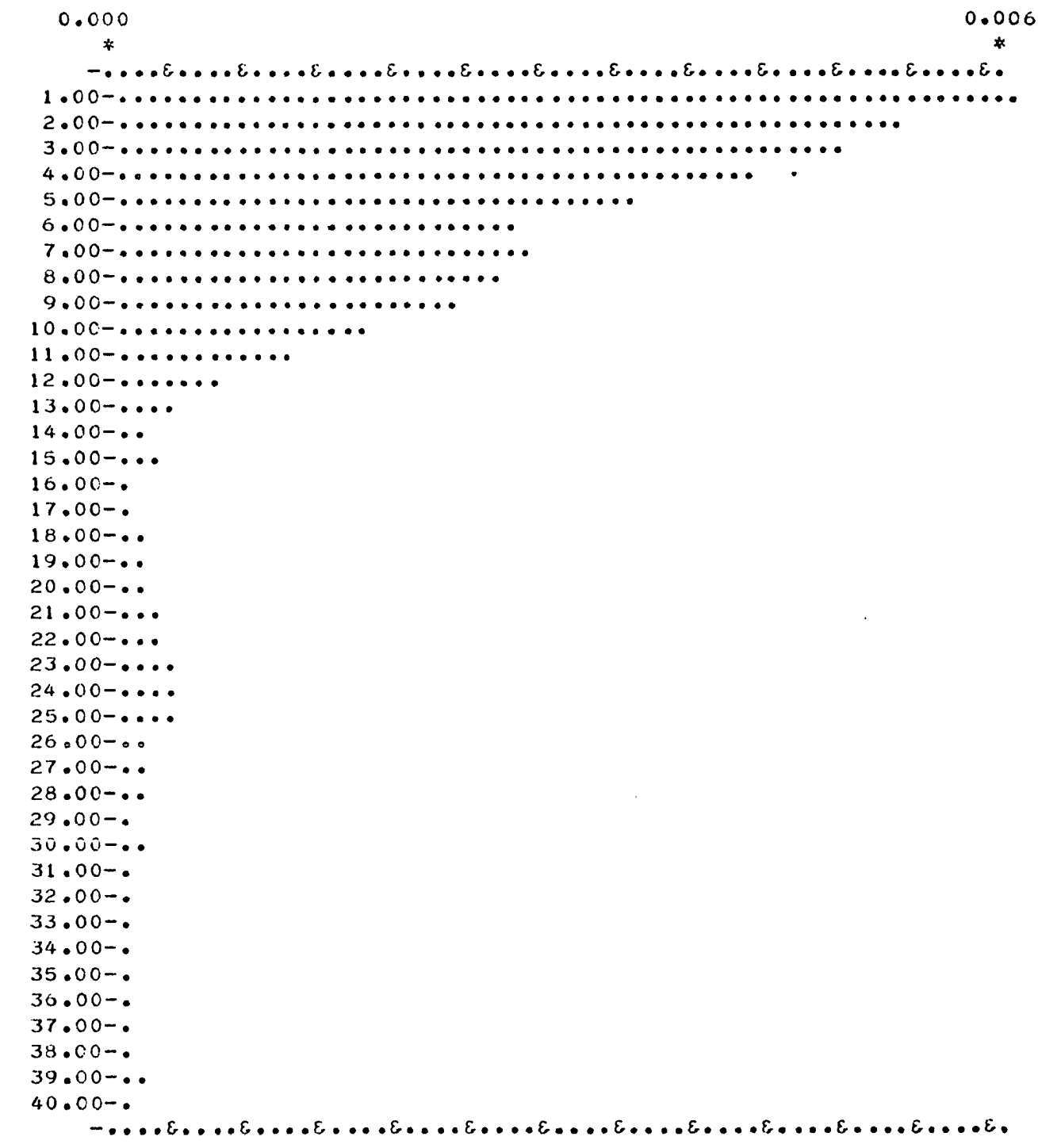

Fig. 25a

THE SCALING FACTOR IS... 0.00010

NUMBER OF RAYS CONTRIBUTE TO THE INTENSITY ARE NN# 346 166 1761

SCLUTICN BY MCDE METHCD

FCLLCWINGS ARE MIRR.SEP.,SCURCE LCC.,WAVELENGTH AND SCREEN LOC.,NC.CELL AND NC.
C.100 5.000 3990.000 170.000 40.000 250.000 24.000

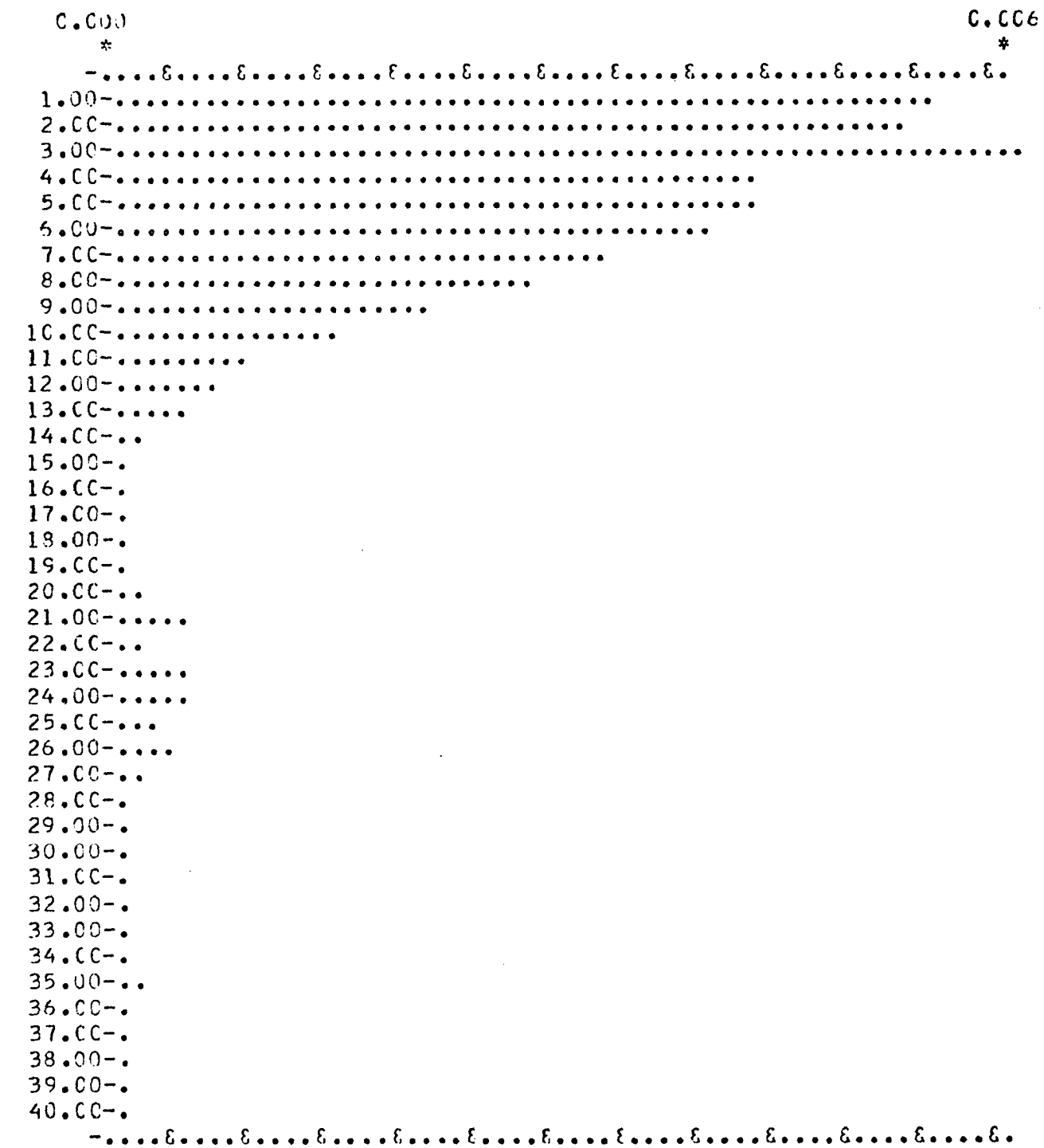

Fig. 25b

THE SCALING FACTOR IS... 0.00010

SOLUTION BY IMAGE METHOD

FOLLOWINGS ARE MIRR.SEP.,SOURCE LOC.,WAVELENGTH AND SCREEN LOC.

0.100 4.000 4000.000 174.000 40.000 22.000 21.000

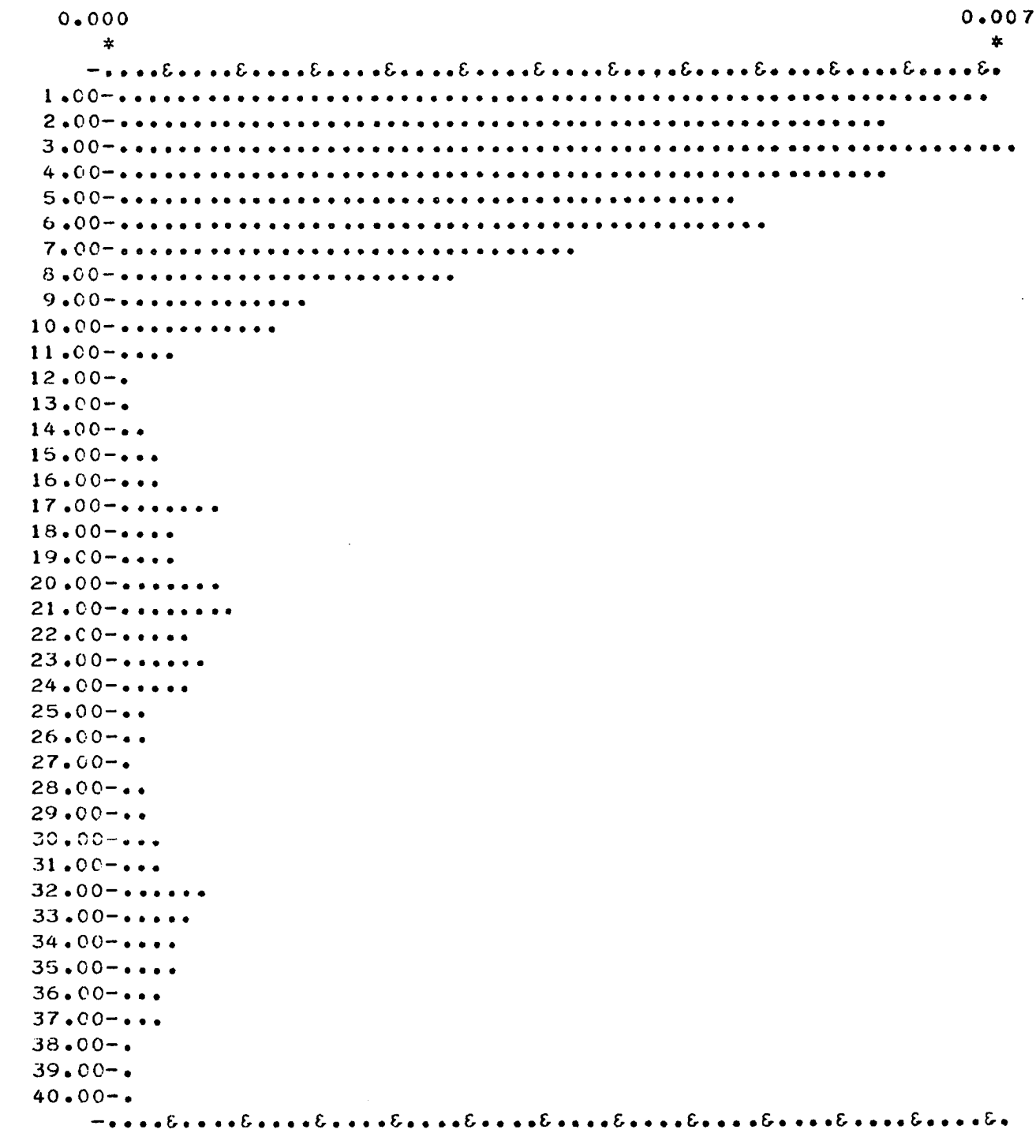

Fig. 26a

THE SCALING FACTOR IS... 0.00012

NUMBER OF RAYS CONTRIBUTE TO THE INTENSITY ARE NN# 44& 21& 22&1

SOLUTION BY MODE METHOD

FOLLOWINGS ARE MIRR.SEP.,SOURCE LOC.,WAVELENGTH AND SCREEN LOC.,NO.CELL AND NO
0.100 4.000 4000.000 170.000 40.000 250.000 24.000

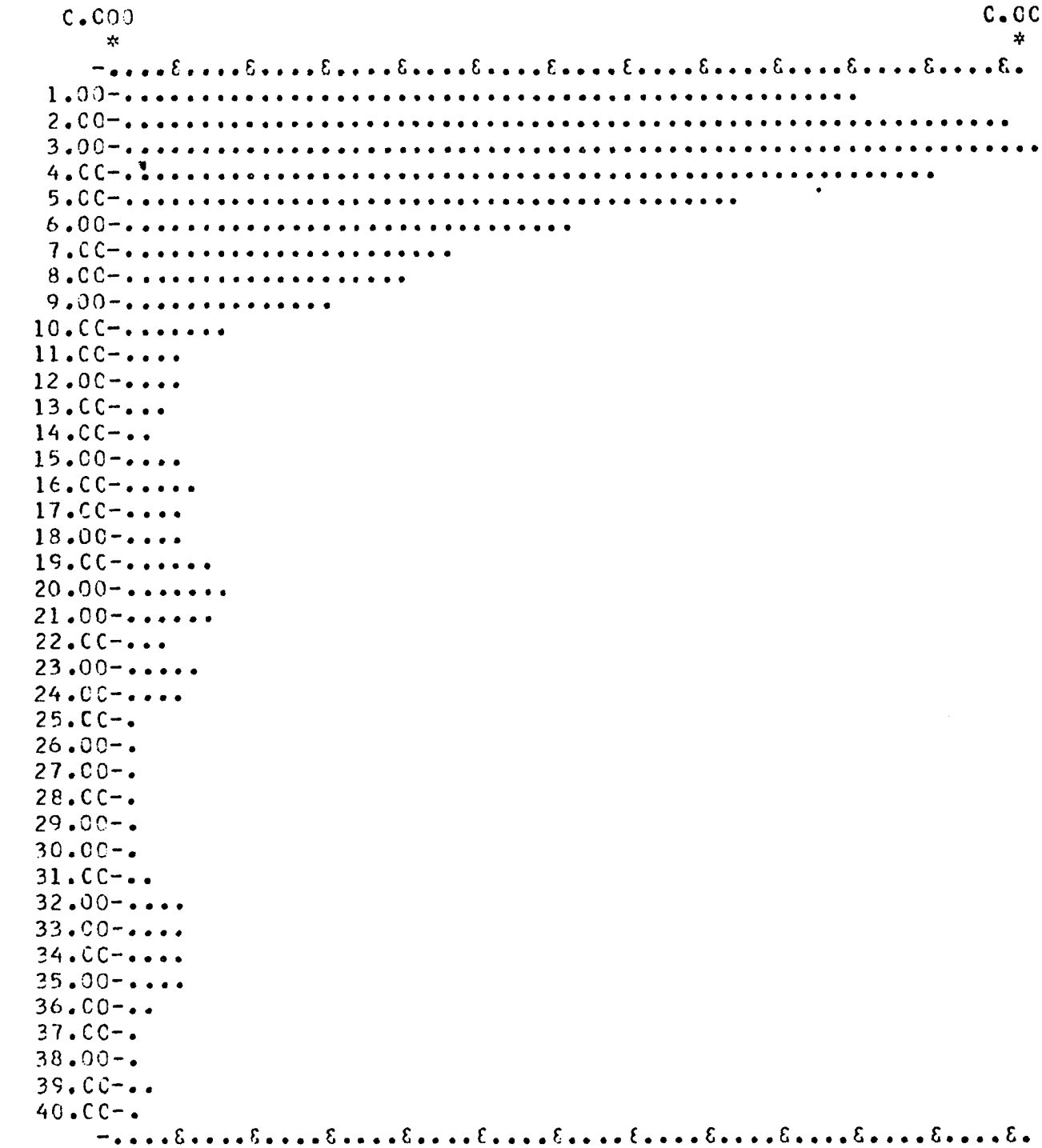

Fig. 26b

THE SCALING FACTOR IS... 0.00014

SOLUTION BY IMAGE METHOD

FOLLOWINGS ARE MIRR.SEP.,SOURCE LOC.,WAVELENGTH AND SCREEN LOC.

0.500	5.000	4000.000	175.000	40.000	17.000	17.000

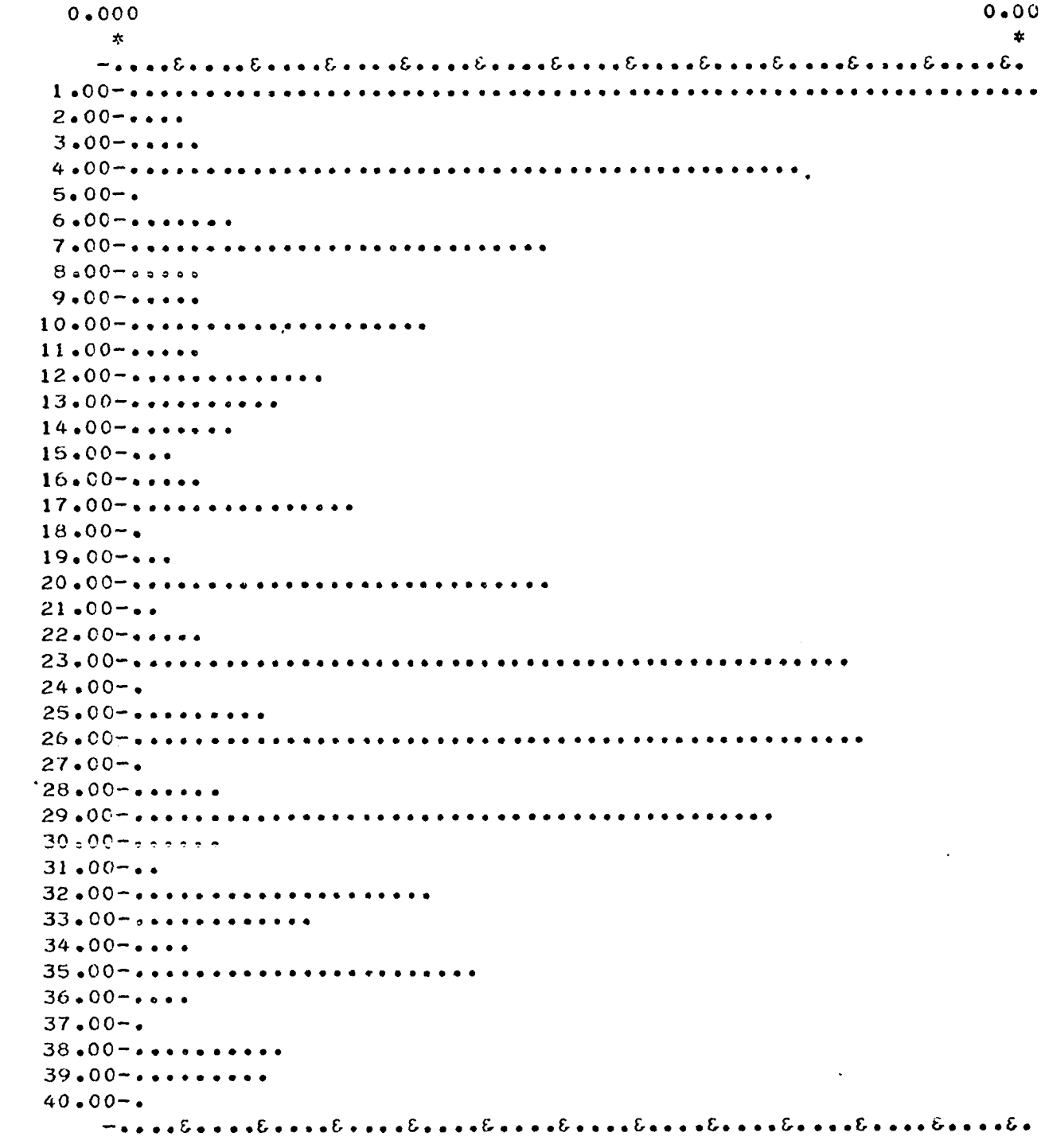

Fig.27

THE SCALING FACTOR IS... 0.00009

NUMBER OF RAYS CONTRIBUTE TO THE INTENSITY ARE NN# 356 176 1761

mirrors. For a separation of 2 millimeter there is a need for a computer time of around 5 hours and in our facility a straight run of this duration is not obtainable.

One set of data, with a mirror separation of .5 mm, was obtained using the image method only. The results obtained resemble actual experimental results from GIMBI.

3. Conclusions

In our calculations, we assumed that the mirrors are perfect conductors. In the Appendix the effect of the conductivity of the mirrors are calculated and it is shown that for optical frequencies and for silver mirrors having vacuum between them, no correction must be made in our results.

The study of computer outputs for different sets of data indicates that both the image and mode methods employed to solve GIMBI are in agreement. The image method involves much less computer time, so it is best suited for GIMBI. The mode method gives easier variation of source-to-screen distances.

Also an examination of intensity patterns for different sets of data, especially variation of wavelength around a central frequency, shows the high sensivity of GIMBI for the use in spectral analysis. This high sensitivity of GIMBI, to other parameters determining the intensity, could be taken advantage in other areas of technology such as communication.

Filmed as received

without page(s) 76 .

UNIVERSITY MICROFILMS.

APPENDIX

Attenuation:

1) Attenuation in image method.

It was shown that the intensity of light on a screen, in this method, is due to the effect of direct and reflected rays of light from the source and mirrors. The rays of light will have losses in each reflection. This loss depends on the angle of incident light and the material property of the mirrors and of the filling between them. The formula for reflectivity is: [11]

$$R_{\perp} = \rho_{\perp}^2 \text{ and } \rho_{\perp} = \frac{(\mu_2 q - \mu_1 \alpha_2 \cos\theta_o)^2 + \mu_2^2 p^2}{(\mu_2 q + \mu_1 \alpha_2 \cos\theta_o)^2 + \mu_2^2 p^2} \tag{A1}$$

$$\tan\delta_{\perp}^{1} = \frac{2\mu_1\mu_2\alpha_2 p \cos\theta_o}{\mu_1^2\alpha_2^2\cos^2\theta_o - \mu_2^2(q^2+p^2)} \tag{A2}$$

where

$$p = \eta(\beta_1 \cos\gamma + \alpha_1 \sin\gamma) \tag{A3}$$

$$q = \eta(\alpha_1 \cos\gamma - \beta_1 \sin\gamma) \tag{A4}$$

$$\eta^2 \cos 2\gamma = 1 - (a^2 - b^2)\, sm^2\theta_o \tag{A5}$$

$$\eta^2\ sm\ 2\gamma = 2\,a\,b\,sm^2\theta_o \tag{A6}$$

$$a = \frac{\alpha 2 \alpha 1}{\alpha_1^2+\beta_1^2}\ ,\quad b = \frac{\alpha_1\beta_1}{\alpha_1^2+\beta_1^2} \tag{A7}$$

$$\alpha_1 = \{\omega\mu_1 (\omega^2\varepsilon_1^2+\sigma_1^2)^{1/2}\}^{1/2} \cos(\tan^{-1}\frac{\sigma_1}{\omega\varepsilon}) \tag{A8}$$

$$\beta_1 = \{\omega\mu_1 (\omega^2\varepsilon_1^2+\sigma_1^2)^{1/2}\}^{1/2} \sin(\tan^{-1}\frac{\sigma_1}{\omega\varepsilon}) \tag{A9}$$

$$\alpha_2 = \omega\sqrt{\varepsilon_2\mu_2} \tag{A10}$$

For typical values: silver mirrors with vaccume between them the material properties are:

i) vacuum

$$\varepsilon_2 = \frac{1}{36\pi} \times 10^{-9} \quad \text{Farad/meter}$$

$$\mu_2 = 4\pi \times 10^{-7} \quad \text{Henry/meter}$$

ii) silver with λ 5893 A°

$$\varepsilon_1 = - \frac{1.95}{\pi} \times 10^{7} \quad \text{Farad/meter}$$

$$\mu_1 = \mu_2$$

$$\sigma_2 = 6.14 \times 10^{7} \quad \text{mhos/meter}$$

ε is obtained from:

$$\varepsilon = n^2 (1 - \kappa^2) \qquad [12]$$

where κ is the attenuation index and n is refractive index of silver

for $\lambda = 5893\ A^{\circ}$, $n = \cdot\ 2$ and $n\kappa = 3.44$ [13]

with the above data relations (A8), (A9) and (A10)

give:

$$\alpha_1 = 0.92 \times 10^{14}$$

$$\beta_1 = 0 \qquad (A11)$$

$$\alpha_2 = 1.03 \times 10^{7}$$

The insertion of values found in (A11) in relations (A7) one obtains:

$$\alpha = - 1.2 \times 10^{-6} \text{ and } b = 0$$

The magnitude of a and h is such small that practically $\eta = 1$ and angle $\gamma = 0$. Finally the values n, β_1, α_1, and γ which were calculated above are inserted in relations (A3) and (A4) to find:

$$p = 0 \qquad (A12)$$

$$q = .92 \times 10^{14}$$

From (A1) and (A2) we can write:

$$\rho_{\perp}^{2} = 1$$

$$\tan \delta_{\perp} = 0 \qquad \delta = 0$$

Also considering $\mu_2 = \mu_1$ for above data ρ_{11} will be:

$$\rho_{||}^{2} = \frac{(\alpha_1^2 \cos \theta_o - \alpha_2 \, q)^2}{(\alpha_1^2 \cos \theta_o + \alpha_2 \, q)^2} \tag{A13}$$

$\rho_{||}^{2}$ for grazing incidence is equal to zero. To show this we set the numerator of (A13) to zero and calculate θ_o

$$\alpha_1^2 \cos\theta_o - \alpha_2 \gamma = 0 \tag{A14}$$

substituting (A11) and (A12) in (A14) we find:

$$\cos \theta_o = \frac{\alpha_2}{\alpha_1} = \frac{1 \cdot 3}{\cdot 92} \times \frac{10^7}{10^{14}}$$

which indicates θ_o is around 90 degrees.

These results for the value of reflectivity implies that in the calculation of the intensity on a screen one needs to consider the perpendicular polarization with reflectivity equal one which means no losses and ignore the other component of polarization.

2) Attenuation in mode method.

There are two kinds of attenuation in the solution of the problem by mode method. (a) Attenuation due to the number of modes and (b) attenuation due to the resistivity of the mirrors. The attenuation factor contains above two kinds and has for the TE modes the formula:

$$\gamma_{TE} = \frac{2\eta^2 \pi^2 \sqrt{\omega \mu m / 2\sigma m}}{\omega\mu \, a^3 \sqrt{\omega^2 \mu\varepsilon - (\frac{n\pi}{a})^2}} \tag{14}$$

In the optical frequency the ohmic attenuation is almost zero. Therefore, its effect is not considered in the calculation. It can, also, be seen from above formula TE modes as an attenuation proportional to the square of the number of modes. This implies that in the calculation of the intensity few lower modes have to be considered.